Escola Universitària d’Enginyeria Tècnica
de Telecomunicació La Salle

Treball Final de Màster

Màster Universitari en Enginyeria de Telecomunicació

On the Analysis and Design of 5G Antenna Arrays

Alumne

Aitor Moreno Laparte

Professor Ponent

Dr. Jaume Anguera Pros
Dra. Aurora Andújar Linares

ACTA DE L'EXAMEN
DEL TREBALL FI DE MÀSTER

Reunit el Tribunal qualificador en el dia de la data, l'alumne

D. AITOR MORENO LAPARTE

va exposar el seu Treball de Fi de Màster, el qual va tractar sobre el tema següent:

On the Analysis and Design of 5G Antenna Arrays

Acabada l'exposició i contestades per part de l'alumne les objeccions formulades pels Srs. membres del tribunal, aquest valorà l'esmentat Treball amb la qualificació de

Barcelona,

VOCAL DEL TRIBUNAL

VOCAL DEL TRIBUNAL

PRESIDENT DEL TRIBUNAL

Abstract

The research conducted during this project has been supervised by PhD. Jaume Anguera and PhD. Aurora Andújar.

This project is based on the challenge to "get on the wave" of the upcoming 5G technology by analyzing the feasibility of a 5G Antenna Array operating at the millimeter-Wave (mmW) frequencies.

The goal is to design and analyze a feasible 5G Antenna Array solution solving the challenges that the mmW frequencies present such as design complexity due to the extremely high frequencies, transmission losses, the required high antenna Gain and high antenna Directivity.

In order to achieve the goal, a project plan is defined with the steps followed and the tasks needed to achieve the goal. In this plan, several experimental phases have been carried out. A preliminary electromagnetic analysis of a single antenna has been performed at a certain mmW frequency, continuing with an electromagnetic analysis of an Antenna Array at the same mmW frequency, the basis of this project, and a feasibility study of its functionality as a real 5G antenna solution to be presented on the market.

The results obtained in the development of the project prove that the 5G Antenna Array solution presented along this project is a real candidate to be implemented as an antenna solution for the upcoming 5G technology's wireless devices.

Resumen

La investigación llevada a cabo durante este proyecto ha sido supervisada por el Dr. Jaume Anguera y la Dra. Aurora Andújar.

Este proyecto se basa en el desafío de "subirse a la ola" de la tecnología emergente del 5G mediante el análisis de viabilidad de un Array de Antenas 5G que trabaja a las frecuencias de onda milimétrica (mmW).

El objetivo es diseñar y analizar una solución de Array de Antenas 5G viable que resuelva los desafíos que presentan las frecuencias mmW, como la complejidad del diseño debido a las frecuencias extremadamente altas, las pérdidas de transmisión, la necesaria alta Ganancia de antena y alta Directividad de la antena.

Para lograr el objetivo, se define un plan de proyecto con los pasos seguidos y las tareas necesarias para alcanzar el objetivo. En este plan, se han llevado a cabo varias fases experimentales. Se realizó un análisis electromagnético preliminar de una sola antena a una cierta frecuencia de mmW; continuando con un análisis electromagnético de un Array de Antenas a la misma frecuencia de mmW, la base de este proyecto, y un estudio de viabilidad de su funcionalidad como una antena 5G real para ser presentada en el mercado.

Los resultados obtenidos en el desarrollo del proyecto demuestran que la solución de Array de Antenas 5G Array presentada a lo largo de este proyecto es una verdadera candidata para ser implementada como una solución de antena para los dispositivos inalámbricos de la emergente tecnología 5G.

Resum

La investigació duta a terme durant aquest projecte ha estat supervisada pel Dr. Jaume Anguera i la Dra. Aurora Andújar.

Aquest projecte es basa en el repte de "pujar a l'onada" de la tecnologia emergent del 5G mitjançant l'anàlisi de viabilitat d'un Array d'Antenes 5G que treballa a les freqüències d'ona mil·limètrica (mmW).

L'objectiu és dissenyar i analitzar una solució d'Array d'Antenes 5G viable que resolgui els desafiaments que presenten les freqüències mmW, com la complexitat del disseny a causa de les freqüències extremadament altes, les pèrdues de transmissió, el necessari alt Guany d'antena i l'alta Directivitat de l'antena.

Per aconseguir l'objectiu, es defineix un pla de projecte amb els passos seguits i les tasques necessàries per assolir l'objectiu. En aquest pla, s'han dut a terme diverses fases experimentals. Es va realitzar una anàlisi electromagnètic preliminar d'una sola antena a una certa freqüència de mmW; continuant amb una anàlisi electromagnètic d'un Array d'Antenes a la mateixa freqüència de mmW, la base d'aquest projecte, i un estudi de viabilitat de la seva funcionalitat com una antena 5G real per a ser presentada al mercat.

Els resultats obtinguts en el desenvolupament del projecte demostren que la solució d'Array d'Antenes 5G presentada al llarg d'aquest projecte és una veritable candidata per ser implementada com una solució d'antena per als dispositius sense fils de l'emergent tecnologia 5G.

Keywords

ENGLISH

Antennas, Antenna Array, Microstrip Patch Antenna, 5G, millimetre-Wave (mmW), Extremely High Frequency (EHF), Beam Steering, Gain, Directivity.

SPANISH

Antenas, Array de Antenas, Microstrip Patch Antenna, 5G, onda milimétrica (mmW), Frecuencia Extremadamente Alta (EHF), Direccionamiento del Haz de la Antena, Ganancia, Directividad.

CATALAN

Antenes, Array d'Antenes, Microstrip Patch Antenna, 5G, ona mil·limètrica (mmW), Freqüència Extremadament Alta (EHF), Direccionament del Feix de l'Antena, Guany, Directivitat.

Acknowledgement

This project has been sponsored by the technology company Fractus Antennas S.L. (Sant Cugat del Vallès) and conducted under the collaboration of Fractus Antennas S.L. and the Department of Electronics and Communications in La Salle, Ramon Llull University (Barcelona).

I would like to express my gratitude to the company Fractus Antennas, S.L. for allowing me to carry out the research presented in this project and for providing me the necessary resources to carry it out.

To PhD. Jaume Anguera and PhD. Aurora Andújar for their great help and collaboration provided throughout this research project, not only on a professional way but also on a personal way.

To the teachers and classmates of La Salle Universitat Ramón Llull, who have accompanied and taught me along my stay at the university.

To my family, especially to my mother María Ángeles, my father Ramón, my brother Edgar and my grandparents for their unconditional support, affection and trust during all these years.

To my girlfriend Anna, for her patience, understanding and unconditional support along the whole Master course and its project. You are a key part of the project’s success.

To my friends, for listening, supporting and encouraging me to move on. Thank you for being not only in good moments.

Thank you so much to all of you, you have encouraged me to make it possible!

Index

1 Introduction

1.1 Scope

It is an innate behavior on human beings to live in society and in constant contact with the people around us, such as family, friends, etc. Consequently, throughout the history of humanity, we have tried to find new ways whose allow us to be closer to other people.

From a technological point of view, the most important technologies that have covered this necessity on the human beings are the Mobile Technology and Internet Technology. But, it was not since Internet was released in 1985 and the first ".com" domain was registered [1] , when a revolution on the "Technology World" started changing completely the way we live, communicate and relate with other human beings.

Several mobile generations have been released since its creation, but it was not until the third generation (3G) when both Mobile and Internet technology merged, integrating the most important technologies in one device.

Nowadays, this necessity of being connected with others has been extrapolated to be connected with other people and the things we have around, in a faster and more precisely way [2] .

At this point, the market is demanding a technology that the current 4G Mobile technology does not support. So, for this reason, a new generation is needed, to cover the expectations and needs of the market. This new generation is stated as 5G.

Therefore, this project aims to investigate a feasible antenna solution for the upcoming 5G technology, focusing on the importance of the challenges that this technology demands.

1.2 Objectives

In a personal way, this project allows me to acquire a maturity and experience in the telecommunications sector, especially in the field of antennas, since this project aims to investigate an upcoming technology which requires an optimal research and study of the cases presented to analyze their future implementation feasibility.

An important objective set for this project is to properly plan and schedule all the required steps for the project development, to ensure the best resolution and to properly manage the resources and efforts needed to achieve a successful study. This will provide me the experience to better plan and to properly size the resources for current and future projects in a real-world environment.

From an R&D point of view, it is an extraordinary opportunity to work on the steps required for a proper product research and development; since it comes from an initial idea and will lead to a solution which could be implemented in a future.

The objectives of this project are divided in three parts which will merge on the final conclusions to solve the investigation conducted during this project and the main goal of it: develop and study a 5G Antenna Array solution for a real-world application which will solve the challenges that 5G technology presents.

More precisely, understand the need of the market and provide a solution for the upcoming 5G technology achieving the best performance for the millions of applications the market will demand.

The three parts of the objectives set for this project are:

1) From a previous analysis point of view, an electromagnetic analysis will be carried out in order to understand how 5G antennas perform and how they need to be designed for the purposes of this project.
2) Once this previous analysis is done, study and develop the 5G antenna array solution that better covers the demands of the market in terms of performance, space, etc.
3) Finally, analyze the results obtained to set a path to follow for a future implementation of the 5G Antenna Array solution presented along this project.

1.3 5G

The upcoming 5G technology is, nowadays, the main challenge for the Information and Communications Technology sector. Within this section, it is intended to expose from a general point of view what 5G is, how will affect our life and the challenges needed to be achieved from the ICT sector.

1.3.1 What is 5G?

5G is the fifth generation of mobile communications, which appears from the needs of the Internet of Things' and Smart Cities' development that 4G cannot cover. The upcoming 5G technology needs to achieve 8 specifications main requirements:

1. Up to 10Gbps data rate.
2. 1-millisecond latency.
3. 1000x bandwidth per unit area (compared with 4G LTE).
4. Up to 100x number of connected devices per unit area (compared with 4G LTE).
5. 99.999% availability.
6. 100% coverage.
7. 90% reduction in network energy usage.
8. Up to 10-year battery life for low power IoT devices.

All these requirements come from the necessity that the market demands on the Internet of Things' and Smart Cities' development. The 4G generation was obsolete due to the limitations on the specifications. However, 5G will improve almost all the technical specifications in order to achieve the European Commission goal (Figure 1) [3] .

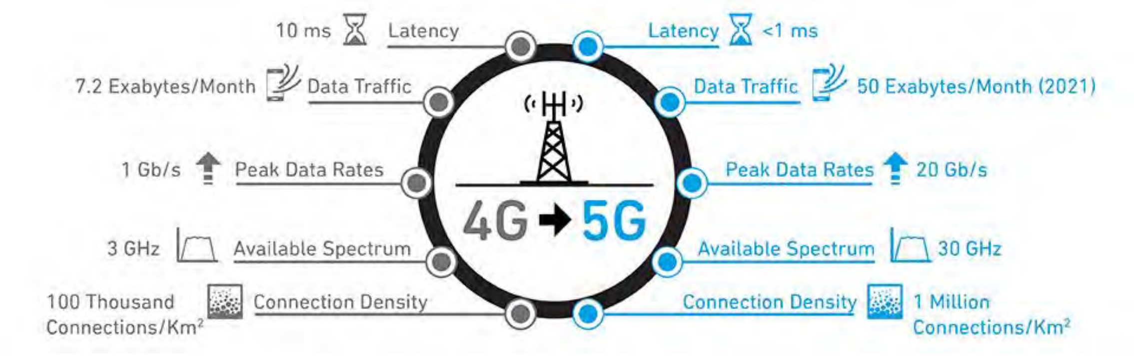

Figure 1. Differences between 4G and 5G [4] .

5G is a key asset for the next years global economy; since it would allow plenty of applications that we cannot even imagine which will change how we see the world and, specially, how we interact with the world [5] .

1.3.2 5G in our life

Since 5G first discussions and symposiums, it has been presented as an improvement of all the technical specifications of 4G. Nevertheless, it should not be forgotten that 5G is not simply an "improved version" of 4G (as it was 4G from 3G); 5G new technical specifications are only the tip of the iceberg of the million changes we will all face in our daily life during the upcoming years.

A 5G connected city will be an extremely close approach to the "Digital City" by definition; with connected cars and remote medical operations, among millions of other applications. Smart cities have been so far focused in only gather information from citizens interactions, but with no real time action using this big amount of data. 5G cities will allow to directly act using the data from the citizens interactions. This is going to be the big change thanks to the high capacity and extremely low latency of the new 5G network [6] .

As an example of new actions 5G cities will be able to do, it would be possible to avoid a car crash remotely; not only due to the onboard computer, even more by using external actors and sensors that will detect the possibility of a crash and will tell the onboard computer of the car what to do to avoid it in real time. Hence, the amount of security measures that will be created using these interactions will lead to improve 5G cities quality of life.

Figure 2. Autonomous vehicle interacting with external actors [7] .

When talking about 5G applications, most popular among the society are the autonomous car and remote medical operations/actions. Nevertheless, 5G is going to arrive much further in almost all fields in our daily life with real time actions in sectors such as:

- **Mobility:** autonomous vehicles (not only cars), traffic management, smart parking and car-to-car communication, for example.
- **Communications:** faster and higher quality communications with full coverage.
- **Security:** real-time security actions, new prevention methods, etc.
- **Basic resources:** water quality and management, waste management, energy optimization, etc.
- **Domotics:** house automatization, resources management, etc.
- **Healthcare:** remote visits and operations using virtual and augmented reality, amount of information available about the patients in real time, etc.
- **Entertainment:** gaming, smartphone applications, virtual and augmented reality, etc.

Figure 3. 5G applications [8] .

To provide all these services and applications, it is needed research and development from the industry, universities and innovation centers to develop the technology needed to achieve 5G expectations. This process is leading to the fourth industry revolution, popularly named as “Industry 4.0”.

As already known, 5G will also affect the industry in several ways, since with 5G a full automation will be possible, reducing operation times and costs in all the productive chain in Manufacturing industries for instance. Main impacts and improvements in the industry will be present on automation using robotics, virtual reality experiences, real time remotely actions to control different processes, big amount of data generated and sent, etc.

Nevertheless, it is a key part of 5G success that country’s and local’s institutions invest resources to achieve the challenging goals 5G present, in order to provide to their citizens all these million applications. If public institutions promote on 5G, new business models, that cannot even be imagined, are going to appear taking profit of 5G opportunities, improving the way we see and interact with our world.

1.3.3 5G Implementation Plan

The 5G Implementation Plan is a strategic European Commission initiative to be in forefront of the Information and Communication Technologies (ICT) sector and the entire economy, contributing to the digital transformation of Europe business and society [5] .

Europe's commitment with 5G is due to the opportunity to promote the European economy, scheduling Euro2020 football games as the deadline to ensure 5G as a reality in our life. At that time, very high-capacity networks like 5G will be a key asset for Europe to compete in the Global market, with 5G revenues for mobile operators expected to reach 225B€ annually by 2025 [8] .

The European Commission launched in 2014 the 5G Public-Private Partnership (5G-PPP) [5] to improve and implement research and development in 5G technology, providing a new vision of the new technology applications. Together with the 5G-PPP, the European 5G Action Plan was presented [3] , and within this action plan, it is identified a number of challenges to promote the deployment, implementation and commercialization of 5G; achieving the goals set for this upcoming technology.

The time plan presented in this action plan (Figure 4), ensured the launch of extensive large scale trials of 5G systems & technology in 2017, early 5G networks at the end of 2018 and pretend a full commercial 5G infrastructure deployment in 2020.

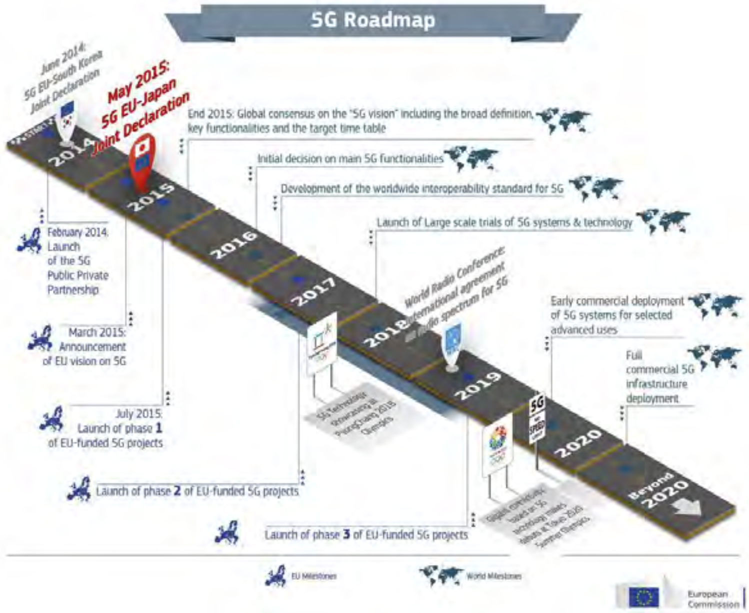

Figure 4.European Commission 5G Roadmap [8] .

Furthermore, the action plan identifies the frequency bands to be harmonized across Europe and adopted by the PAN-Europe member states: 700MHz band, 3.4-3.8GHz band and the 24.25-27.5 GHz band [5] .

The 5G-PPP presented the time plan for the different standards and trials in the key cities all over Europe (Figure 5) to achieve the EU Commission action plan Euro2020 target.

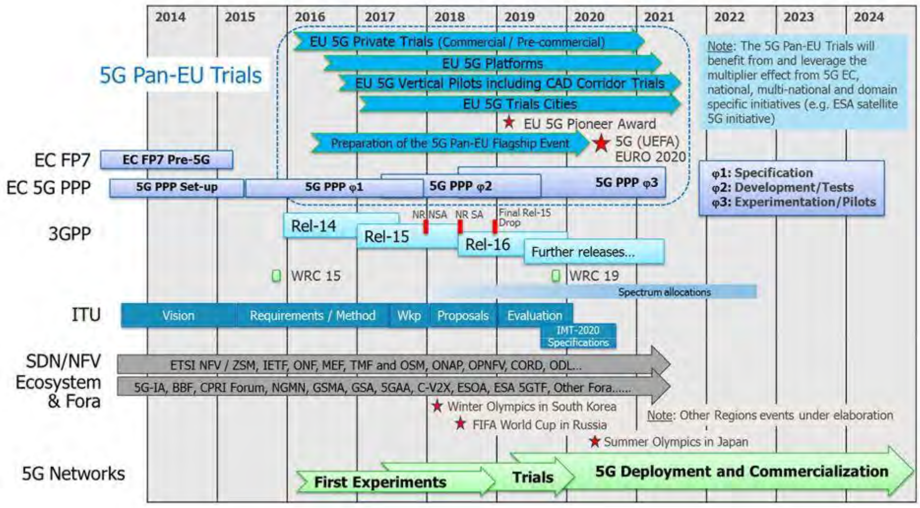

Figure 5. 5G-PPP standards and trials time plan [3] .

Therefore, from the 5G-PPP time plan, it can be extracted that the first 5G cities should start in second half of 2019, with the release of devices that will support the EU configuration in bands 42 and 43 (3.4GHz – 3.8GHz):

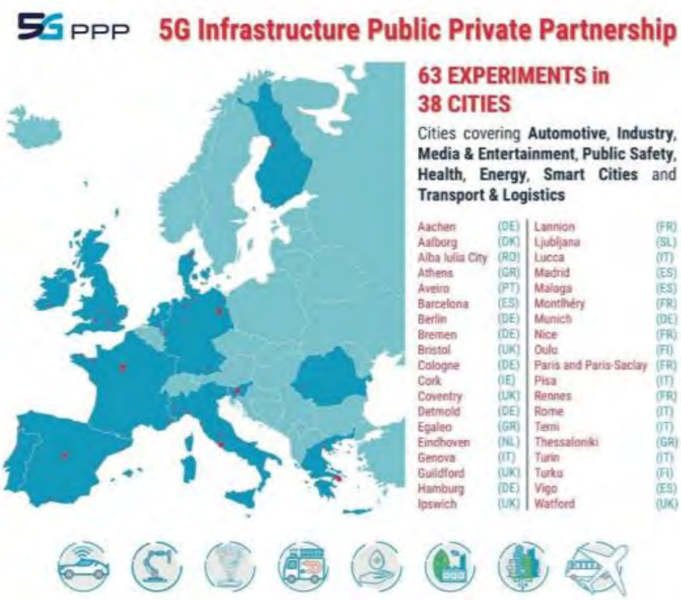

Figure 6. Cities for the 5G Trials [3] .

In essence, the European vision of 5G as the enabler for the Gigabit Society is exposed as the key part for the 5G to be implemented. The 5G Implementation Plan presents several challenges that should be achieved to continue being in forefront of the Global Economy in the ICT sector.

1.4 Structure

As explained on section 1.2, this project aims to achieve various objectives. In order to achieve the objectives, the project has been structured following several chapters.

The first chapter is an introduction of the project and the need of the research developed, presenting the different technologies which take part of the investigation. Along the first chapter, the basic concepts to understand the investigation carried out on this project are presented.

In the second chapter, the project definition is presented including all the steps performed during the project development. This planning provides an overview of the project from an organizational point of view, allowing to better understand the parts of the project and the reason of each step forward done.

In the third chapter, the state of the art is reviewed to see what is being done and what might be expected from the project. After reviewing several articles, you will get a conclusion choosing a path to follow. An investigation is carried out within the existing sources of information and documents and works are studied to know the state of the art.

Throughout the fourth chapter, an electromagnetic analysis of single antenna solutions is presented. This chapter will allow to get familiarized with the technology and the antennas studied in this project. As a second part of this chapter, and the basic part of the investigation, an electromagnetic analysis is carried out considering an antenna array of the antenna studied on the previous chapter's section. As conclusion of this chapter is presented a summary of the results obtained.

In the fifth chapter, it is simulated an antenna array but considering the impact of a wireless device cover. Along this section, it will be studied the "optimal thickness" for the cover impact to be transparent for the antenna array.

In the sixth chapter, the final conclusions of the investigation are presented. A summary compiling the results is concluded and the path to follow for future implementations.

1.5 Methodology

To implement the project, several processes will be followed. First, a study of the state of the art was carried out, which has acquired the knowledge and information necessary to understand the basic parameters of a 5G Microstrip Patch Antenna.

The electromagnetic simulation was performed with the IE3D program and Microwave Office AWR.

The IE3D and the Microwave Office AWR are simulation programs, with licenses at Fractus Antennas, S.L. The IE3D is the first scalable EM design and verification platform that provides modelling accuracy for the combined needs of high frequency circuit design engineers and signal integrity in multi-domain design.

Once the first designs have been implemented with the IE3D software, they are exported to the AWR to see their behavior. If the behavior in terms of antenna impedance are the once expected, an analysis using the IE3D Pattern View and AWR is done to obtain the required information to study every case.

Finally, the antenna solutions and their results are presented and deeply analyzed along this report.

1.6 Basic Concepts

Along this chapter, the basic concepts that are needed to understand the cases exposed during this project are introduced.

All the concepts explained below can be found in J. Anguera and A. Pérez “Teoría de Antenas” [9] book.

1.6.1 Antenna Impedance

The antenna impedance is the relationship between the voltage and the input port current. This impedance has a real and an imaginary part. Both depend in frequency.

On the one hand, an antenna can be resonant at several frequencies but will only resonate when its impedance imaginary part is 0.

On the other hand, the real part from the antenna impedance can be separated into the radiation impedance and the loss impedance which represents the energy or power that the antenna will radiate and the loss that the antenna will have.

The main goal when designing an antenna system is to have the antenna adapted in order to be more efficient and by so the radiation will be greater.

$$R_A + jX_A = Z_A$$

Equation 1. Antenna Impedance (Z_A) equation where R_A is the real part and X_A is the imaginary part

$$R_r + R_L = R_A$$

Equation 2. Antenna Resistance (R_A) equation where Rr is the radiation resistance of the antenna and R_L is the loss resistance of the antenna.

The maximum power delivered to the antenna occurs when we have conjugate matching, that is when:

$$R_A = R_g$$

Equation 3. Antenna resistance (R_A) need to be equal to the generator resistance impedance (R_g)

$$X_A = -X_g$$

Equation 4. Antenna reactance (X_A) needs to be equal to minus the generator resistance reactance (X_g)

1.6.2 Directivity

Directivity is a measure of how directional an antenna's radiation pattern is, i.e. it measures the direction of radiation of an antenna.

Mathematically, it is defined as the ratio of its radiation intensity in a given direction over that of an isotropic source, understanding as an isotropic source an antenna which radiates equally in all directions.

$$D = \frac{U}{U_0} = \frac{4\pi U}{P_{rad}}$$

Equation 5. Directivity (D) at a certain direction equation where U is the radiation intensity of the antenna, U_0 the radiation intensity of an isotropic antenna and P_{rad} is the total radiated power of the antenna.

If the direction is not specified, the direction of maximum radiation intensity is defined as:

$$D_{max} = D_0 = \frac{U_{max}}{U_0} = \frac{4\pi U_{max}}{P_{rad}}$$

Equation 6. Maximum Directivity (D_0) equation where U_{max} is the maximum radiation intensity of the antenna, U_0 the radiation intensity of an isotropic antenna and P_{rad} is the total radiated power of the antenna.

1.6.3 Gain

The gain of an antenna is closely related to the directivity; however, it also takes into consideration the efficiency of the antenna.

Gain of an antenna (in a given direction) is defined as the ratio of the intensity, in a given direction, to the radiation intensity that would be obtained if the power accepted by the antenna were radiated isotropically. The radiation intensity corresponding to the isotropically radiated power is equal to the power accepted (input) by the antenna divided by 4π.

$$Gain = 4\pi \frac{Radiation\ intensity}{total\ accepted\ power} = 4\pi \frac{U(\theta,\varphi)}{P_{in}}$$

Equation 7. Gain of an antenna.

Nevertheless, the Gain of an antenna could also be obtained if the transmission coefficient between two antennas (S_{21}) is known. This implies a system set-up where two antennas take part and are transmitting and receiving signal from each other.

$$Gain\ (dB) = \frac{S_{21} - 20 * log_{10}(\frac{300}{4\pi * D * f_0})}{2}$$

Equation 8. Gain of an antenna in dB where S_{21} is the transmission coefficient between two antennas, D is the distance between both antennas and f_0 is the central frequency of the signal transmitted by the antennas.

1.6.4 Friis' Transmission Equation

The Friis' Transmission Equation relates the power received to the power transmitted between two antennas separated by a distance $R > 2D^2/\lambda$, where D is the largest dimension of either antenna.

Even the original Friis' Transmission Equation considers the Gain and Directivity in different directions, for reflection and polarization-matched antennas aligned for maximum directional radiation and reception, the equation reduces to:

$$\frac{P_r}{P_t} = \left(\frac{\lambda}{4\pi R}\right)^2 G_{0t}G_{0r}$$

Equation 9. Friis' Transmission Equation for reflection and polarization matched antennas where R is the distance between both antennas and G_{0r} and G_{0t} the isotropic Gain of the reception and transmission antenna respectively.

1.6.5 S-Parameters and VSWR

The S-parameters can be defined as a relationship of power waves between the incident and the reflected. Those waves are related to the characteristic impedance of the system.

Depending of the number of ports, a matrix defining the relationship mentioned can be analyzed. The S_{11} parameter gives information of the relationship of the reflected signal and the S_{21} parameter gives information about the coupling between them.

$$a_n = \frac{V_n^+}{\sqrt{Z_0}}\ ,\ b_n = \frac{V_n^-}{\sqrt{Z_0}}$$

Equation 10. Incident power wave (a_n) and reflected power wave (b_n) equations.

$$\begin{pmatrix} b_1 \\ b_2 \end{pmatrix} = \begin{pmatrix} S_{11} & S_{12} \\ S_{21} & S_{22} \end{pmatrix} \begin{pmatrix} a_1 \\ a_2 \end{pmatrix}$$

$$b_1 = S_{11}a_1 + S_{12}a_2$$

$$b_2 = S_{22}a_2 + S_{21}a_1$$

Equation 11. Reflected power waves equation of a 2-ports systems, where it is expressed in function of the S-parameter matrix and the incident power wave.

The Voltage Standing Wave Ratio relates the standing wave maximum voltage with the standing wave minimum voltage. It therefore relates to the magnitude of the voltage reflection coefficient.

Mathematically could be expressed as:

$$VSWR = \frac{1 + |S_{11}|}{1 - |S_{11}|}$$

Equation 12. VSWR in function of the reflection coefficient S_{11}.

1.6.6 Radiation Efficiency

The radiation efficiency can be defined as the relationship between the power radiated and the power given to the antenna system.

$$\eta_r = \frac{P_r}{P_r + P_L} = \frac{I^2 \cdot R_r}{I^2(R_r + R_L)} = \frac{R_r}{R_r + R_L}$$

Equation 13. Radiation Efficiency equation where Rr is the radiation resistance of the antenna and R_L is the loss resistance of the antenna.

1.6.7 Antenna Efficiency

While the radiated efficiency (η_r) only considers the efficiency over the Ohmic losses, the antenna efficiency (η_a) considers the impedance matching of the antenna (S_{11}).

$$\eta_a = \eta_r \cdot (1 - |S_{11}|^2)$$

Equation 14. Antenna Efficiency equation expressed in function of the impedance matching of the antenna.

1.6.8 Radiation Pattern

A radiation pattern defines the variation of the power radiated by an antenna as a function of the direction away from the antenna represented on a space coordinate system (Figure 7). This power variation as a function of the arrival angle is observed in the antenna's far field.

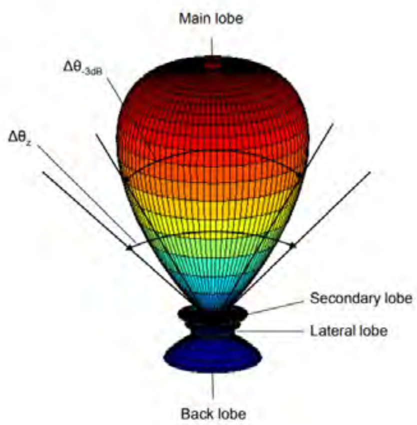

Figure 7. Coordinate system for antenna analysis [9] .

The radiation pattern of an antenna presents several characteristics which are used to analyze and define the antenna performance for a required application. The main characteristics that can be analyzed from a radiation pattern are:

- **Radiation lobes**: "portion of the radiation pattern bounded by regions of relatively weak radiation intensity". There could be different radiation lobes represented on a radiation pattern:
  - Main lobe: it represents the direction where the highest amount of radiation is directed to.
  - Side lobe, Minor lobe, Back lobe (secondary lobes): represent the directions where the radiation of the antenna is not directed to (or its power is highly decreased).

  The difference between the "Main Lobe" and the "Secondary Lobes" is a critical point when designing an antenna, since they would affect the directivity and gain of the antenna that the designer want to achieve.

- **HPBW and FNBW:** correspond to the Half-power Bandwidth (-3dB from the Main Lobe maximum) and First-null Bandwidth respectively.

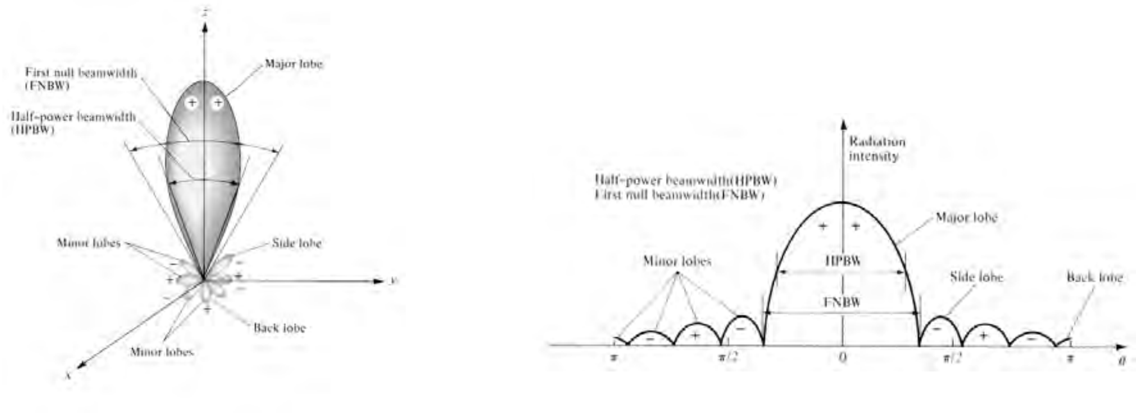

Figure 8. Radiation pattern characteristics represented on a 3D coordinate system and on 2D coordinate system respectively [10] .

The most common radiation patterns could be summarized to three different types: Isotropic, Directional and Omnidirectional patterns:

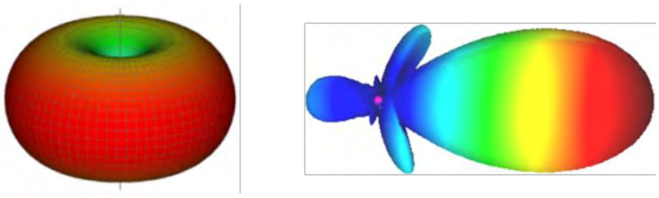

Figure 9. Isotropic/Omnidirectional and Directional radiation pattern examples respectively.

In summary, the radiation pattern is a representation which allows us to visualize where the antenna transmits or receives power.

1.6.9 Microstrip Patch Antennas

In high-performance aircraft, spacecraft, satellite, and missile applications, where size, weight, cost, performance, ease of installation, and aerodynamic profile are constraints, low-profile antennas may be required. Presently there are many other government and commercial applications, such as mobile radio and wireless communications, that have similar specifications. To meet these requirements, Microstrip Patch Antennas can be used [9] .

These antennas are low profile, conformable to planar and nonplanar surfaces, simple and inexpensive to manufacture using modern printed-circuit technology, mechanically robust when mounted on rigid surfaces, compatible with MMIC designs, and when the particular patch shape and mode are selected, they are very versatile in terms of resonant frequency, polarization, pattern, and impedance.

Microstrip Patch Antennas consist of a very thin metallic strip (patch) placed above a ground plane. The Microstrip Patch is designed so its pattern maximum is normal to the patch (broadside radiator) [9] . This is accomplished by properly choosing the mode (field configuration) of excitation beneath the patch.

The Microstrip Patch Antenna transmission line and ground plane are made of high conductivity metal, like copper, of thickness t. The patch is of length L, width W, and placed on the top of a substrate of thickness h (Figure 10).

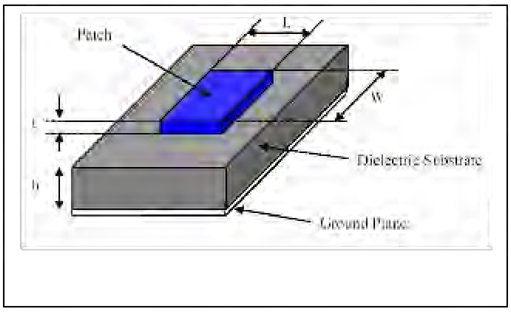

Figure 10. Microstrip Patch Antenna dimensions [10] .

Several geometries could be achieved when designing a Microstrip Patch Antenna (Figure 11) as well as other shapes based on fractal geometries and genetic based antennas [11] [12] [13] [14] :

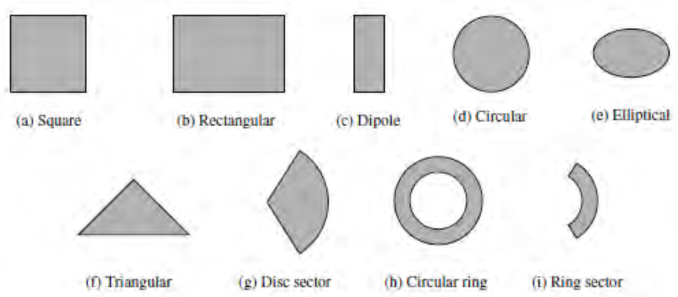

Figure 11. Different geometries of Microstrip Patch Antennas [10] .

Linear and circular polarizations can be achieved with either single elements or arrays of Microstrip Patch Antennas.

A Microstrip Patch Antenna could be feed in several ways (Figure 12), the type of feeding implemented on the patch would set the polarization of the patch antenna [9] .

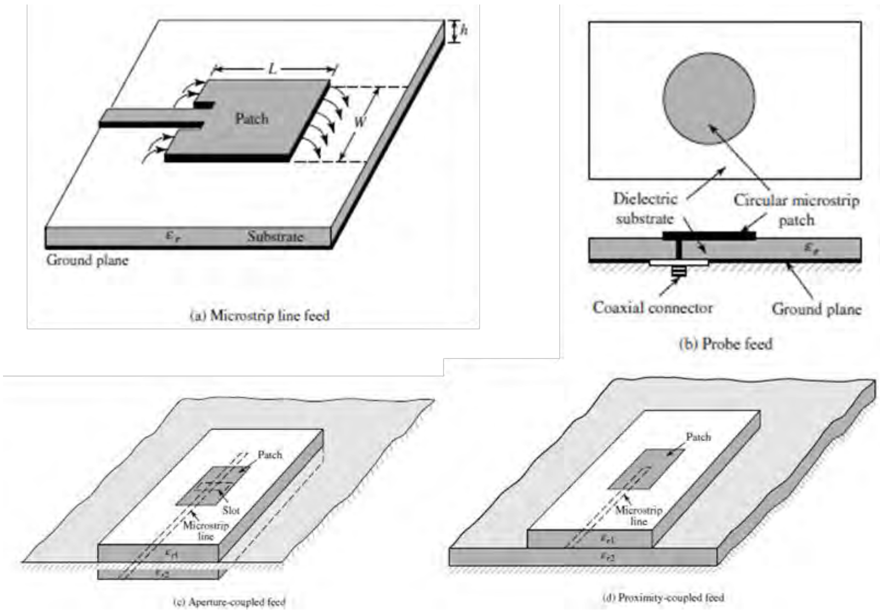

Figure 12. Different feeding methods of a Microstrip Patch Antenna [10] .

On the current project electromagnetic analysis and measurements, the chosen feeding method is the Probe-feed. As it will be seen later on, this type of feeding allows obtaining circularly polarized Microstrip Patch Antenna at a certain frequency.

In order to set the values of the parameters which characterize a Microstrip Patch Antenna, some equations will be presented on Section 4.2.

1.6.10 Antenna Array

An antenna array can be defined as an aggrupation of minimum two antennas.

Usually the radiation pattern of a single element is relatively wide, and each element provides low values of directivity and gain. “*In many applications it is necessary to design antennas with very directive characteristics (very high gains) to meet the demands of long-distance communication. This can only be accomplished by increasing the electrical size of the antenna. Enlarging the dimensions of single elements often leads to more directive characteristics. Another way to enlarge the dimensions of the antenna, without necessarily increasing the size of the individual elements, is to form an assembly of radiating elements in an electrical and geometrical configuration. This new antenna, formed by multi-elements, is referred to as an array.”* [10] .

To meet the objective of an antenna array and achieve very high gains it is necessary to consider different characteristics which will define the antenna array performance:

1. Geometrical configuration of the array (linear, 2D or 3D).
2. Distance between the elements (ideally should be λ/2).
3. Excitation amplitude and phase of the individual elements.
4. Radiation pattern of the individual elements.

Figure 13. Antenna array examples.

Apart of the array characteristics presented above, there is one important function in array theory, and it is named as Array Factor (AF). The Array Factor is a function of the positions of the antennas in the array and the weights used. By tailoring these parameters, the antenna array's performance can be optimized to achieve desirable properties. For example, the antenna array can change the direction of maximum radiation or reception by changing the weights in the array.

The Array Factor is calculated as:

$$AF = \sum_{i=1}^{N} w_i e^{-jkr_i}$$

Equation 15. Array Factor, where N is the array's number of elements.

1.6.11 Beam steering

Beam steering is a new concept which appears due to the upcoming 5G technology. It is based on the concept to dynamically change the signal beam direction of an antenna array, and comes from the concept named as “Beam Forming” of controlling the shape and direction of an antenna array signal beam by changing the phase and spacing between the antenna array single elements [15] .

As said before, the signal beam direction and shape can be modified by altering the signal phase and spacing between the antenna array elements. Nevertheless, on a real-world environment where antenna arrays are physically fixed, the single elements of an antenna array do have a fixed spacing between them. Therefore, changing the signal phase is the main tool that can be used to modify a signal beam direction of an antenna array.

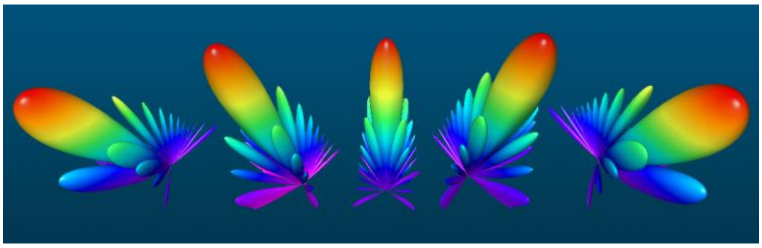

Figure 14. Different signal beam directions by using Beam Forming and Beam Steering techniques [16] .

At this point is where beam steering concept appears, since it allows to dynamically change the signal phase in a digital way. By doing so, the antenna array signal beam can be directed to many different points of its total coverage, enabling to have continuous and full coverage in a certain region.

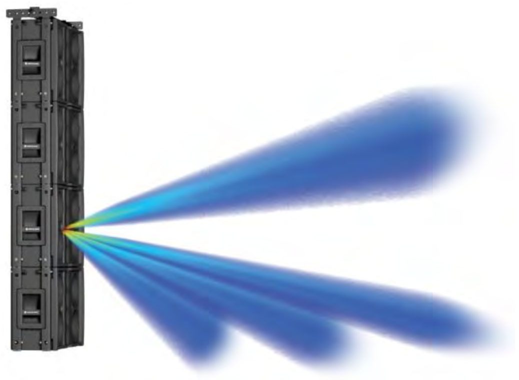

Figure 15. Beam Steering technique [17] .

There are several digital techniques to achieve beam steering on a certain antenna array, and by using them, each antenna has its own transceiver and data converters. They can handle multiple data streams and generate multiple beams simultaneously from one array.

Therefore, when using beam steering techniques, it is possible to generate several sets of signals. By doing so, it enables a single antenna array to serve multiple beams, and hence multiple users in a scenario like 5G.

The challenges that beam steering technique presents, require more hardware and a highly demanding environment on the signal processing in the digital domain, but enables much greater flexibility and capability.

2 Project Plan

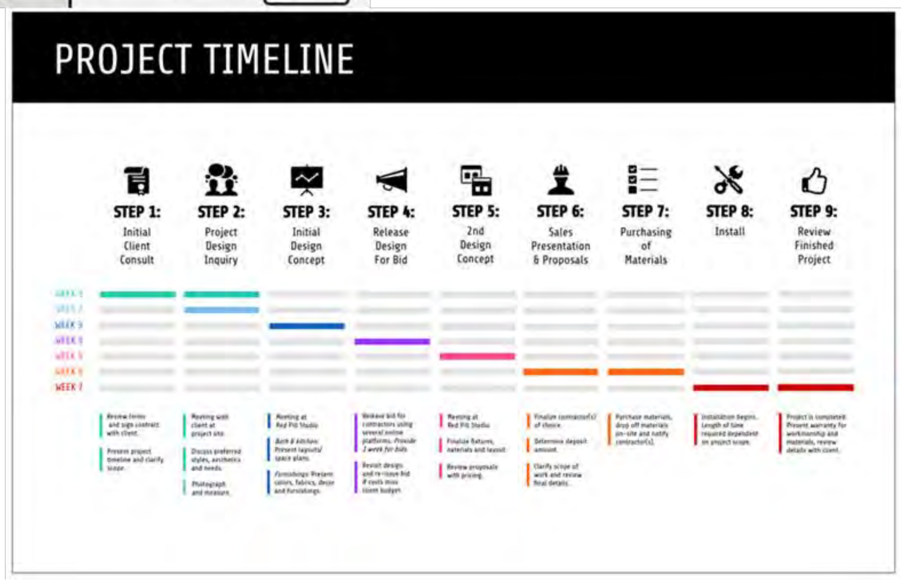

2.1 Introduction

Along this section, the project definition is presented including all the steps performed during the project development.

This planning provides an overview of the project from an organizational point of view, allowing to better understand the parts of the project and the reason of each step forward done.

2.2 Project Definition

This project has been designed to study and develop an Antenna Array solution for the upcoming 5G technology focused on solving the challenges this technology present.

With this research and development, it is intended to analyze a market which will grow up extremely fast along the upcoming years and to provide a solution which will be used for plenty of 5G applications.

The work done and presented along this report, will give an advantage in this field, being able to strategically open this market for current and new customers interested to implement a 5G Antenna Array solution.

2.3 Tasks List

Below is presented the proposed implementation approach for this project. The key activities and tasks to do are as follows:

- **Project Definition, Design and Start:**
  - Initial meeting for project presentation.
  - Define requirements and key objectives of the project.
  - 5G General Information.
  - Study 5G Implementation Plan.
  - Benefits/improvements included within 5G.
  - 5G Applications.
  - Solutions that the market demands.
  - Meeting for project design and scope validation.
- **Review of Prior Art.**
  - Benchmark of current solutions.
  - Analysis of the solutions studied.
  - Meeting to discuss and validate Prior Art studied.

- **Single Antenna Electromagnetic Simulation:**
  - Solution characteristics benchmark.
  - Meeting to set and define the solution to be studied.
  - Calculations and design.
  - Simulation.
  - Results study and conclusions.
  - Meeting to discuss and validate the solution design and results.
- **Antenna Array Electromagnetic Simulation:**
  - Solution characteristics benchmark.
  - Meeting to set and define the solution to be studied.
  - Calculations and design.
  - Simulation.
  - Results study and conclusions.
  - Meeting to discuss and validate the solution design and results.
- **Project Report:**
  - Report the information, Prior Art, simulations, results and conclusions created/obtained during the project duration.
  - Feasibility study of the solution and creation of the path to follow.
  - Meeting to discuss and validate the project report.
- **Project Presentation:**
  - Creation of the project presentation to be exposed during the final evaluation.
  - Meeting to discuss and validate the project presentation.
- **Project Close:**
  - Final meeting before the final evaluation to analyze:
    - Project Execution.
    - Objectives achieved.
    - Define further actions if agreed.
  - Project presentation and evaluation.

2.4 Execution Plan

The execution plan defined for the key activities and tasks to do is presented below in a timeline scheme. This execution plan is intended to schedule properly all the tasks involved in the project execution to ensure good project timings:

Vacation period

Active period

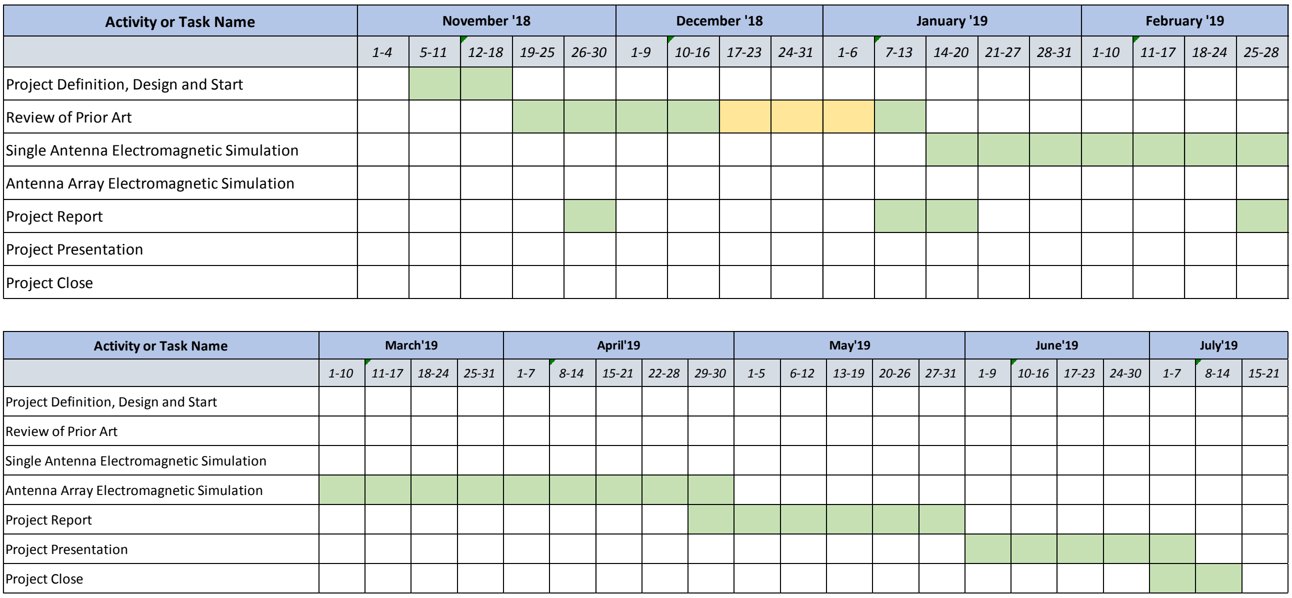

Figure 16. Execution Plan defined for the project development and closing from November '18 to July '19.

2.5 Conclusions

It is a key part of a project's success to clearly plan and schedule the project timings along its duration.

In this section it has been presented the project definition, basis of this project's objectives, and the steps needed to successfully develop it. These steps have been fully followed enabling good timings on each key part of the project execution.

3 State of the art

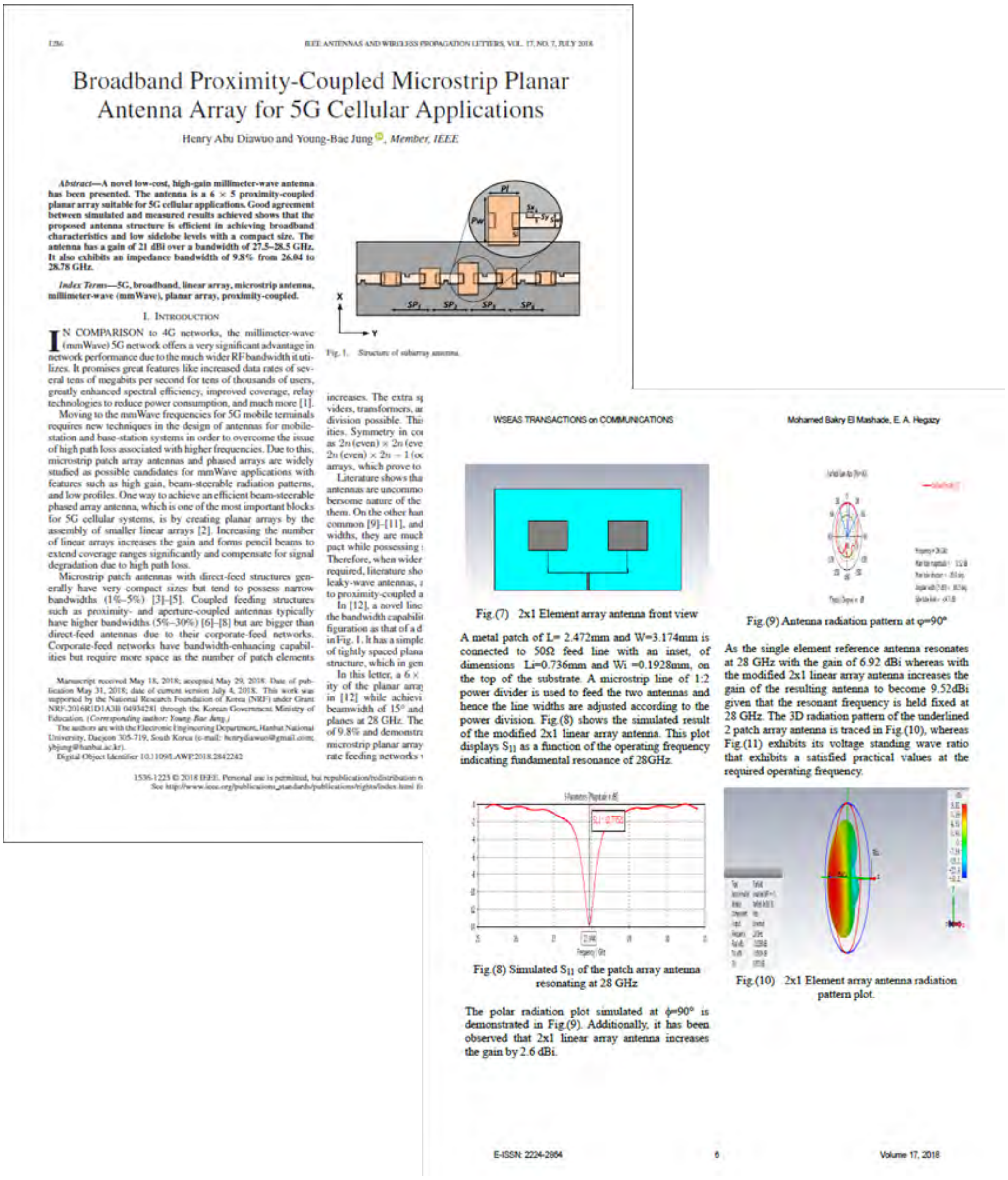

1286 IEEE ANTENNAS AND WIRELESS PROPAGATION LETTERS, VOL. 17, NO. 7, JULY 2018

Broadband Proximity-Coupled Microstrip Planar Antenna Array for 5G Cellular Applications

Henry Abu Diawuo and Young-Bae Jung, *Member, IEEE*

***Abstract*—A novel low-cost, high-gain millimeter-wave antenna has been presented. The antenna is a 6 × 5 proximity-coupled planar array suitable for 5G cellular applications. Good agreement between simulated and measured results achieved shows that the proposed antenna structure is efficient in achieving broadband characteristics and low sidelobe levels with a compact size. The antenna has a gain of 21 dBi over a bandwidth of 27.5–28.5 GHz. It also exhibits an impedance bandwidth of 9.8% from 26.04 to 28.78 GHz.**

***Index Terms*—5G, broadband, linear array, microstrip antenna, millimeter-wave (mmWave), planar array, proximity-coupled.**

I. Introduction

IN COMPARISON to 4G networks, the millimeter-wave (mmWave) 5G network offers a very significant advantage in network performance due to the much wider RF bandwidth it utilizes. It promises great features like increased data rates of several tens of megabits per second for tens of thousands of users, greatly enhanced spectral efficiency, improved coverage, relay technologies to reduce power consumption, and much more [1].

Moving to the mmWave frequencies for 5G mobile terminals requires new techniques in the design of antennas for mobile-station and base-station systems in order to overcome the issue of high path loss associated with higher frequencies. Due to this, microstrip patch array antennas and phased arrays are widely studied as possible candidates for mmWave applications with features such as high gain, beam-steerable radiation patterns, and low profiles. One way to achieve an efficient beam-steerable phased array antenna, which is one of the most important blocks for 5G cellular systems, is by creating planar arrays by the assembly of smaller linear arrays [2]. Increasing the number of linear arrays increases the gain and forms pencil beams to extend coverage ranges significantly and compensate for signal degradation due to high path loss.

Microstrip patch antennas with direct-feed structures generally have very compact sizes but tend to possess narrow bandwidths (1%–5%) [3]–[5]. Coupled feeding structures such as proximity- and aperture-coupled antennas typically have higher bandwidths (5%–30%) [6]–[8] but are bigger than direct-feed antennas due to their corporate-feed networks. Corporate-feed networks have bandwidth-enhancing capabilities but require more space as the number of patch elements

Manuscript received May 18, 2018; accepted May 29, 2018. Date of publication May 31, 2018; date of current version July 4, 2018. This work was supported by the National Research Foundation of Korea (NRF) under Grant NRF-2016R1D1A3B 04934281 through the Korean Government Ministry of Education. (*Corresponding author: Young-Bae Jung.*)

The authors are with the Electronic Engineering Department, Hanbat National University, Daejeon 305-719, South Korea (e-mail: henrydiawuo@gmail.com; ybjung@hanbat.ac.kr).

Digital Object Identifier 10.1109/LAWP.2018.2842242

Fig. 1. Structure of subarray antenna.

WSEAS TRANSACTIONS on COMMUNICATIONS — Mohamed Bakry El Mashade, E. A. Hegazy

Fig.(7) 2x1 Element array antenna front view

A metal patch of L= 2.472mm and W=3.174mm is connected to 50Ω feed line with an inset, of dimensions Li=0.736mm and Wi =0.1928mm, on the top of the substrate. A microstrip line of 1:2 power divider is used to feed the two antennas and hence the line widths are adjusted according to the power division. Fig.(8) shows the simulated result of the modified 2x1 linear array antenna. This plot displays S_{11} as a function of the operating frequency indicating fundamental resonance of 28GHz.

Fig.(8) Simulated S_{11} of the patch array antenna resonating at 28 GHz

The polar radiation plot simulated at ϕ=90° is demonstrated in Fig.(9). Additionally, it has been observed that 2x1 linear array antenna increases the gain by 2.6 dBi.

Fig.(9) Antenna radiation pattern at φ=90°

As the single element reference antenna resonates at 28 GHz with the gain of 6.92 dBi whereas with the modified 2x1 linear array antenna increases the gain of the resulting antenna to become 9.52dBi given that the resonant frequency is held fixed at 28 GHz. The 3D radiation pattern of the underlined 2 patch array antenna is traced in Fig.(10), whereas Fig.(11) exhibits its voltage standing wave ratio that exhibits a satisfied practical values at the required operating frequency.

Fig.(10) 2x1 Element array antenna radiation pattern plot.

E-ISSN: 2224-2864 6 Volume 17, 2018

3.1 Introduction

Along this section, a series of scientific papers are revised and discussed in order to analyze the state of the art in the field of Antenna Arrays for 5G Technology.

As exposed along section 1.3, 5G is intended to be fully deployed around mid-2020. To achieve this challenging deadline, research and development is essential to be ready from radiofrequency side, providing antenna solutions capable to perform as expected and as the million applications will demand.

From this analysis, it will be extracted how the current market products are designed and performing. It is important to have a clear view of the timings and expects we should have from this upcoming technology.

Finally, some conclusions about the prior art are extracted in order to set the path to follow for next experiments.

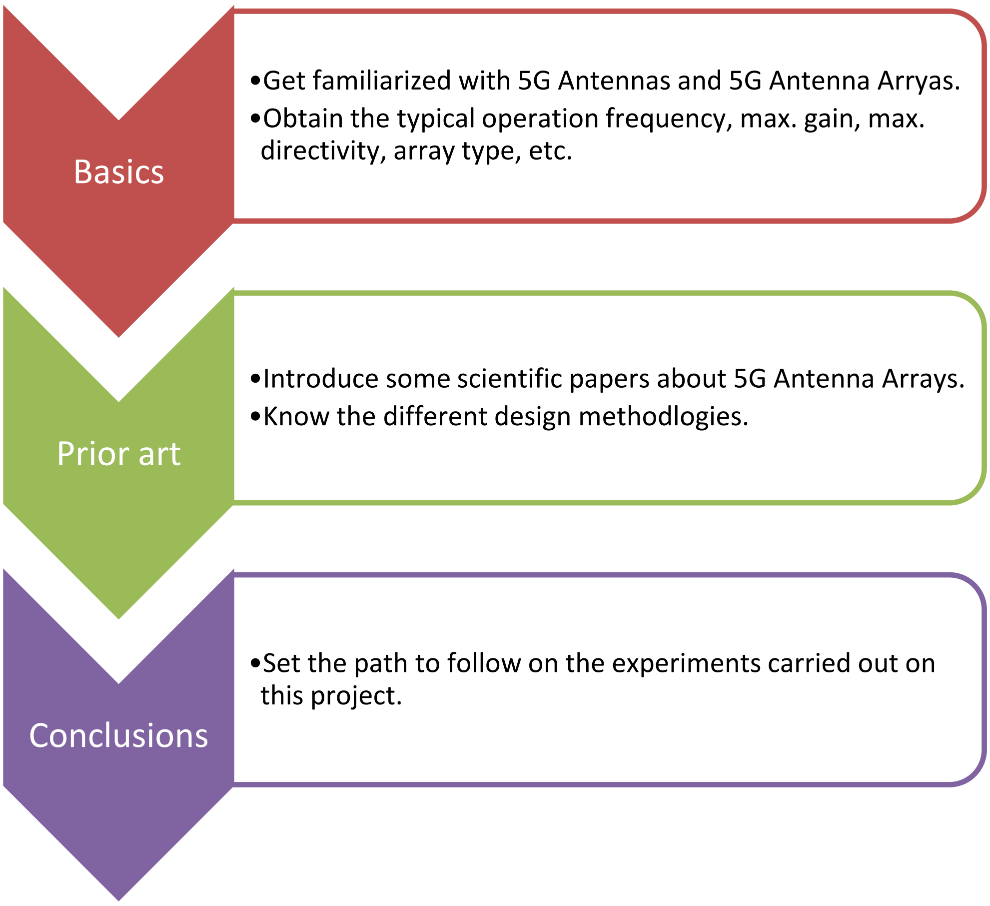

3.2 Review of Prior Art

During this section, some scientific papers will be presented and analyzed in order to get familiarized with the current products present on the market and what has been done in terms of investigation regarding 5G Antenna Arrays.

3.2.1 8x8 Phased Series Fed Patch Antenna Array at 28GHz for 5G Mobile Base Station Antennas

Along this article [18] , is presented a 64 element, 8x8 phased series fed patch antenna array, operating at 28GHz frequency. The phased array steers its beam along the horizontal axis to provide the coverage to the users in different directions. The series fed array is designed to mix standing wave and travelling wave behavior, where the initial seven elements show a standing wave and the eight element shows a travelling wave behavior.

It is arranged an 8x8-element series fed array to form an 8x8 patch array with vertical inter-element spacing of d=λ/2=3.54mm.

Parameter	Value (mm)
W_p	3.539
W_C	0.494
L_C	3.539
W_m	2.727
L_m	0.6269
W_f	0.72

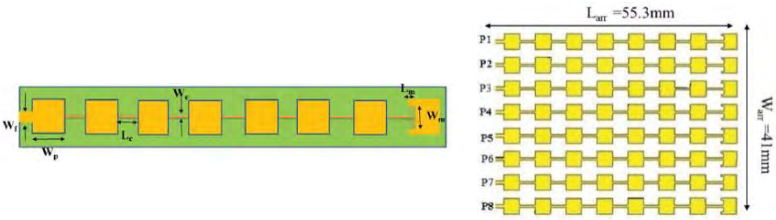

Figure 17. 8x8 Series-fed patch array

The simulated results of the 8x8 array are:

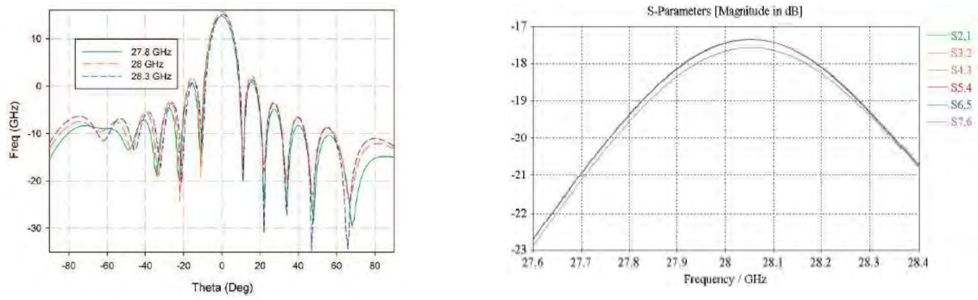

Figure 18. 8x8 Series-fed patch array Radiation Pattern and Mutual Coupling (below -15dB)

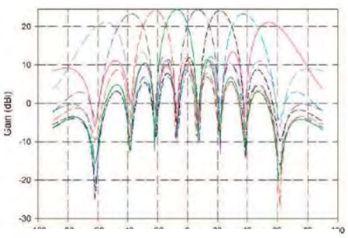

Figure 19. Multibeam Radiation Pattern in H-Plane.

The array is operating from 27.9GHz-28.4GHz with a 500MHz impedance bandwidth. The gain of the array is 24.25dBi, with a suppression of the side lobes of -14dB. The beam steering is performed obtaining eight beam steering angles: ±55°, ±37°, ±22°, ±15°, ±7.5°; which shows a stable side lobe level.

3.2.2 A Compact Millimeter-Wave Slot Antenna Array for 5G Standards

In this paper [19] , a millimeter wave (mmW) two-dimensional slot antenna array, operating at 28GHz, is designed.

The antenna array consists of 8 elements in a 2x4 configuration. A 1-to-4 power divider is feeding the 2x4 slot antenna array in both schemes; parallel and series. This power divider is constructed by microstrip lines, operated at 28GHz and implemented on an RO3003 substrate (εr = 3) of thickness 0.13mm, the realized line widths were found to be 0.35mm and 0.18mm corresponding to 50Ω and 70.7Ω. After integrating and optimizing the slot antenna array with the feed network to operate at the desired frequency, the slot length and width are found to be 3.15mm and 0.45mm, respectively.

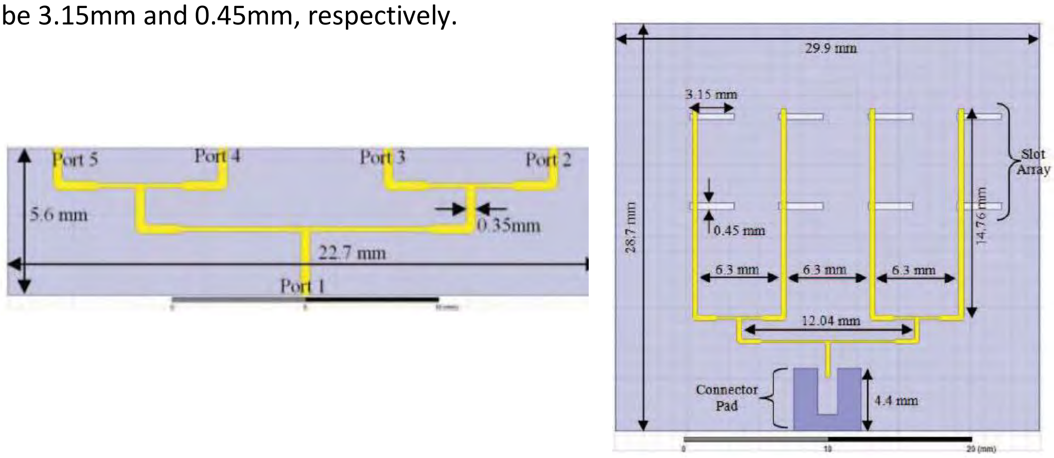

Figure 20. Power divider configuration and Complete System configuration.

The 2x4 slot antenna array alone has a resonance centered at 28.1GHz with -10dB BW of 950MHz, while the complete integrated system is resonating at 28.2GHz and the -10dB BW is 1.38GHz. The antenna system provides a maximum gain of 9dB directed towards 0 and 180 from the z-axis.

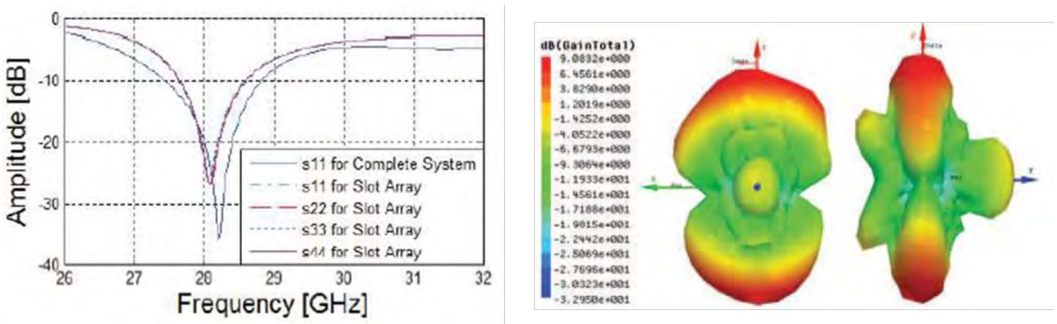

Figure 21. Reflection Coefficients and 3D Gain Pattern for the slot antenna array.

Such a design can be very attractive to be integrated in future mobile terminals for short range 5G communications.

3.2.3 A High Gain Steerable Millimeter-Wave Antenna Array for 5G Smartphone Applications

During this paper [20] , a phased array antenna is designed at mm-W frequency bands for future 5G based smartphone applications. The proposed antenna is a slot-PIFA antenna made on a low cost FR4 board. The 8-element antenna array is located at the bottom edge of the mobile phone chassis (130mm x 74mm). A standard low cost FR4 epoxy of a relative dielectric constant 4.4 and loss tangent 0.25 is used as the substrate for PCB. The proposed antenna is a simple elliptical PIFA with an open slot on the system ground plane.

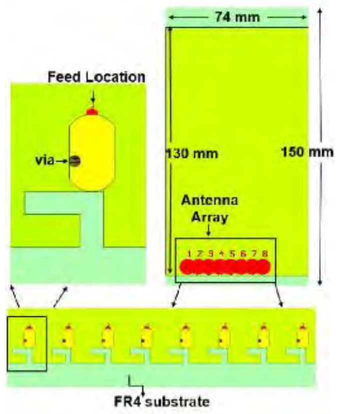

Figure 22. Proposed antenna design and array location in mobile phone.

The proposed antenna is arranged as an 8-element array with a separation of λ/2 between each element to ensure good isolation between the antenna elements and minimize the grating lobes.

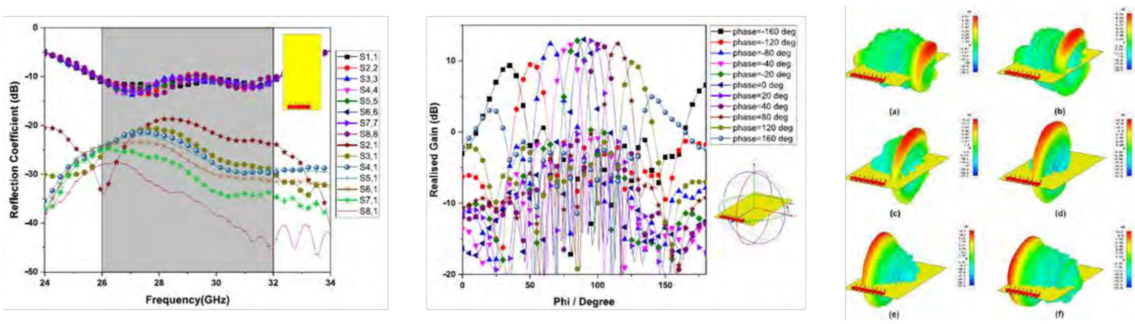

Figure 23. Reflection Coefficient, Realized Gain for scanned pattern in the Phi-plane and Simulated scanned pattern for proposed antenna at various tilt (-60°, -45°,-30°, 0°, 15°,45°).

The antenna array covers a frequency range of 26-32GHz with a 6GHz -10dB bandwidth. The antenna exhibits a very good radiation pattern when integrate with the mobile phone chassis. The maximum gain is around 13dBi. The pattern can be steered by varying the phase shift at each antenna element. The steered pattern in the Phi-plane shows a gain of 10dBi maintained for about 60°.

3.2.4 A Multiband Millimeter-Wave 2-D Array Based on Enhanced Franklin Antenna for 5G Wireless Systems

Along this paper [21] , is presented a novel and compact antenna array. The extension of the standard narrowband Franklin linear antenna array in a compact two-dimensional assembly is proposed and multiband response is accomplished in this work which fulfils demands of future 5G systems. The proposed 2D antenna arrays is designed to operate at licensed frequency bands of 28GHz and 37GHz-39Gz.

Antenna design is initiated by altering the parameters of array geometry with the objective of extending the concept of the Franklin array in order to generate multiple frequency bands, rather than a single resonant frequency. The antenna solution is composed of a series of radiating patches and folded-dipole-like antennas, where the resonant frequency is controlled by the radiating length of the stubs.

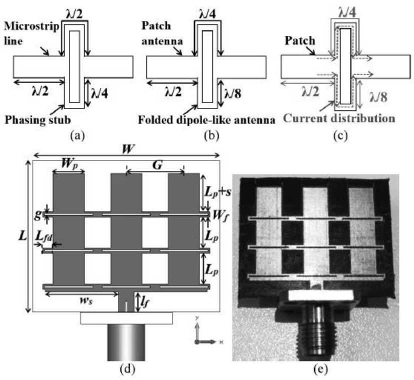

Symbol	Parameters	(mm)
L_p	Length of patch	4.3
W_p	Width of patch	4.34
s	Extended length of terminating patches	1.0
G	Gap between centres of two parallel patches	8.0
L_{fd}	Length of folded-dipole	1.4
W_f	Width of folded-dipole	0.7
w_s	Width of matching stub	10.15
l_f	Length of feed	2.8
g	Gap of folded-dipole	0.26
L	Length of array prototype	21.0
W	Width of array prototype	26.0

Figure 24. Proposed 2D antenna array: (a) Franklin array unit-cell; (b) array unit-cell; (c) array current distribution; (d) simulated prototype with te optimized dimensions; (e) fabricated antenna prototype.

The results obtained are:

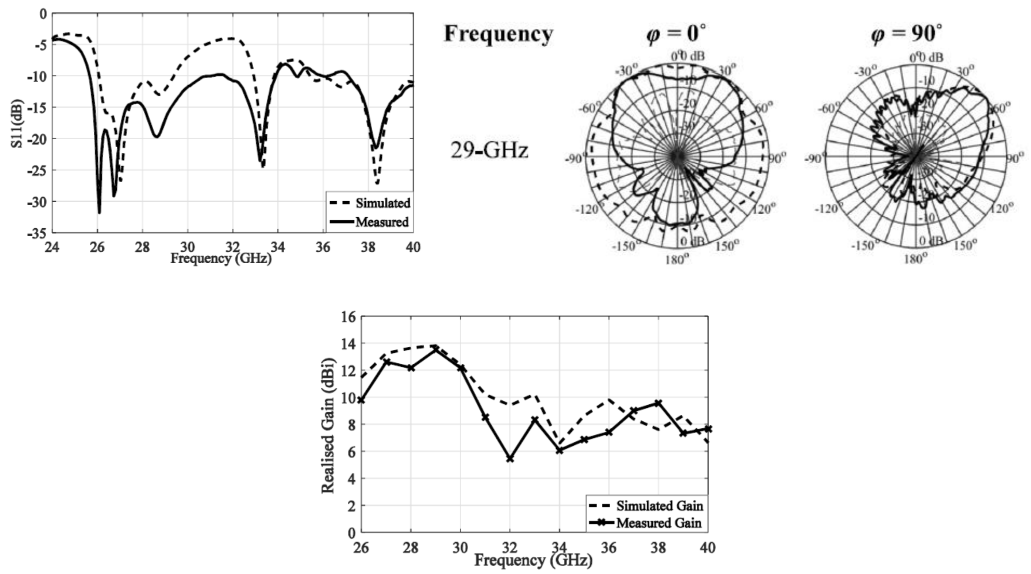

Figure 25. Reflection Coefficient, Radiation Pattern and Realised Gain for the complete system

3.2.5 A Switchable 3-D-Coverage-Phased Array Antenna Package for 5G Mobile Terminals

In this paper [22] , is proposed a new design of a mmW array antenna package with beam steering characteristic for the 5G mobile applications. Three identical subarrays of patch antennas have been compactly arranged along the edge region of the mobile phone PC to form the antenna package. By switching the feeding to one of the sub arrays, the desired direction of coverage can be achieved.

The proposed antenna package can operate either in diversity or MIMO mode at 21-22GHz:

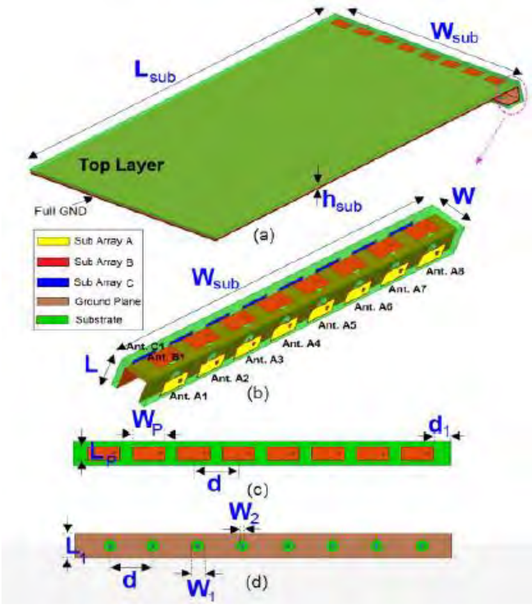

Parameter	W_{sub}	L_{sub}	h_{sub}	W_P	L_P	d
Value (mm)	55	110	0.787	4.32	2	6.5
Parameter	d_1	W	L	W_1	L_1	W_2
Value (mm)	4.5	4.574	3.787	1.72	3	0.5

Figure 26. Proposed design of three identical sub arrays of patch antennas operating at 5G frequencies.

The results obtained on the analysis of the antenna package are shown below for each sub-array:

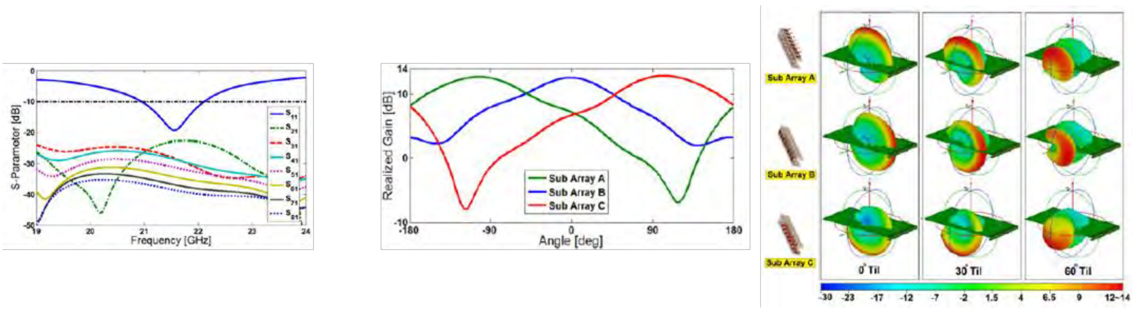

Figure 27. Reflection Coefficient, Realized Gain and Radiation Pattern for each sub-array

The proposed design has >10dB gain in the upper spherical space, good directivity and efficiency, which is suitable for 5G mobile communications. Consisting of three sub arrays, each sub array is steerable in the scan range of ±90°.

3.2.6 Broadband Proximity-Coupled Microstrip Planar Antenna Array for 5G Cellular Applications

During this paper [23] , a novel low-cost, high-gain millimeter-wave antenna is presented. The antenna is a 6x5 proximity coupled planar array and has a bandwidth of 9.8% and demonstrates a way of forming proximity-coupled microstrip planar arrays without the use of cumbersome corporate feeding networks with the ability to easily form any planar suitable for 5G mobile applications.

The antenna operates from 27.5 to 28.5 GHz with a center frequency of 28 GHz and is constructed from two stacked Taconic TLY-5 substrates (εr = 2.2) with thicknesses of 0.508mm each. A 50 Ω microstrip line on the lower substrate feeds the resonant microstrip patch elements on the upper substrate with spacings of SP1 to SP4.

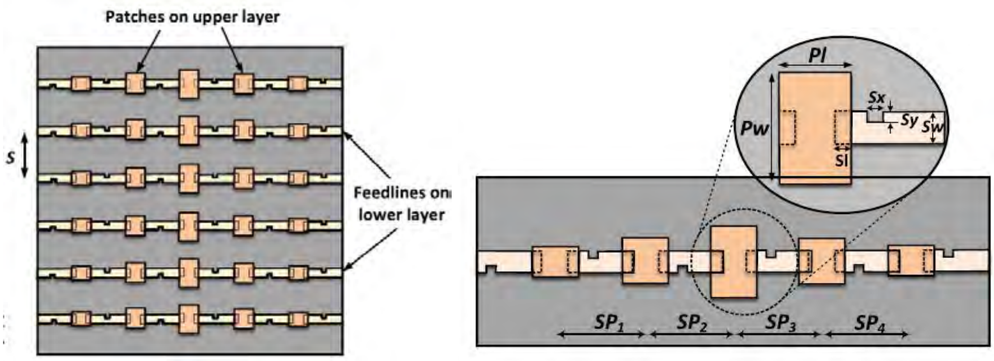

Figure 28. Proximity-Coupled Microstrip Planar Antenna design.

The antenna has a gain of 21dBi over a -10dB bandwidth 27GHz-28.5GHz.

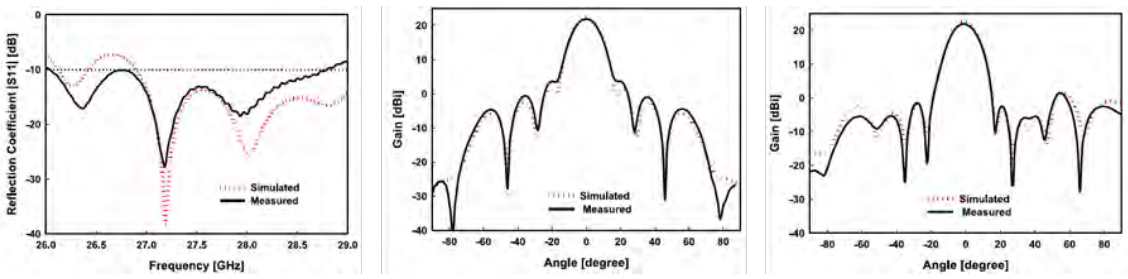

Figure 29. Reflection Coefficient, H-Plane radiation pattern and E-Plane radiation pattern.

The proposed 6 × 5 array has a gain of 21.86 dBi in its H-plane and 21.95 dBi in its E-plane at 28GHz with an impedance bandwidth of 9.8%. The stability of the structure is illustrated by the similarities in the simulated and measured results, making it very suitable for integration in 5G applications.

3.2.7 Design and Analysis of 28GHz Rectangular Microstrip

Along this paper [24] , is presented the design of four elements 28GHz microstrip patch array antenna for future 5G mobile phone applications. The designed antenna can be implemented using low cost FR-4 substrates and can maintain good performance in terms of gain and efficiency.

The 4-element rectangular microstrip patch array is formed by 4 microstrip patch antennas with substrate height of 0.1mm, dielectric constant of 4.35 and a negligible tangent loss was employed. A metal patch of length (L=2.503mm) and width (W=3.215mm) was connected to 50Ω feed line with an inset on the top of the substrate. The dimensions of inset feed were Li=2.896mm and Wi=0.1928mm.

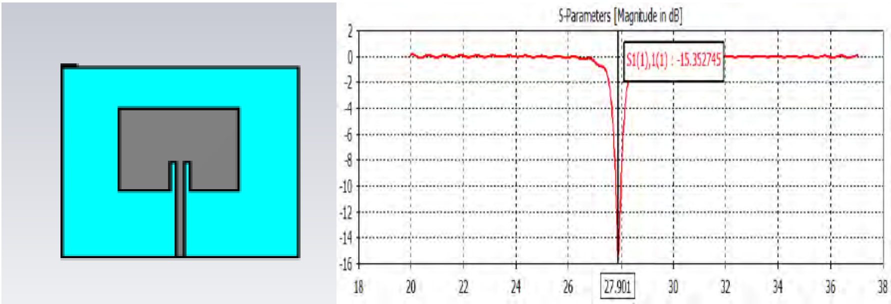

Figure 30. 28GHz Microstrip Patch Antenna design and Reflection Coefficient

The 4-element array is formed using power dividers and it is outlined in the figure below. The Table summarizes the geometry dimensions of the suggested 4x1 element array microstrip patch antenna.

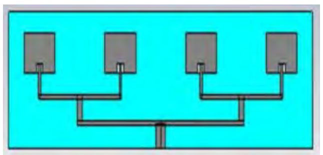

Parameters	L	W	εr	substrate Height	Fi	ground length	ground width
mm	2.303	3.215	4.35	0.5	0.5556	7.07	31.677

Figure 31. 4-element Microstrip Patch antenna array and its parameters

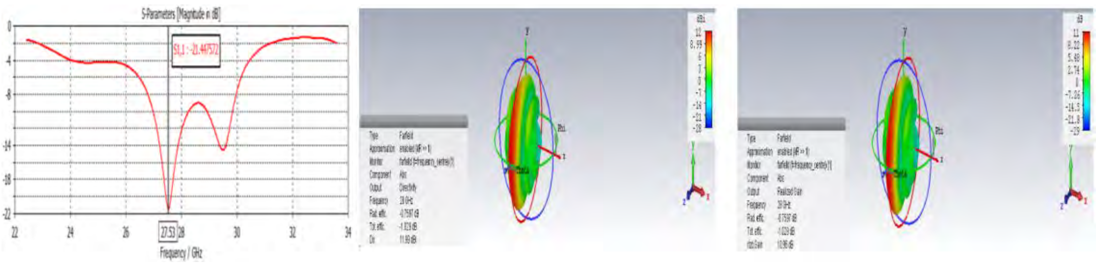

From the simulation results, it has been observed that 4x1 linear array resonates at 28 GHz with a gain of 11.2 dBi. Its performance regarding the Reflection Coefficient, it resonates at 28GHz at -14dB and with a -10dB bandwidth between 27GHz and 28.5GHz.

3.2.8 Design of Efficient Microstrip Linear Antenna Array for 5G Communications Systems

During this paper [25] , is presented a design of an efficient microstrip antenna array for 5G communication systems. The single element has gap-coupled feeder and the antenna is designed on low-loss Teflon based RT/Duroid 5880 substrate with dielectric constant 2.2 and substrate thickness of 0.381mm. Below is presented the design, where Lp = 3.27mm, Wp = 4.343mm and feeder width is 1.187mm (50Ω).

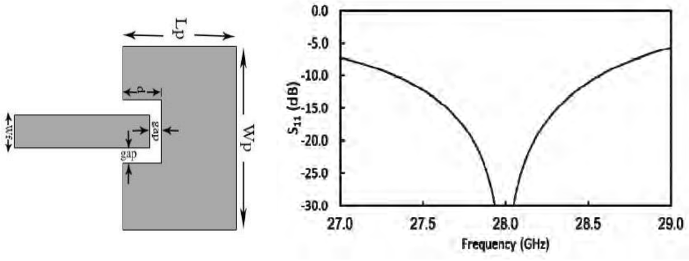

Figure 32. Single element design

The antenna operates at 28GHz and it is formed of 16 elements of rectangular patches arranged in a linear configuration. A defected ground structure (DGS) in the form of rectangular slots is employed in the array design to reduce the mutual coupling between adjacent elements.

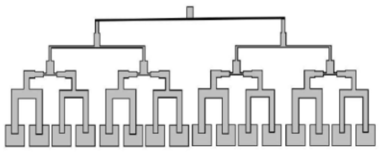

Figure 33. 16-element microstrip patch antenna array.

The 16-element array has a 10dB bandwidth of 2GHz and a maximum gain of 17.4dBi at 28.4GHz.

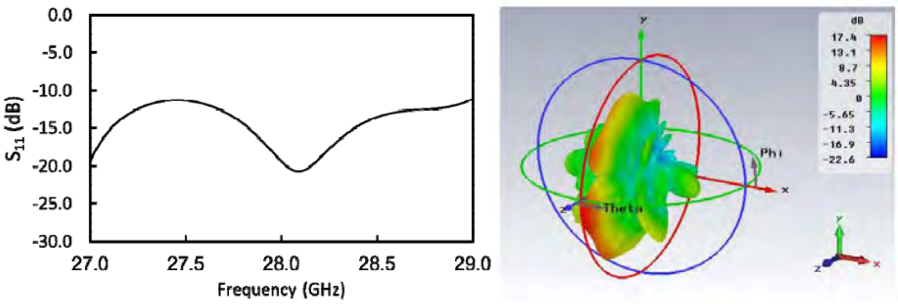

Figure 34. 16-element Reflection Coefficient and Realised Gain

The performance of the proposed antenna satisfies the requirements of 5G communications systems in terms of high gain, high radiation efficiency and adequate bandwidth.

3.2.9 Design of Phased Arrays of Series-Fed Patch Antennas with Reduced Number of Controllers for 28-GHz mm-W Applications

Along this paper [26] , a new modified 2x2 and 3x3 series-fed patch antenna arrays with beam steering capability are designed. In the designs, the patches are connected to each other continuously and in symmetric 2-dimensional format using the high impedance microstrip lines.

In this work, a low thickness Rogers RT/Duroid 5880 substrate with dielectric constant 2.2, height 0.25mm and loss tangent 0.001 is used in the designs. The proposed cell is employed to design the 2x2 and 3x3 series-fed array:

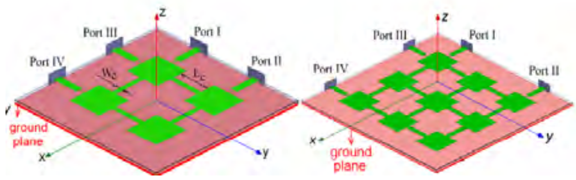

Figure 35. 2x2 and 3x3 series-fed arrays

The arrays will have maximum gain and good matching at $\theta = \varphi = 0^{\circ}$. The S-Param of the optimized arrays are presented below that show a good matchin around 28GHz and 820MHz 10dB bandwidth.

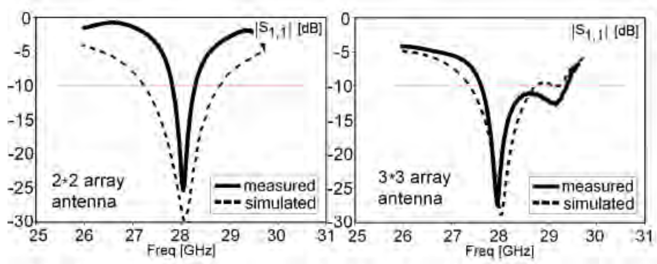

Figure 36. S-Parameters of the 2x2 and 3x3 series-fed arrays.

In the first design, 3-dimensional beam scanning range of ±25° and good radiation and impedance characteristics were attained by using only one phase shifter. In the second one, good scanning performance of a range of ±20°, acceptable side lobe level and gain of 15.6 dB are obtained.

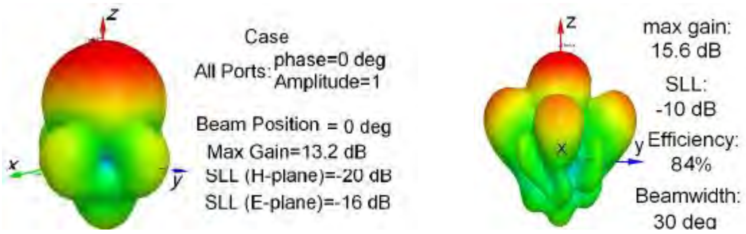

Figure 37. Radiation Pattern of 2x2 and 3x3 series-fed array respectively.

3.2.10 Directive Antennas for Future 5G Mobile Wireless Communications

In this paper [27] , several gain enhancement techniques for a single directive antenna for 5G mobile communications including antenna arrays, metallic horn, dielectric horn, superstrate, homogenous hemisphere lens and convex hyperbolic lens are presented.

The single element antenna configuration and geometry is presented below. The elliptical patch is printed on a low permittivity (dielectric constant 2.2) grounded substrate with a 0.254mm thick and fed by a 50Ω microstrip line on the backside of a second thin dielectric layer with a higher permittivity (dielectric constant 10.2) and 0.254mm thick through an elliptical aperture etched in the ground plane with a width nearly equals to half wave length of the centre frequency 28GHz.

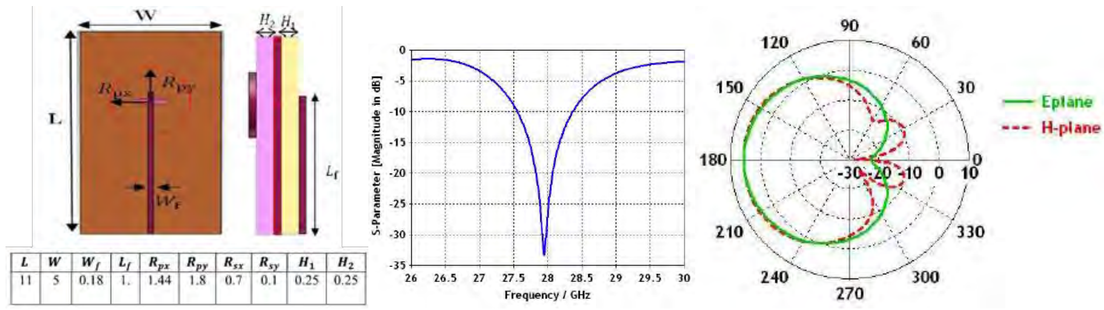

Figure 38. Single element design and results.

Different gain enhancement techniques are studied. Here it is presented the series-fed array technique. The spacing among radiation elements is optimized at 28GHz to decreases the side lobe level. This type antenna array does not affect the bandwidth, on the contrary to the traditional antenna arrays.

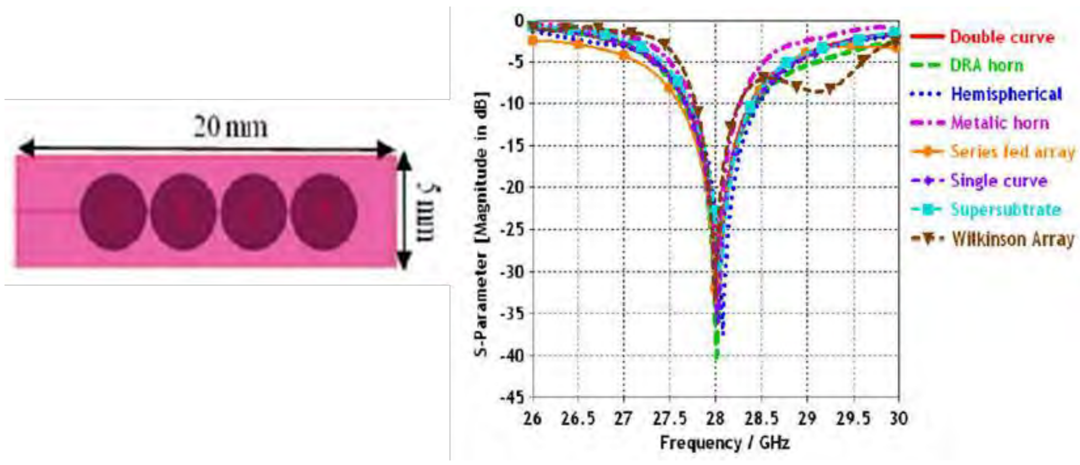

Figure 39. Series-fed array design and simulated results of the different gain enhancement techniques.

A single directive antenna for the future 5G mobile networks has been presented. A realized gain of more than 10dB with small side lobe level has been achieved.

3.2.11 Exposure to RF EMF from Array Antennas in 5G Mobile

Along this paper [28] , radio-frequency electromagnetic field (RF EMF) exposure evaluations are conducted in the frequency range 10GHz – 60GHz for array antennas intended for user equipment (UE) and low-power radio base stations in 5G mobile communication systems. A systematic study based on numerical power density simulations considering effects of frequency, array size, array topology, distance to exposed part of human body, and beam steering range is presented whereby the maximum transmitted power to comply with RF EMF exposure limits specified by the International Commission on Non-Ionizing Radiation Protection (ICNIRP), the US Federal Communications Commission (FCC) and the Institute of Electrical and Electronics Engineers (IEEE) is determined.

To analyze these limits, it is intended to simulate an antenna configuration:

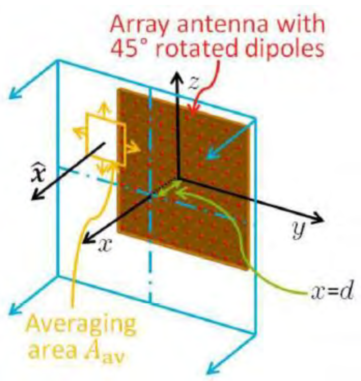

Figure 40. Square-shaped array antenna and definition of area over which the power density is averaged.

It is studied the RF EMF exposure limits and limits on maximum equivalent isotropically radiated power (EIRP) and the Power density and maximum transmitted power allowed for the different regions:

	f (GHz)	Array area (cm^2) 2 × 2 – 10 × 10 elements	Maximum transmitted power (dBm)			Maximum EIRP (dBm)		
			ICNIRP	FCC	IEEE	ICNIRP	FCC	IEEE
Portable[1] applications (d = 0.5 cm)	10	9.0 – 230	13 – 20	7 – 18	16 – 28	24 – 45	18 – 43	27 – 53
	20	2.3 – 56	13 – 16	2 – 13	12 – 24	24 – 41	13 – 38	23 – 49
	30	1.0 – 25	13 – 14	1 – 10	11 – 20	24 – 39	12 – 35	22 – 45
	40	0.56 – 14	13	1 – 8	9 – 20	24 – 38	12 – 33	20 – 45
	50	0.36 – 9.0	13	1 – 6	9 – 18	24 – 38	12 – 31	20 – 43
Mobile[2] applications (d = 20 cm)	10	9.0 – 230	20 – 26	18 – 26	27 – 31	37 – 45	37 – 43	42 – 53
	20	2.3 – 56	16 – 26	14 – 26	24 – 28	37 – 41	37 – 39	39 – 49
	30	1.0 – 25	16 – 26	13 – 26	21 – 27	37 – 41	37 – 38	38 – 46
	40	0.56 – 14	15 – 26	13 – 26	21 – 27	37 – 40	37 – 38	38 – 46
	50	0.36 – 9.0	15 – 26	13 – 26	21 – 27	37 – 40	37 – 38	38 – 46

[1] FCC terminology used to denote devices intended to be used at a distance of less than 20 cm from the human body.
[2] FCC terminology used to denote devices intended to be used at a distance of 20 cm or more from the human body.

Table 1. Summary of maximum transmitted power and maximum EIRP to comply with the ICNIRP [7], FCC [8,9,19] and IEEE [10,11] RF EMF exposure limits.

For mobile devices very similar results are obtained for the FCC and ICNIRP limits as the difference between the spatially averaged power density over 1 cm^2 and 20 cm^2 is small in a large part of the parameter space where far-field conditions apply.

3.2.12 Handheld Beamforming Antennas Adoptable to 5G Wireless Connectivity

Along this paper [29] , is presented the design of high-frequency handheld beamforming antennas for 5G mobile applications. A proposed 4-element antenna array resonating at 24GHz fits the placement in the top side of a handset phone.

The radiating elements are microstrip patches designed to resonate at 24GHz with 29.4mm, 8mm, 3.3mm, 3.2mm and 2.2mm as W, L, D, Wpatch, Lpatch respectively. This array antenna is fed by the feed network whose multi-port blocks can be configured out by an optimization process to scan the beam over the 120°-range in the broadside.

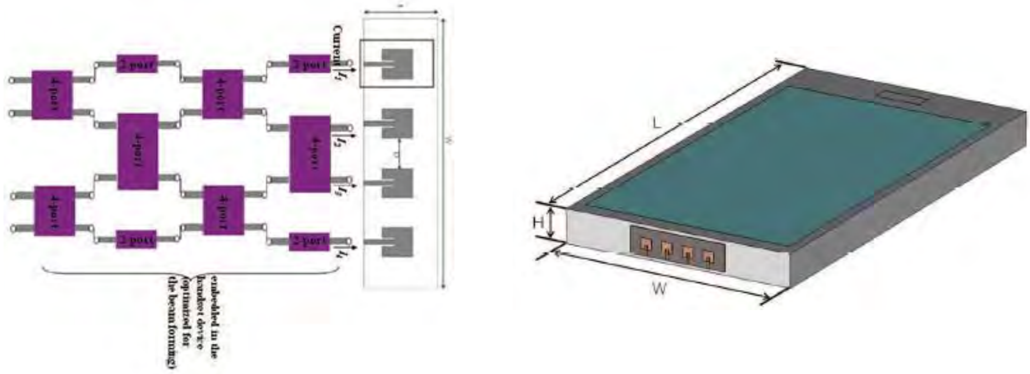

Figure 41. 4-element antenna array configuration.

The proposed 4-element antenna array scans the upward 120°-range in the elevation plane with the movable main-beam of the antenna efficiency over 70% and the peak-gain greater than 8dBi up to 10.5dBi at the target mmW frequency.

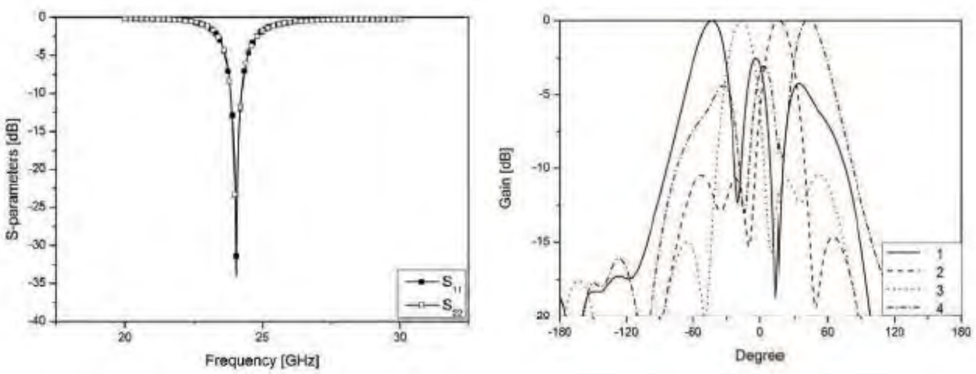

Figure 42. 4-element antenna array Return Loss and Far-field patterns of the movable beam.

A small beamforming antenna for the handset phone was designed with a feed network adapted to be optimized feeding scheme. The proper antenna performance is demonstrated, so it is a suitable solution for 5G mobile communications.

3.2.13 Optically Upconverted, Spatially Coherent Phased-Array-Antenna Feed Networks for Beam-Space MIMO in 5G Cellular

During this paper [30] , it is presented a new approach to realizing extreme spatial discrimination based on optically upconverted, spatially coherent phased-array feed networks. The details of its approach, presented herein, include the design and initial demonstration of both transmit (Tx) and receive (Rx) array systems that are used in tandem to form a down-/up-link for the purpose of characterizing both array and link performance. Design parameters and initial link characterization results are presented.

It is proposed an alternative Beam-Forming concept for RX and TX, relying on optical up conversion of RF signals in a spatially coherent phase-array antenna to enable analog beam forming in a planar/conformal array form factor.

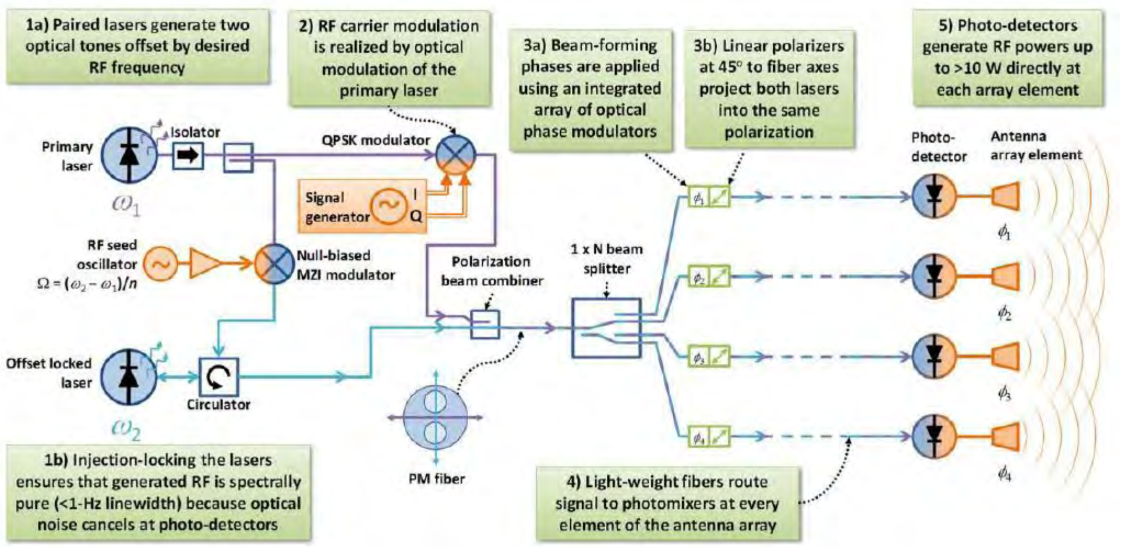

Figure 43. Schematic layout of an optically fed phased-array antenna network for analog beam forming on a Tx array.

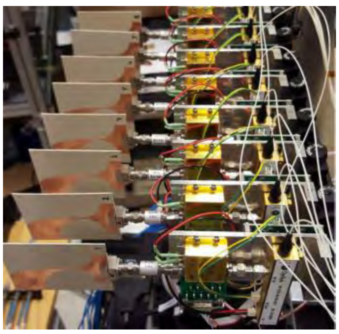

Figure 44. Photograph of the 1 × 8 imaging receiver system's RF front end.

A unique aspect of this paper was in the system-level integration of Tx and Rx optical processors that consists of eight channels for application in the realization of beam space MIMO up-/down-link demonstration. In this paper, we demonstrated data rates up to 200 Mbps in data transmission with an SNR commensurate with error-free transmission. Finally, the developed transmitting phased array and the imaging receiver Rx array antenna have been demonstrated in conjunction to show an end-to-end system demonstration, where microwave communications signals have been generated, steered, received, down converted, and recovered using photonic techniques.

3.2.14 Stacked Patch Antenna with Dual-Polarization and Low Mutual Coupling for Massive MIMO

In this paper [31] , it is presented a dual-polarized antenna array with 144 ports for Massive MIMO operating at 3.7GHz.

The proposed array consists of 18 low profile subarrays, and each subarray consists of four single units. Each single antenna consists of one vertically polarized port and one horizontally polarized port connected to power splitters, which serve as a feeding network. The design and configuration of each subarray is:

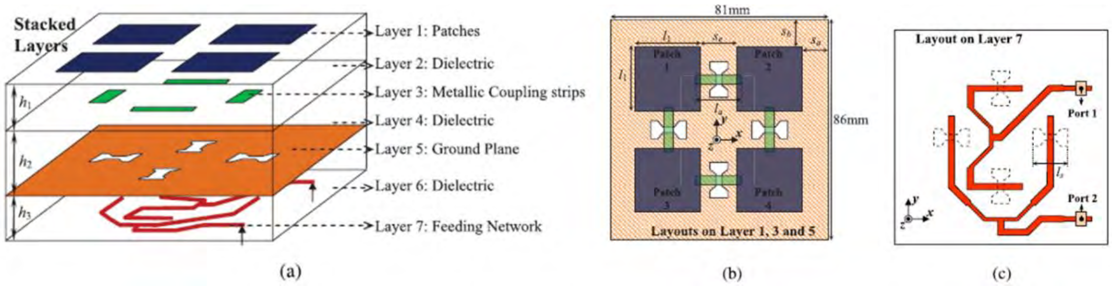

Figure 45. Structure of the proposed antenna unit. (a) Prospective view. (b) Layouts on Layers 1, 3, and 5. (c) Layout on Layer 7. [With h1 = (1/2) h2 = h3 = 0.762, l1 = w1 = 23.7, la = 16.6, se = 13.7, sa = 10.0, and sb = 12.5, all dimensions are in mm.

The proposed Massive MIMO antenna array consists of 18 elements of each subarray presented above providing a gain of 15dBi. The array configuration is based on the Turning Torso building.

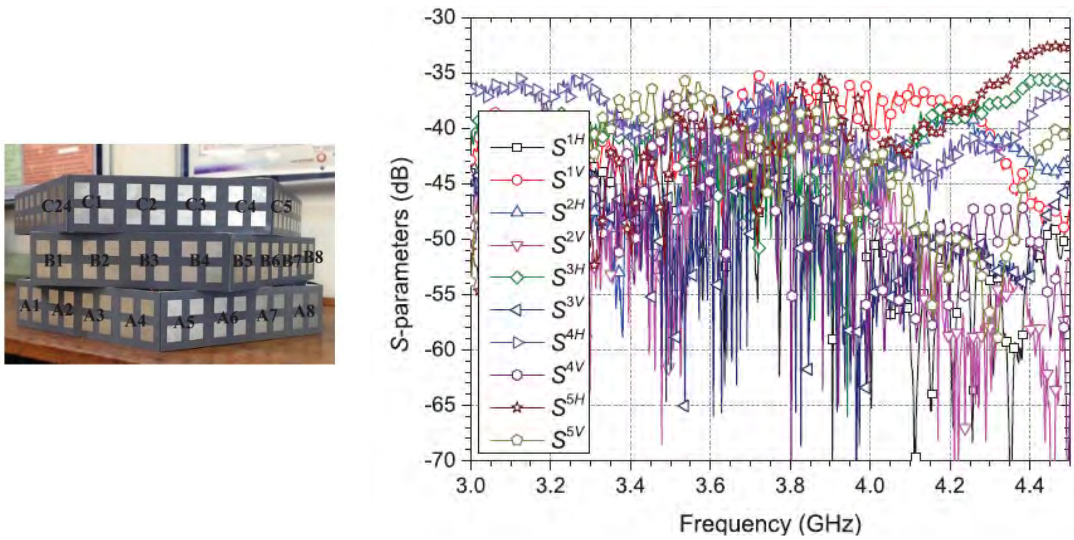

Figure 46. Configuration of three-level Turning Torso antenna array and Mutual coupling levels.

The proposed array could be a strong contender for the small cell base station deployment in the urban area with high-density buildings for 5G wireless systems.

3.2.15 User Effects on the Circular Polarization of 5G Mobile Terminal Antennas

Along this paper [32] , it is studied the effects of the user on a circularly polarized phased array for 5G mobile applications for frequencies around 28GHz. The single element used to construct the array consists of a magnetic dipole and an electric dipole. The proposed phased array includes a total of 8 elements combined into a linear array on the short edge of the ground plane.

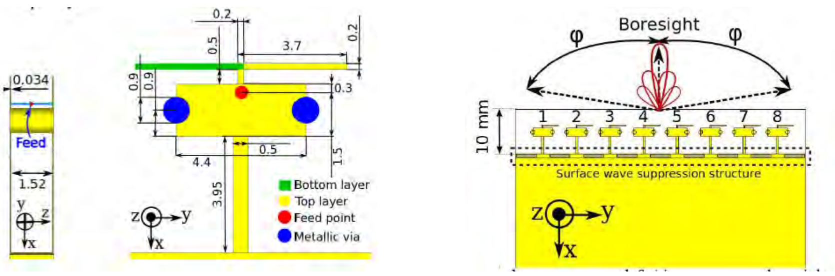

Figure 47. Single element geometry and Proposed phased array.

When user effects are introduced, the Axial Ratio (AR) bandwidth becomes approximately 0.8 to 1.3GHz narrower.

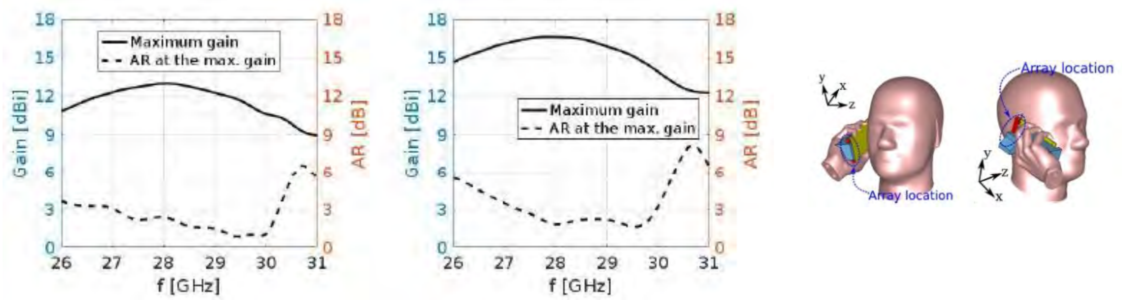

Figure 48. AR and Maximum gain for (a) talk mode-bottom short edge; (b) talk mode-top short edge.

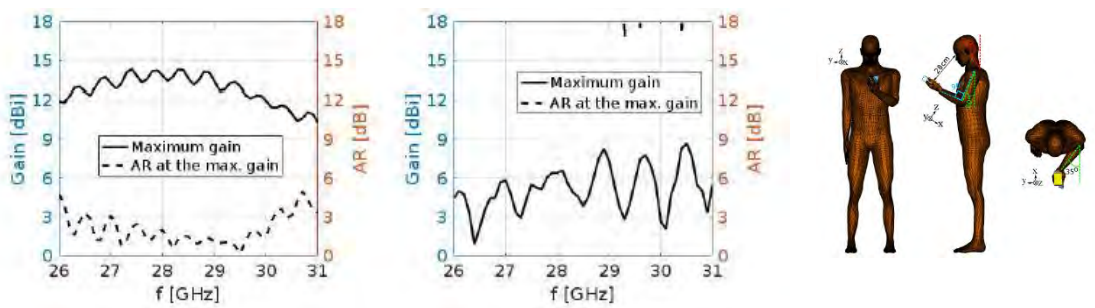

Figure 49. AR and Maximum gain for (a) data mode-bottom short edge; (b) data mode-top short edge

To realize the optimal CP performance and reduce the user effects of the CP coverage efficiency, a CP array at the bottom short edge of the ground plane should be chosen in talk mode, while the top short edge location should be chosen in data mode.

3.3 Conclusions

It has been observed along the previous section, that there are several antenna array configurations to be implemented for the upcoming 5G technology, from an array for Massive MIMO purposes to simple antenna arrays for mobile communications.

In Table 2 below are represented the main and most important characteristics extracted from each paper, in order to have a clear view about what the current solutions in the market are proposing.

	N-Element Antenna Type	fo	Bandwidth -10dB	Location	Boresight Gain	Max. Scan Angle	Array Type	Beam steering
3.3.1	64 Patch Antennas	28GHz	0.5GHz (1.8%)	-	24.3dBi	±55°	2D	Phase shifters
3.3.2	8 Slot Antennas	28GHz	1.4GHz (4.9%)	-	9.0dBi	-	2D	-
3.3.3	8 Slot PIFA Antennas	26GHz-32GHz	6.0GHz (21.4%)	PCB Top Edge	13.0dBi	±60°	Lineal	Phase shifters
3.3.4	9-Enhanced Franklin Antenna	28GHz, 37GHz and 39GHz	6.0GHz (21.4%)	-	12.0dBi	-	2D	-
3.3.5	24 Patch Antennas	21.5GHz	1.0GHz (4.7%)	PCB Top Edge	12.5dBi	±90°	3D	Phase shifters
3.3.6	30 Proximity-Coupled Planar	28GHz	1.5GHz (5.4%)	-	21.0dBi	-	2D	-
3.3.7	4 Patch Antennas	28GHz	1.5GHz (5.4%)	-	11.2dBi	-	Lineal	-
3.3.8	16 Patch Antennas	28GHz	2.0GHz (7.2%)	-	17.4dBi	-	Lineal	-
3.3.9	4-9 Patch Antennas	28GHz	0.8GHz (2.8%)	-	15.6dBi	±25°	2D	Phase shifters
3.3.10	4 Patch Antennas	28GHz	0.8GHz (2.8%)	-	10.7dBi	-	Lineal	-
3.3.11	-	-	-	-	-	-	-	-
3.3.12	4 Patch Antennas	24GHz	-	PCB Top Edge	10.5dBi	±60°	Lineal	Phase shifters
3.3.13	-	-	-	-	-	-	-	-
3.3.14	72 Patch Antennas	3.7GHz	-	-	15.0dBi	-	3D	-
3.3.15	8 Dipole Antennas	28GHz	-	-	16.0dBi	-	2D	-

Table 2. Summary of the Prior Art antenna solution most important characteristics.

From the table above, it can be extracted that the main characteristics used for designing a 5G antenna array solution are:

- **N-elements Antenna type:** 4, 16 or greater – Microstrip Patch Antenna Array.
- **Operating frequency:** 28GHz.
- **-10dB bandwidth:** 0.5GHz (1.8%) to 2GHz (7.2%). Achievable for an antenna array. Not needed to develop sophisticated wideband techniques.
- **PCB Location:** top or bottom short edge.
- **Gain in boresight:** >12.0dBi.
- **Max scan angle:** ±60°.
- **Array type:** Linear or 2D.
- **Beam steering mechanism:** phase shifters.

These characteristics will be used on further sections to design, analyze and provide a suitable solution for the market demands.

4 Analysis & Design of 5G Solutions

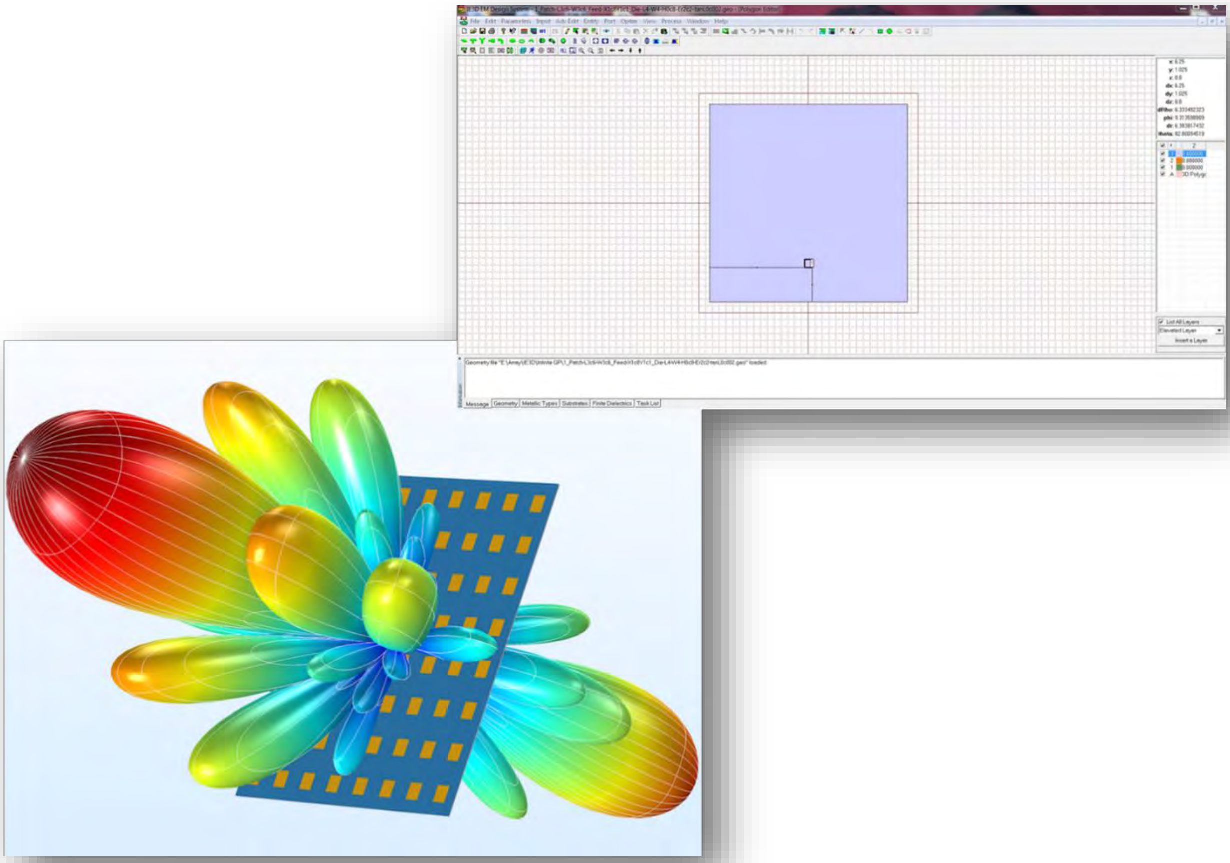

4.1 Introduction

It has been seen so far that plenty of applications will be a reality with the arrival of 5G. Nevertheless, both the hardware and software must reach the technical requirements to allow the correct functionality of every of those applications. Hence, this project is focused on one part of the hardware side: the antenna solution for 5G; one of the most important parts for the technology success.

During previous section 3.2, several types of different antenna arrays already developed for 5G applications have been presented and studied, showing the current solutions present in the market from an antenna point of view. So, at this point, it is time to design and evaluate an antenna array to be implemented for the upcoming 5G technology, beating all the challenges this technology present such as high gain and directivity, high radiation efficiency, small dimensions and beam steering for instance.

Therefore, to accomplish the required 5G Antenna Array solution and the main objective of this project, it is previously analyzed a single element antenna, which will be replicated and grouped to form the final antenna array solution.

4.2 5G Microstrip Patch Antenna

Nowadays, several type of Microstrip Patch antennas are present on the market, but basically, Microstrip Patch antennas can be differentiated by the geometry and the feeding technique.

Nothing is fixed in this sense, lots of geometries and feeding techniques combinations can be used to design a Microstrip Patch antenna for any application. In the particular case presented in this project, a squared geometry and a probe-feed to patch technique have been used to design the 5G Microstrip Patch antenna. The design procedure and considerations are presented from scratch in next point.

Indeed, the objective of this first experiment is to find the correct Microstrip Patch dimensions to resonate at the required 5G frequency obtaining high gain/directivity, with an extend -10dB bandwidth and a highly efficient antenna. The center frequency (f_0) is selected at 28GHz, based on the analysis of the prior art done on section 3.3. Many cases have been analyzed in order to get the best performance for a 5G solution, considering different dimensions and different feeding point's coordinates. However, only the best candidate is selected to be implemented in the final antenna array.

An important point to consider which should not be forgotten is the importance of the Microstrip Patch dimensions; because it will be used to create an antenna array which will be probably placed into a wireless device (such as a smartphone, drone, etc.). Nevertheless, and thanks to the 5G high frequency, in terms of lambda the electrical dimension of the antenna elements is little enough to not be a problem for any future integration.

4.2.1 Design procedure

As exposed above, there are plenty of design combinations to achieve an optimal Microstrip Patch antenna solution for a desired operating frequency; but in this particular case, a square Microstrip Patch antenna is considered.

To be squared, it is needed to set width and length equally (W=L). Antenna theory states that an antenna element provide maximum radiation when its length is equal to $\lambda/2$. Therefore, the desired Microstrip Patch antenna dimensions should be as close as possible to $\lambda/2$, but in this case, considering the substrate dielectric constant.

- $W = L = \frac{\lambda_0}{\sqrt{\varepsilon_r}*2}$

For the case of study presented in this project, it is used a RT/Duroid 5880 substrate material, since its dielectric constant and loss tangent allow an optimal performance on the desired 5G frequency band of 28GHz. From RT/Duroid 5880 datasheet [33] , it can be extracted the following information:

- $\varepsilon_r = 2.2 \ @ \ 28GHz$
- $tan\delta = 0.002 \ @ \ 28GHz$

PROPERTY	TYPICAL VALUES		DIRECTION	UNITS[3]	CONDITION	TEST METHOD
	RT/duroid 5870	RT/duroid 5880				
[1]Dielectric Constant, ε_r Process	2.33 2.33 ± 0.02 spec.	2.20 2.20 ± 0.02 spec.	Z Z	N/A	C24/23/50 C24/23/50	1 MHz IPC-TM-650 2.5.5.3 10 GHz IPC-TM 2.5.5.5
[4]Dielectric Constant, ε_r Design	2.33	2.20	Z	N/A	8 GHz - 40 GHz	Differential Phase Length Method
Dissipation Factor, tan δ	0.0005 0.0012	0.0004 0.0009	Z Z	N/A	C24/23/50 C24/23/50	1 MHz IPC-TM-650, 2.5.5.3 10 GHz IPC-TM-2.5.5.5

Figure 50. RT/Duroid 5880 Datasheet - Dielectric Constant.

Consequently, once established the design requirements in terms of dimensions and substrate characteristics, the final Microstrip Patch dimensions are obtained:

$$W = L = \frac{\lambda_0}{\sqrt{\varepsilon_r} * 2} = \frac{\frac{c}{f_0}}{\sqrt{\varepsilon_r} * 2} = \frac{\frac{3e10^8}{28e10^9}}{\sqrt{2.2} * 2} = 3.6mm$$

Equation 16. Microstrip Patch antenna dimensions.

Where:

- **W**: width of the Microstrip Patch antenna.
- **L:** length of the Microstrip Patch antenna.
- ε_r**:** RT/Duroid 5880 dielectric constant.
- **c:** speed of light.
- f_0**:** desired center frequency of operation.

Along the design phase, several antenna solutions have been simulated on IE3D. In addition, by using this simulation software, it has been analyzed the antenna performance in terms of radiation pattern and efficiency. Nevertheless, the antenna impedance analysis has been carried out on AWR.

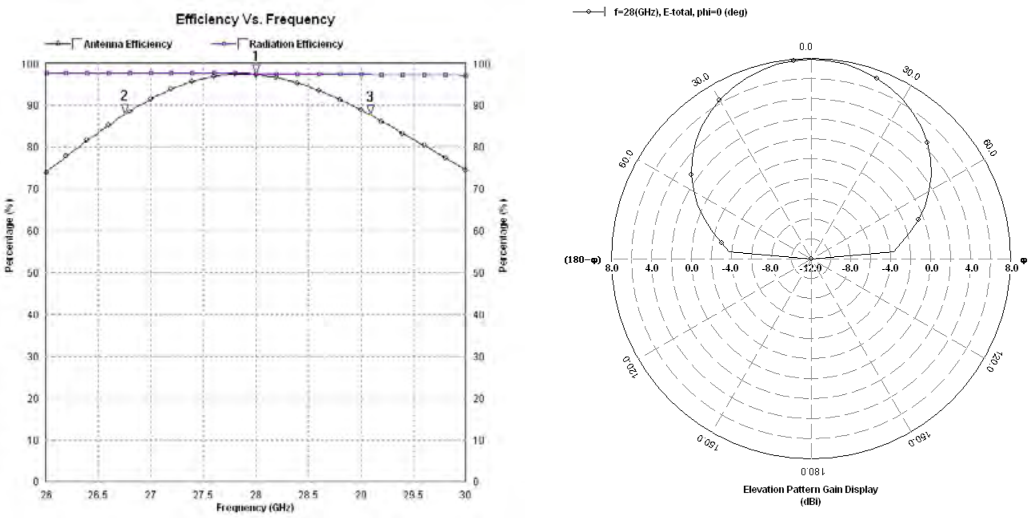

Figure 51. Example of the information obtained and analyzed from IE3D.

Hence, a square 3.6mm x 3.6mm Microstrip Patch antenna is analyzed using IE3D and AWR software to carry out a parametric study. It is observed the impact of the substrate height and the probe-feed to patch points over the Microstrip Patch antenna impedance to achieve the desired antenna performance by tuning these parameters.

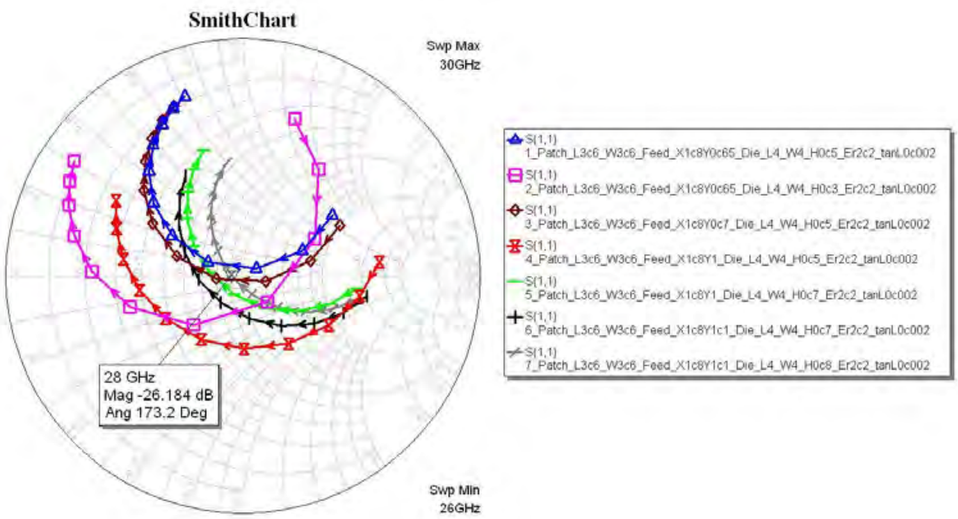

Figure 52. Parametric study of the Microstrip Patch antenna solution.

However, the final and most optimal solution is only presented along this section, since the single element solution found will be analyzed in different array configuration solutions; which is the main objective of this project.

4.2.2 Simulation Set-up

The 3.6mm x 3.6mm square Microstrip Patch antenna solution has been simulated on IE3D software over a frequency range from 26GHz to 30GHz and considering:

- An infinite ground plane at the base of the antenna solution.
- Substrate dielectric constant = 2.2
- Loss tangent = 0.002
- Feeding technique: probe-feed to patch.

In the figure below, it can be observed that the simulated Microstrip Patch antenna fulfills the dimensions obtained from the design procedure's calculus:

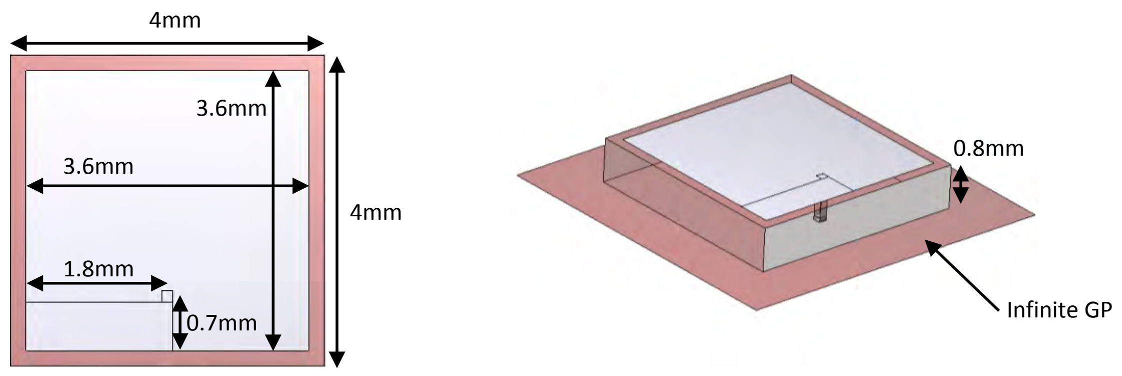

Via: Negative level=0mm, Positive level = 0.08mm, Radius = 0.1mm

Figure 53. Single element Microstrip Patch antenna simulation set-up.

These simulation parameters and considerations have directly influenced on the Microstrip Patch antenna performance analyzed and presented on next point, since they are a key part of the simulation scenario and, therefore, the simulations results.

Moreover, during the design and simulation phase, the first challenge 5G present is faced: the extremely small dimensions of the antenna elements. Due to lambda values at these millimeter-Wave frequencies, the antenna elements must be as small as exposed on the simulation set-up image above (or even smaller).

From a simulation point of view, the upcoming 5G antenna solutions require a really accurate mesh process to correctly carry out the simulation, making difficult the entire simulation process and scenario.

4.2.3 Results

After analyzing several combinations of probe-feed to patch points and substrate heights, the optimal antenna solution is presented.

Different figures are shown in order to characterize the performance of the single element Microstrip Patch antenna solution for 5G application.

Reflection coefficient (S_{11})

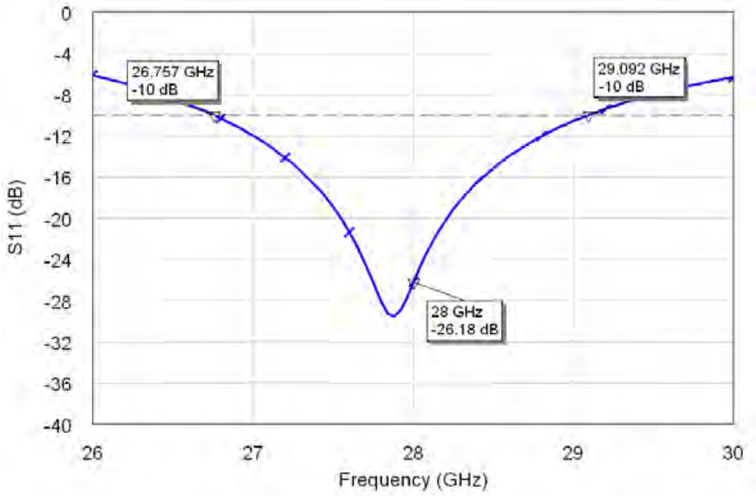

Figure 54. Reflection coefficient of the Microstrip Patch Antenna.

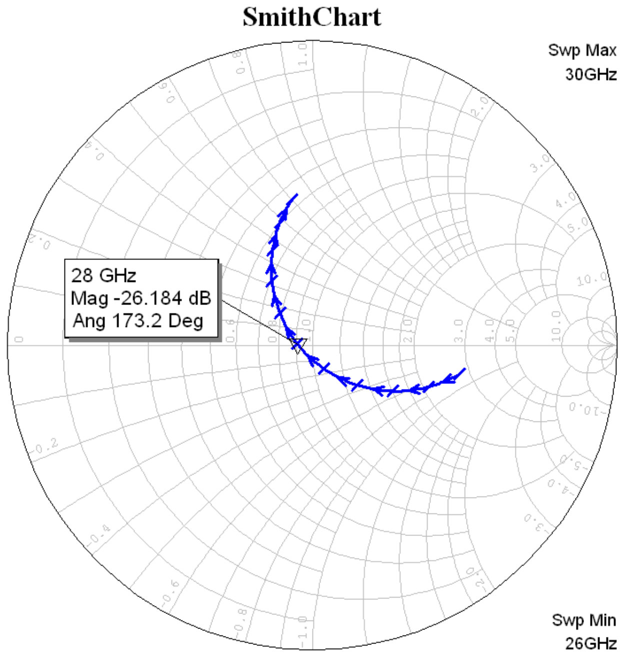

Figure 55. Microstrip Patch antenna impedance shown on Smith Chart.

It can be extracted from both graphics that the designed antenna solution is fully resonating at the desired center frequency of the band (28GHz); since it presents a Reflection Coefficient (S_{11}) below -26dB, which means that more than 95% of the radiation efficiency will be radiated (in a loss-less scenario).

Another key point to be analyzed and extracted from the S_{11} result's graphics is the antenna bandwidth. In this case, it has been intended to achieve the maximum bandwidth below the limit of -10dB, so good antenna performance can be ensured in this range. Hence, the -10dB bandwidth can be extracted:

BW -10db (%) = 29.092-26.757= 2.335GHz (8.3%)

It will ensure high and stable antenna performance over the 2.335GHz frequency range and centered at 28GHz.

Antenna Efficiency and Radiation Efficiency

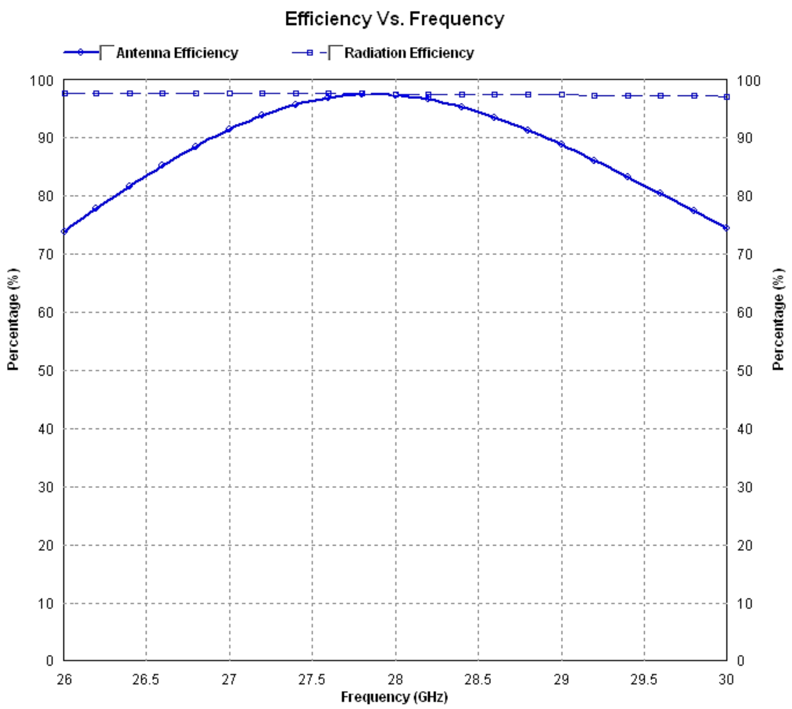

Figure 56. Single element Microstrip Patch Antenna and Radiation Efficiency

The Radiation Efficiency obtained from the single element is 96% throughout the whole -10dB bandwidth frequency range. In this manner, it can be ensured that the design performed is efficient by itself, so well-designed.

On the other hand, the Antenna Efficiency is above 90% in the -10dB bandwidth frequency range, and especially high at 28GHz, reaching completely the Radiation Efficiency limit. Therefore, it is confirmed what was exposed previously, at 28GHz it is radiated more than 95% (in this case 100%) of the radiation efficiency.

Radiation Pattern

As explained on "Basic Concepts" section 1.6.8 about the Radiation Pattern, it is critical to correctly consider the most convenient 2D views of the antenna radiation pattern to properly show the relevant information.

In the case studied, phi = 0° and phi = 90° are shown, since as the Microstrip Patch antenna is designed to radiate in zenithal direction mainly, no relevant patterns can be extracted from theta = 90° view.

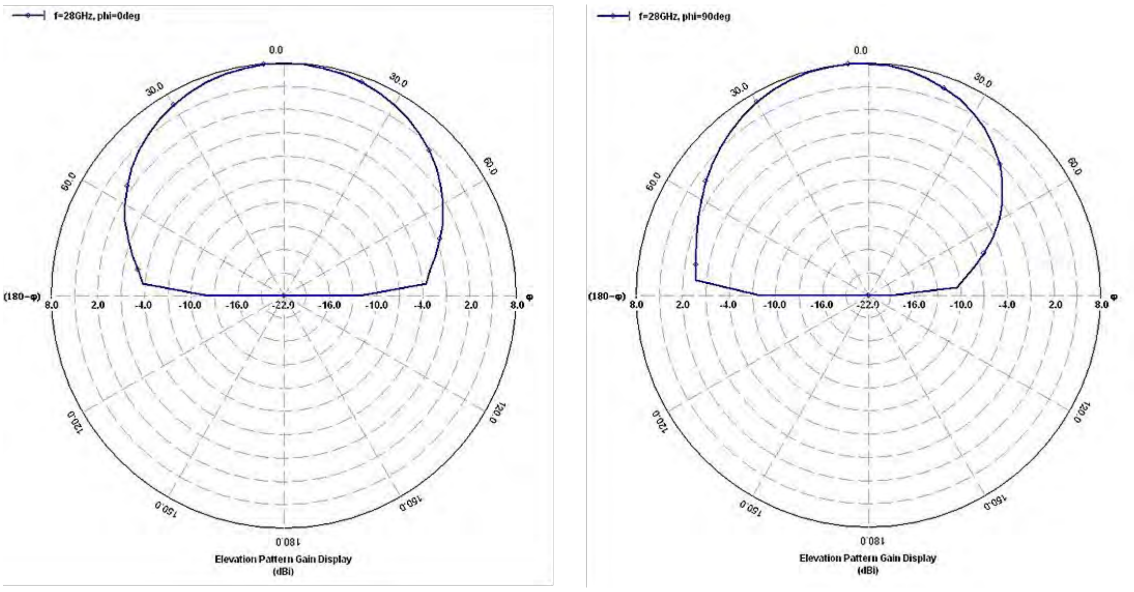

Figure 57. Single element Microstrip Patch antenna Radiation Pattern, phi = 0° and phi = 90° respectively.

In both cases, it is represented the Radiation Pattern considering an axis from maximum gain to -30dB point. Therefore, the Microstrip Patch antenna maximum Gain is 8.0 dBi.

Taking into account the views presented (phi = 0°/plane XZ and phi = 90°/plane YZ), it can be easily seen that the designed antenna is radiating in zenith direction, providing high coverage towards the direction it points to. In addition, someone familiar with this type of antennas can observe that there is no "back" radiation since no lobes are seen in this direction. This phenomenon is due to the infinite ground plane considered for the simulation, which provides an ideal surface to radiate from.

Summary

Results exposed reinforce the importance of a properly designed antenna solution, especially for technologies such as 5G which demand really high performance. Therefore, it is validated the single element design presented to be integrated and grouped to form an antenna array for 5G successfully implementation as it will be done on next section.

4.3 5G Microstrip Patch Antenna Array

Within section 1.3 it has been introduced what 5G is and what challenges this new technology demand from a technological point of view, such as high gain and directivity, high efficiency, broad bandwidth and the ability to provide full coverage in real time. All these requirements are only achievable with an antenna array solution, since its design flexibility allows to achieve high performance in tough and highly demanding environments (section 1.6.10).

Along this point, different antenna array solutions will be studied formed by the single antenna element designed and analyzed in the previous section; considering different configurations to study their performance and obtain the optimal solution for 5G application.

4.3.1 Design procedure

Several characteristics and design techniques are considered when designing Microstrip Patch antenna arrays as it has been seen on the "3.2 Review of Prior Art" previously in this report. Antenna arrays can be either linear or in two-dimension; even more, in some cases three-dimension arrays could fulfill the specific requirements looked for.

In the study carried out within this section, linear and two-dimensional antenna array cases have been considered; since the preferred implementation of the solution sought along this project is for 5G wireless devices, which will demand to be as smallest as possible. For Microstrip Patch antenna array characterization, it has been used the IE3D PatternView "Array Pattern Calculation" tool, which provide an antenna pattern calculation with no mutual couplings between array elements considered. Nevertheless, it provides a great flexibility to analyze several designs and great accuracy for antenna array pattern calculation.

PatternView tool estimates the antenna array behavior by considering the number of elements, the distance and phase step between them. From Antenna Theory, it is extracted that the distance between antenna elements should be < λ to avoid the apparition of grating lobes in the visible range. Also, distance should also consider beam-steering to avoid the apparition of grating lobes when steering the main beam [9] . Therefore, the distance between the antenna array elements center and total distance of the array is calculated as:

$$\frac{Total\ Distance}{N-1} = d = \frac{\lambda}{2} = \frac{c}{2f_0} = \frac{3e8}{2*28e9} = 5.35mm$$

Equation 17. Distance between antenna array elements.

Where:

- **Total Distance**: distance between the center of the first and the last element of the antenna array in the specific direction.
- **N:** total antenna array elements.
- **d:** distance between antenna array elements.
- **c:** speed of light.
- $\boldsymbol{f_0}$**:** desired center frequency of operation.

However, it should be highly considered that if Microstrip Patch antenna dimensions are greater than the calculated λ/2 distance between elements, it must be set a greater distance.

Hence, once obtained the distance between antenna array elements, it is possible to get the Total Array dimensions for each studied case.

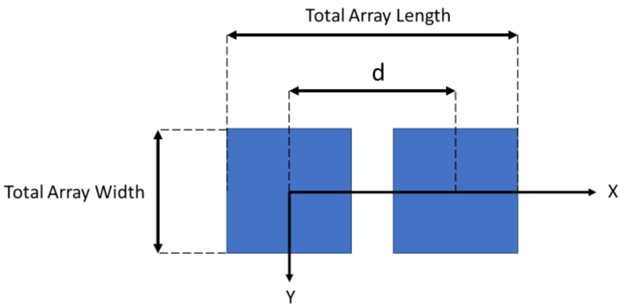

Figure 58. Distance between antenna array elements and Total Array dimensions.

As exposed before, IE3D PatternView "Array Pattern Calculation" tool has been used to characterize the antenna arrays studied in this section. It is considered the number of elements, the total distance and the phase step for each direction:

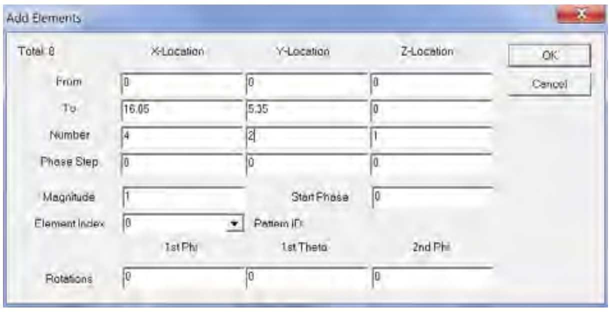

Figure 59. Example of Add Elements to the antenna array.

On the main screen, it is possible to set the "Elevation Angles" and "Azimuth Angles" which will be taken into account when characterizing the Microstrip Antenna array. For all cases presented, it has been considered 73 points on each case.

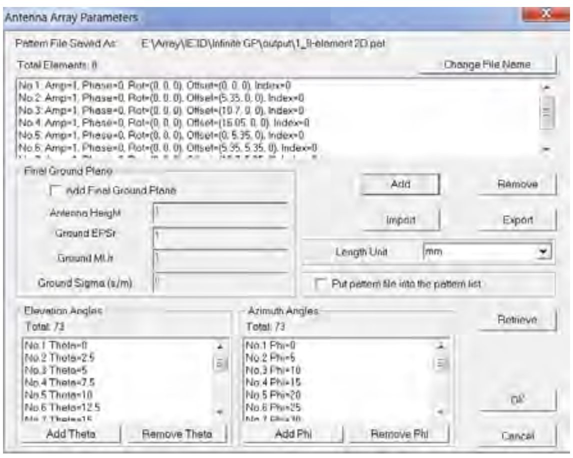

Figure 60. Example of the Antenna Array Parameters.

Once the Microstrip Patch antenna array has been defined, it is possible to analyze the array characterization. The “Array Pattern Calculation” tool allows to generate the data needed to plot the required radiation pattern, directivity, gain and efficiency. Information used to analyze and define next steps on the design phase.

2D Radiation Pattern view is used to obtain the antenna array lobes, gain in boresight and maximum scan angle for the specific Microstrip Patch antenna array.

In addition, the Total Field Directivity and Efficiency can be extracted from this characterization.

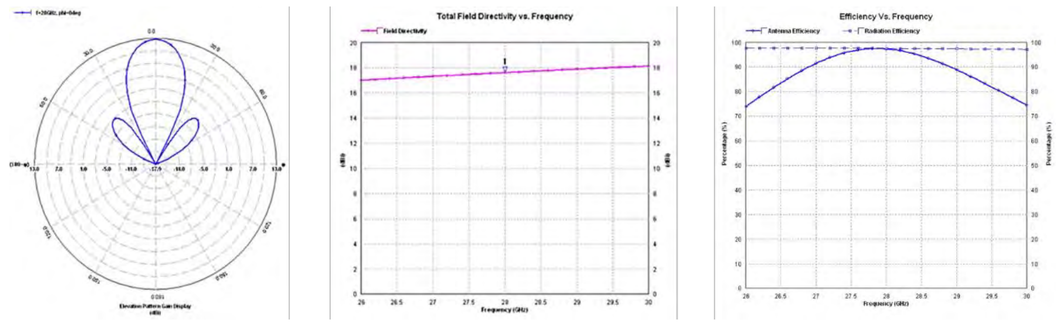

Figure 61. Example of 2D Radiation Pattern, Directivity and Efficiency graphs.

“Array Pattern Calculation” tool provides the required information to correctly characterize and study the different use cases for 5G applications. Moreover, it is a key tool to approach in an easier way, the performance of the analyzed antenna array solution.

4.3.2 Simulation Set-ups

During the design phase, different simulation set-ups have been performed implementing the 3.6mm x 3.6mm square Microstrip Patch antenna solution presented along section 4.2; to generate every antenna array case.

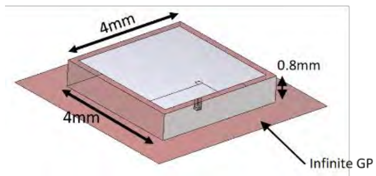

Figure 62. Single element Microstrip Patch antenna dimensions.

As exposed on the “Design Procedure”, in the case of study it has been selected array configurations to be linear or two-dimension, with a number of elements from 4 to 16; since, as said before, it is important to keep small dimensions when designing the Microstrip Patch antenna array solution.

Six Microstrip Patch antenna arrays have been simulated and, for each case, it is presented below the total distance considering the distance between elements exposed on section 4.3.1 of 5.35mm, together with the PatternView “Array Pattern Calculation” tool values.

4-Microstrip Patch linear antenna array

First case of study is a 4-element linear antenna array, which Total Distance between centers of first and last element is calculated as.

$$\frac{Total\ Distance}{N-1} = d \dashrightarrow Total\ Distance = 5.35mm(4-1) = 16.05mm$$

Equation 18. Total Distance between centers of first and last element for a 4-Microstrip Patch linear case.

Hence, and considering the Microstrip Patch dimensions, the Total Array dimensions are as follow:

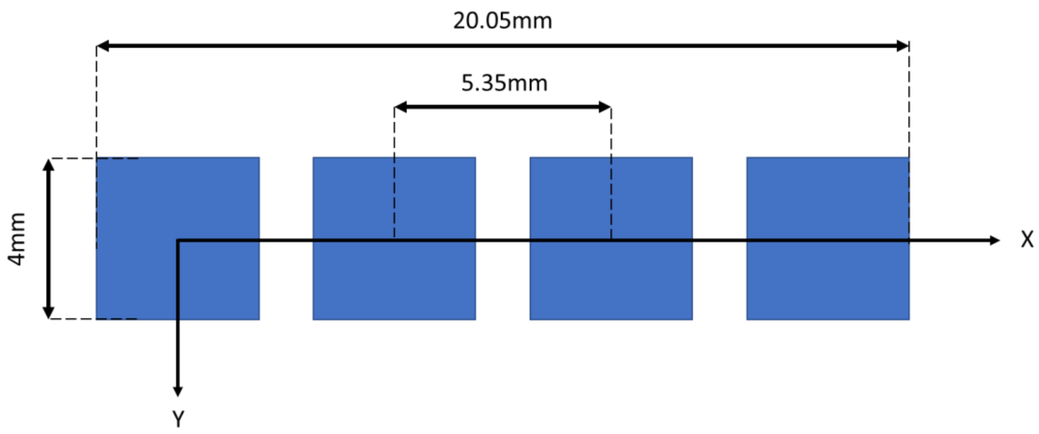

Figure 63. Distance between antenna array elements and Total Array dimensions for a 4-element antenna array.

To generate the required antenna array, on "Array Pattern Calculation" tool it is needed to add the array elements with the previous characteristics. In addition, a phase step between elements is included to analyze the maximum scan angle of the solution.

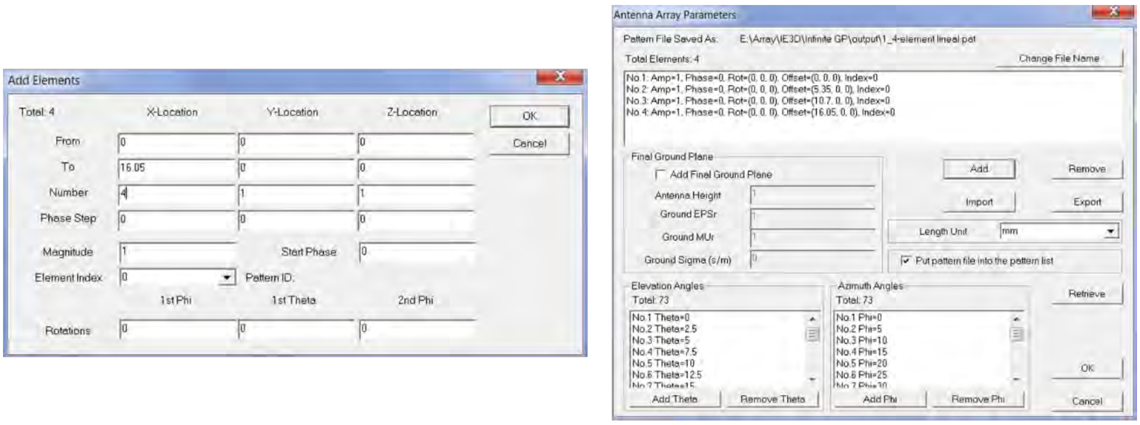

Figure 64. Array Pattern Calculation tool on IE3D PatternView for a 4-element antenna array.

Once created the antenna array elements, an antenna array pattern is generated with the characteristics set to analyze its results.

4-Microstrip Patch 2-D antenna array

For the two-dimension solution, it is needed to set the distance in X and Y direction respectively; so, they are calculated as:

$$Total\ DistanceX = 5.35mm(2-1) = 5.35mm$$

$$Total\ DistanceY = 5.35mm(2-1) = 5.35mm$$

Equation 19. Total Distance between centers of first and last element for a 4-Microstrip Patch 2D case.

Therefore, the antenna array elements on Y direction are increased, which it is directly related to an increase of the width. Total Array dimensions are set as shown below:

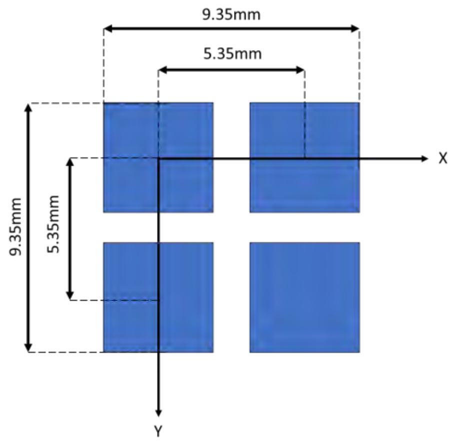

Figure 65. Distance between antenna array elements and Total Array dimensions for a 4-element 2D antenna array.

On a two-dimension antenna array, it is needed to implement the distance between elements on both X and Y direction as shown below. Moreover, when including the phase step, both direction's elements must be analyzed.

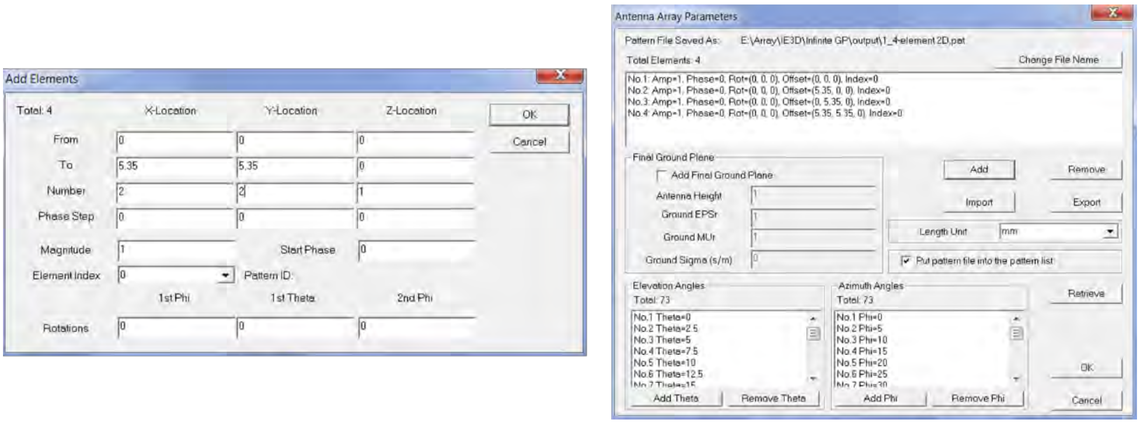

Figure 66. Array Pattern Calculation tool on IE3D PatternView for a 4-element 2D antenna array.

Phase steps of 30, 60, 90, 120 and 150 degrees have been implemented for the scan angle study.

8-Microstrip Patch linear antenna array

As a second case of study considering the number of antenna array elements, it is implemented an 8-element linear Microstrip Patch antenna array; for which the Total Distance is increased till 37.45mm.

$$Total\ Distance = 5.35mm(8-1) = 37.45mm$$

Equation 20. Total Distance between centers of first and last element for an 8-Microstrip Patch linear case.

So, the antenna array for an 8-element linear case taking into account the dimensions previously calculated can be characterized as shown below:

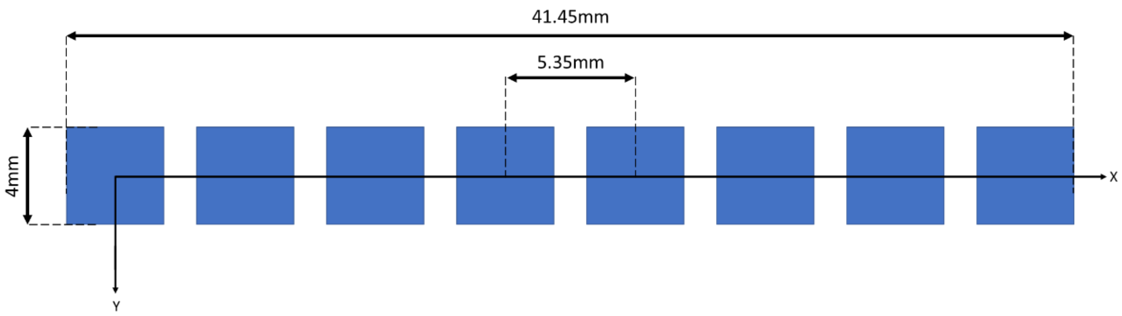

Figure 67. Distance between array elements and Total Array dimensions for an 8-element linear antenna array.

To properly characterize the 8-element antenna array solution, it is needed to generate the elements on the X-direction only, including the Total Distance calculated previously between both first and last element centers and the total number of elements in each direction of the antenna array.

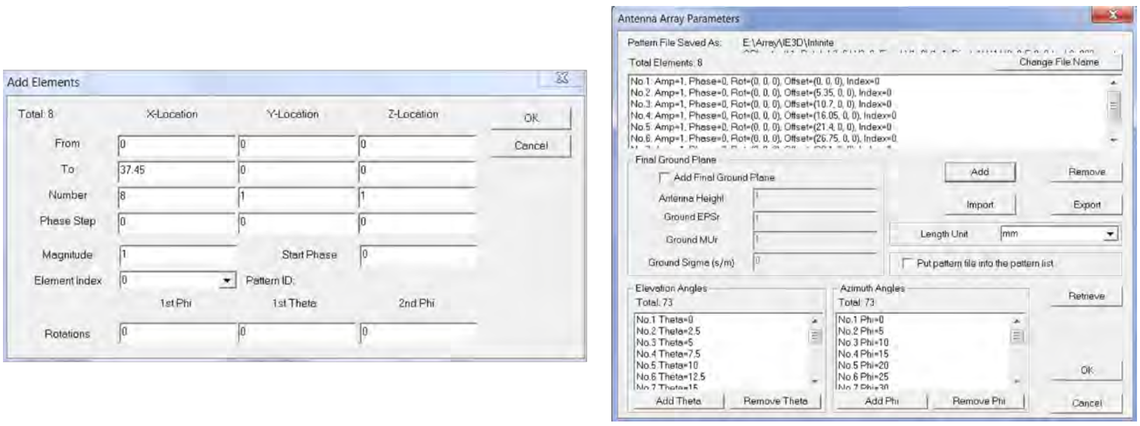

Figure 68. Array Pattern Calculation tool on IE3D PatternView for an 8-element linear antenna array.

For the maximum scan angle analysis, it is needed to increase the phase step value to obtain a characterization of the performance in each phase.

8-Microstrip Patch 2-D antenna array

In this case, as it is an 8-element antenna array solution in two-dimension configurations, it is needed to set a 4 x 2 configuration in X-direction and Y-direction respectively; so, X-direction remains the main direction of the Microstrip Patch antenna array:

$$Total\ DistanceX = 5.35mm(4-1) = 16.05mm$$

$$Total\ DistanceY = 5.35mm(2-1) = 5.35mm$$

Equation 21. Total Distance between centers of first and last element for an 8-Microstrip Patch 2D case.

Total Array dimensions are shown below, where it can be observed that the complete antenna array increases its dimensions in both directions:

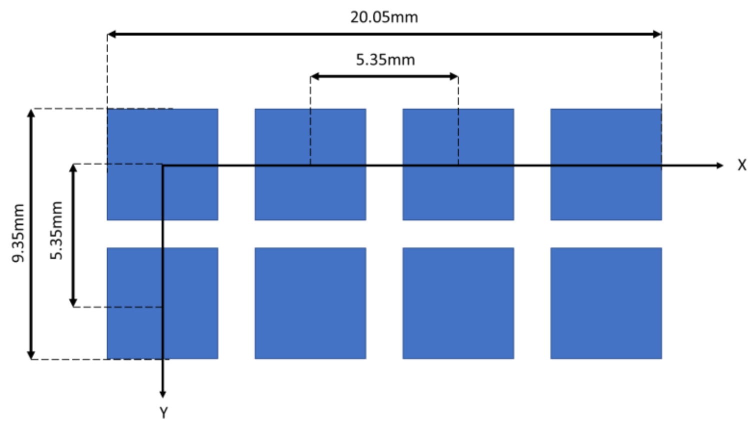

Figure 69. Distance between array elements and Total Array dimensions for an 8-element 2D antenna array.

Eventually, and as it was explained on the 4-element 2D case, it is needed to create antenna array elements considering both directions Total Distances to properly characterize the Microstrip Patch antenna array. For the maximum scan angle, it has been increased the phase step in both array directions, to observe the effect in all directions.

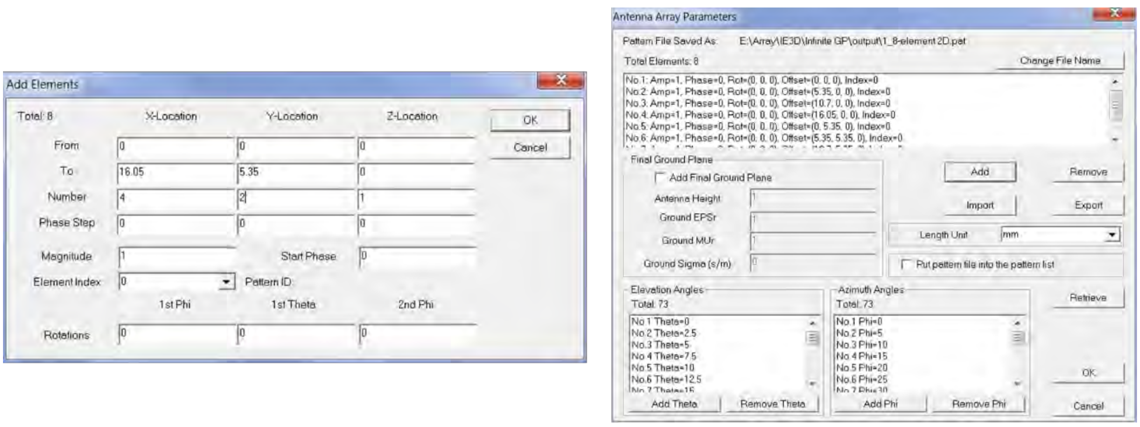

Figure 70. Array Pattern Calculation tool on IE3D PatternView for an 8-element 2D antenna array.

16-Microstrip Patch linear antenna array

Finally, a 16-element linear antenna array is studied. It is set as “the limit” in terms of antenna array elements, since its dimensions start getting too big, which will complicate its implementation on a 5G wireless device. With this configuration, the Total Distance is 80.25mm.

$$Total\ Distance = 5.35mm(16-1) = 80.25mm$$

Equation 22. Total Distance between centers of first and last element for a 16-Microstrip Patch linear case.

As it can see below, there is such a great difference between the Total Array length and Total Array width. For this specific configuration of antenna arrays, it is preferred to implement them in a device short edge; because it will free plenty of space just underneath the area occupied by the antenna array.

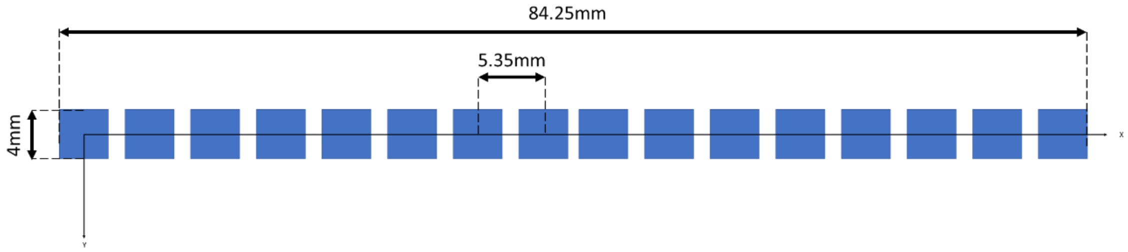

Figure 71. Distance between array elements and Total Array dimensions for a 16-element linear antenna array.

When creating the antenna array elements, and as it has been done in previous linear array cases, it is needed to set the Total Distance in X-direction to generate the 16-element linear antenna array.

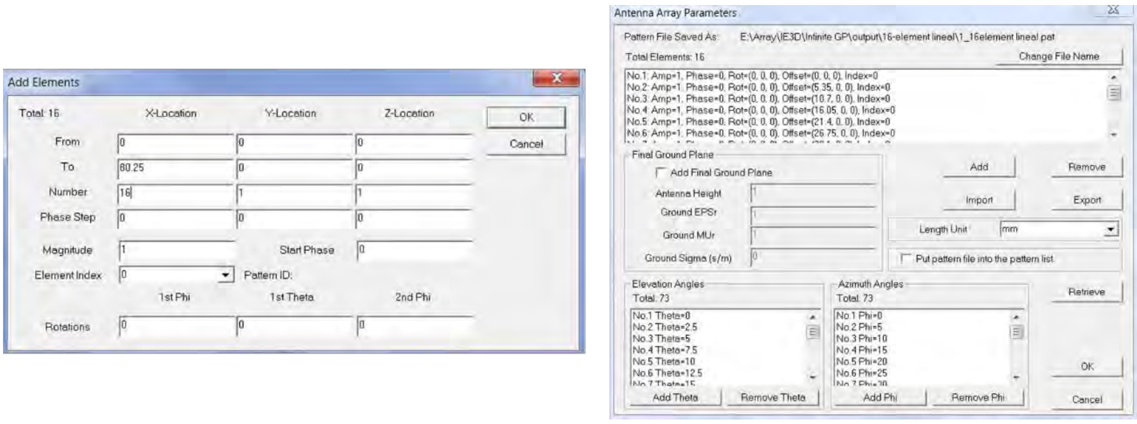

Figure 72. Array Pattern Calculation tool on IE3D PatternView for a 16-element linear antenna array.

In this case, the phase step has been increased only in X-direction; since no elements are present in Y-direction.

16-Microstrip Patch 2-D antenna array

The last case that has been characterized is a 16-element two-dimension antenna array. As it was explained in previous two-dimension solution, it is needed to set two different Total Distances considering the X-direction and Y-direction respectively.

$$Total\ DistanceX = 5.35mm(4-1) = 16.05mm$$

$$Total\ DistanceY = 5.35mm(4-1) = 16.05mm$$

Equation 23. Total Distance between centers of first and last element for a 16-Microstrip Patch 2D case.

Total Array dimensions are shown below, where it can be observed that the complete antenna array increases its dimensions in both directions forming a square of 20.05mm x 20.05mm:

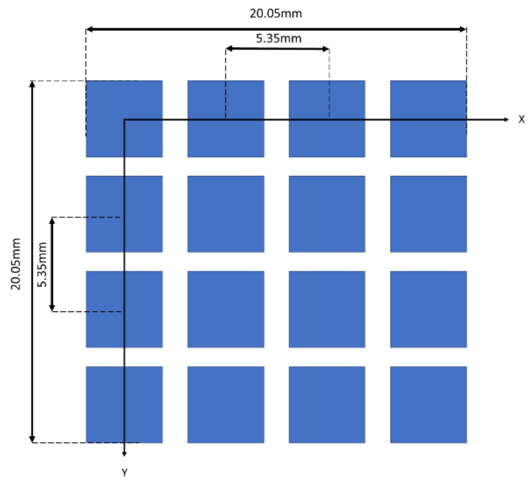

Figure 73. Distance between array elements and Total Array dimensions for a 16-element 2D antenna array.

Finally, it is needed to add the antenna array elements in both directions equally, to generate the desired 16-element two-dimension Microstrip Patch antenna array solution. Phase step is characterized in both directions as well, to observe the impact of the phase difference between elements.

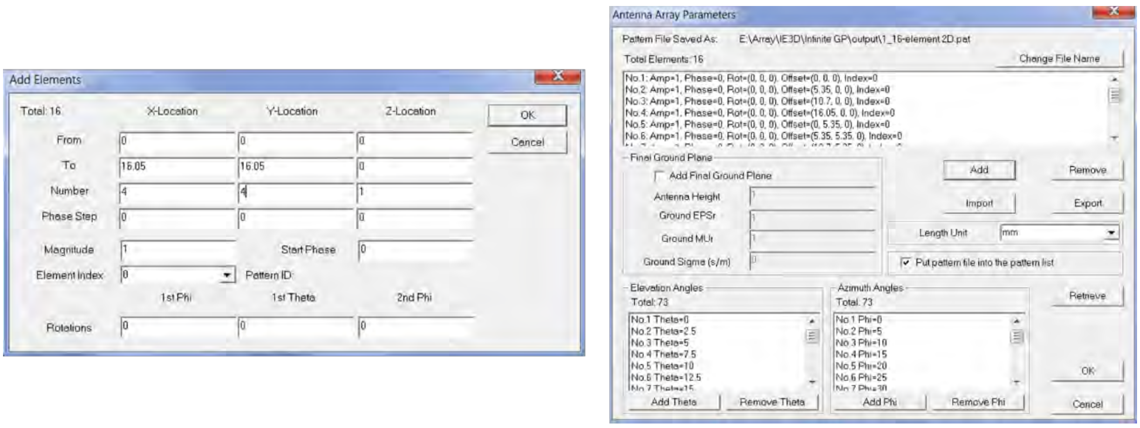

Figure 74. Array Pattern Calculation tool on IE3D PatternView for a 16-element 2-D antenna array.

4.3.3 Results

On previous section, it has been presented all the Microstrip Patch antenna array configurations studied in this project, formed by the single antenna element specifically designed for this purpose.

Henceforth, several figures are shown for each studied case in order to characterize the performance of the desired antenna array solution for the upcoming 5G technology applications. For each solution proposed, it is presented the Radiation Pattern, Directivity, Efficiency and Maximum Scan Angle.

Along “4.3.1 Design Procedure” point, it has been exposed that 2D Radiation Patterns have been used to obtain the gain in boresight of the antenna array solution analyzed, but moreover, to obtain the shape and maximum scan angle of each solution.

In the cases studied, phi = 0° and phi = 90° are shown considering an axis from maximum gain to -30dB point, since as the Microstrip Patch antenna array is designed along X-direction and Y-direction mainly, no relevant patterns can be extracted from theta = 90° view.

4-MICROSTRIP PATCH LINEAR ANTENNA ARRAY

Radiation Pattern

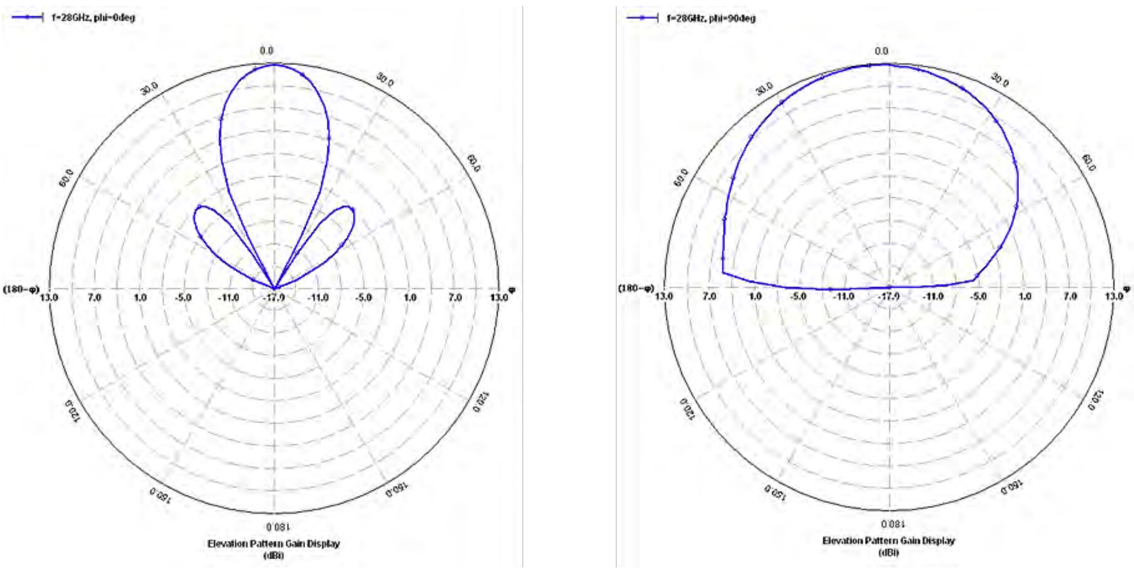

Figure 75. 4-element linear Microstrip Patch antenna array Radiation Pattern, phi = 0° and phi = 90° respectively.

From both radiation pattern graphs, it can be observed that the 4-Microstrip Patch linear antenna array maximum Gain is 12.8 dBi. Side lobes are -10dB from the main lobe maximum, ensuring proper antenna radiation in the desired direction. Antenna array radiation is wider in phi = 90°, since it has been physically designed to be along X-direction.

Directivity and Efficiency

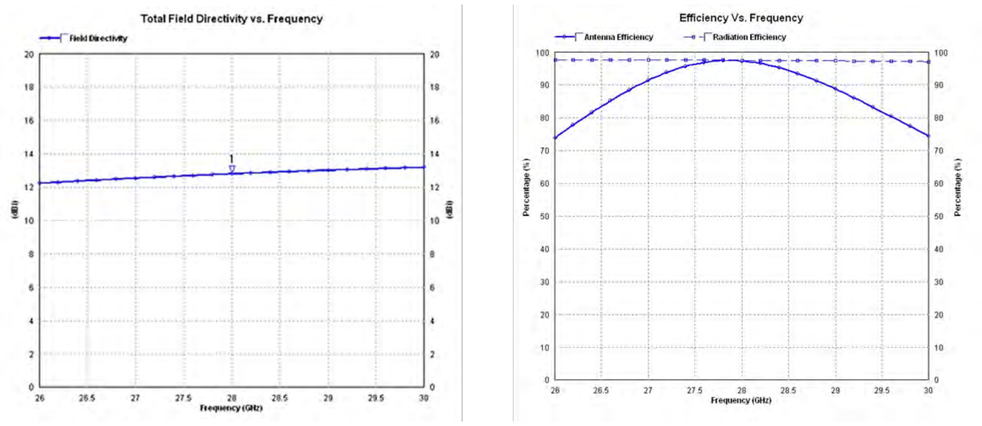

Figure 76. 4-element linear Microstrip Patch antenna array Total Field Directivity and Efficiency respectively.

Total Field Directivity is shown as cartesian plot to crosscheck the maximum Gain obtained from Radiation Pattern graph exposed above. As it can be seen, the Directivity for the 4-element linear antenna array is 12.8 dBi. On the other hand, the antenna array Efficiency is shown, which matches with the Efficiency of the single element presented on section 4.2.3.; since no mutual couplings are considered with the "Array Pattern Calculation" tool, Radiation Efficiency is ideally 100%. For the -10dB bandwidth, the Antenna Efficiency is above 90%.

Maximum Scan Angle

To obtain the Maximum Scan Angle of the 4-Microstrip Patch antenna array solution, it has been considered several phase steps between antenna array elements as explained in "4.3.2 Simulation Set-ups section". By doing so, it is possible to shift the main lobe of the Radiation Pattern. It has been considered the Maximum Scan Angle where the main lobe is -3dB from the Phase Step 0° case.

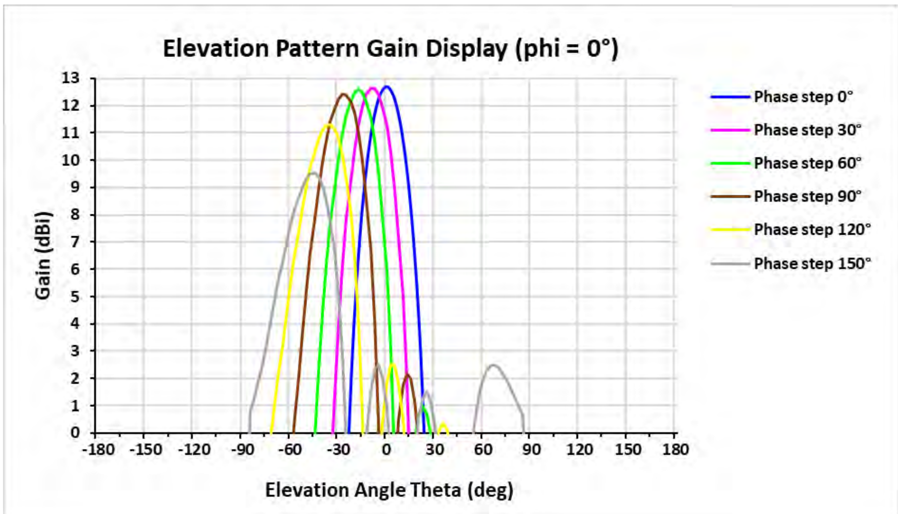

Figure 77. Maximum Scan Angle of the 4-Microstrip Patch linear antenna array solution.

As it can be observed, the Maximum Scan Angle of the present case is ±45°.

4-MICROSTRIP PATCH 2-D ANTENNA ARRAY

Radiation Pattern

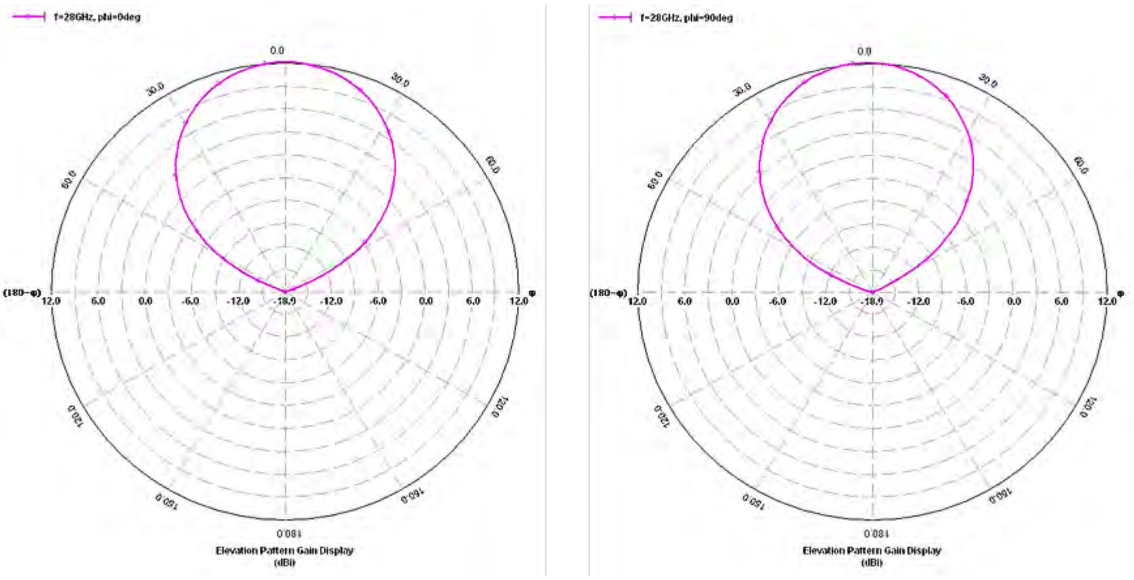

Figure 78. 4-element 2D Microstrip Patch antenna array Radiation Pattern, phi = 0° and phi = 90° respectively.

In a two-dimensional case where in both directions (X and Y) there are the same number of elements, phi = 0° and phi = 90° views have the same behavior. It can be observed that the 4-Microstrip Patch 2D antenna array maximum Gain is 12.1 dBi. And no side lobes are present, only a great main lobe.

Directivity and Efficiency

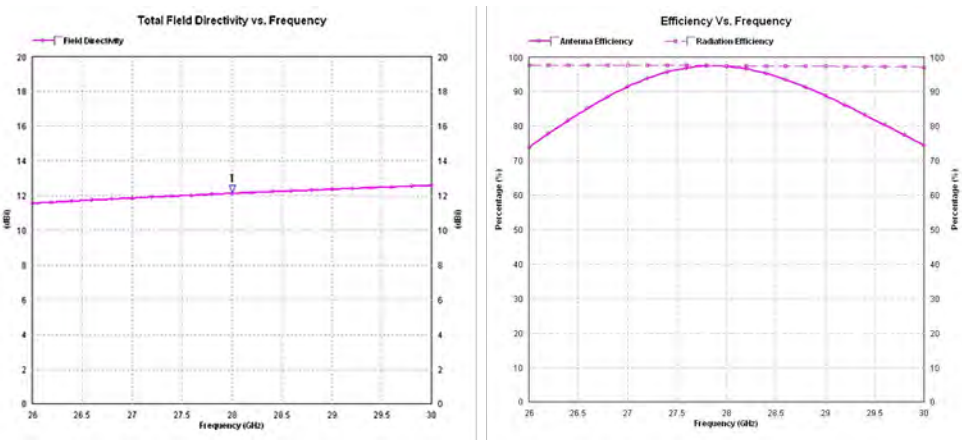

Figure 79. 4-element 2D Microstrip Patch antenna array Total Field Directivity and Efficiency respectively.

As it can be observed, the Directivity for the 4-element 2D antenna array solution is 12.1 dBi. Regarding the Efficiency, same behavior than previous solution is obtained, with an Antenna Efficiency for the -10dB bandwidth above 90%.

Maximum Scan Angle

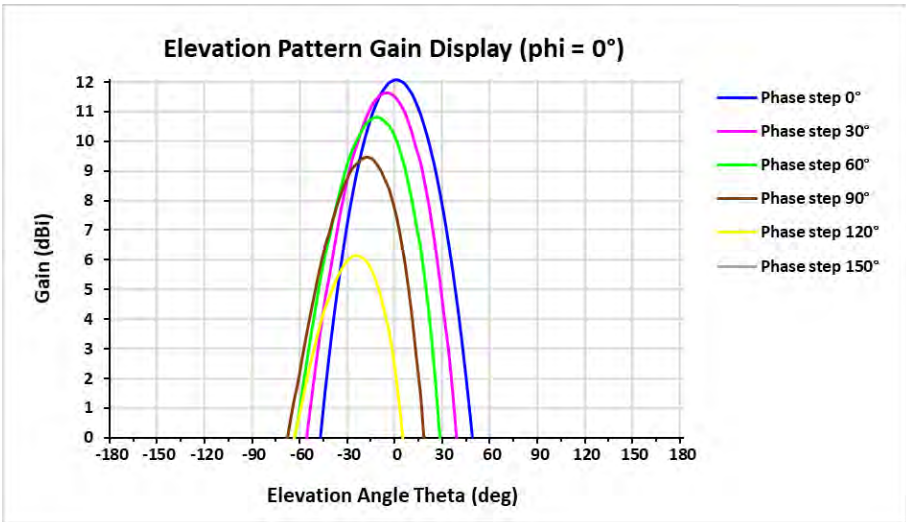

Figure 80. Maximum Scan Angle of the 4-Microstrip Patch 2D antenna array solution.

From the graph above, it is observed that in a two-dimensional configuration the Maximum Scan Angle is reduced to ±30°.

8-MICROSTRIP PATCH LINEAR ANTENNA ARRAY

Radiation Pattern

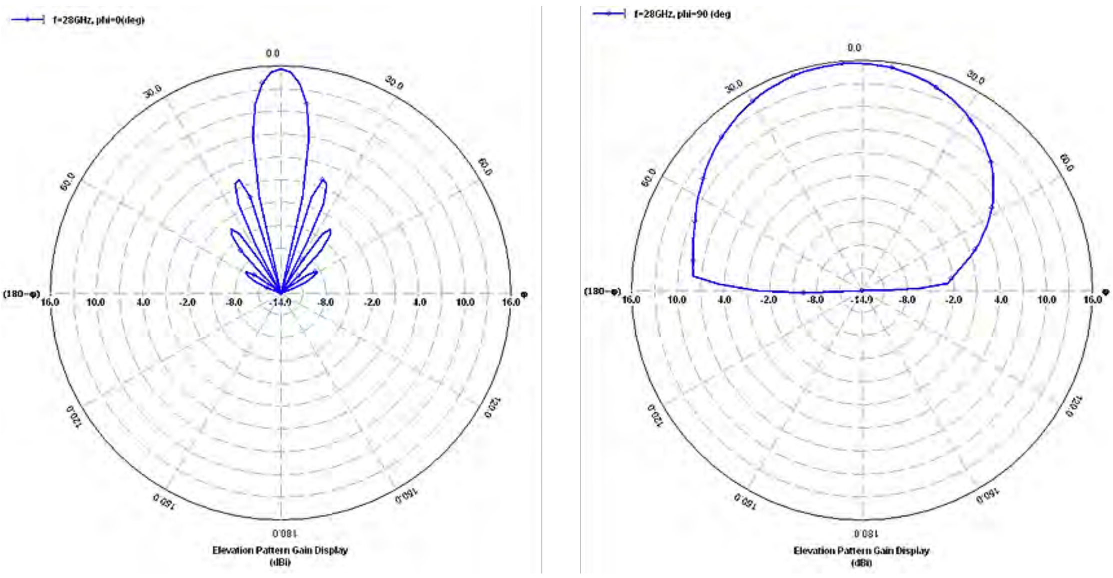

Figure 81. 8-element linear Microstrip Patch antenna array Radiation Pattern, phi = 0° and phi = 90° respectively.

When increasing the number of elements in one specific direction, in this case X-direction, it can be seen on phi = 0° graph that the main lobe becomes narrower and more side lobes appear. However, this side lobes are -10dB lower than the main lobe, which will not distort the antenna array radiation. Another point is the increase of the maximum Gain that is 15.6 dBi.

Directivity and Efficiency

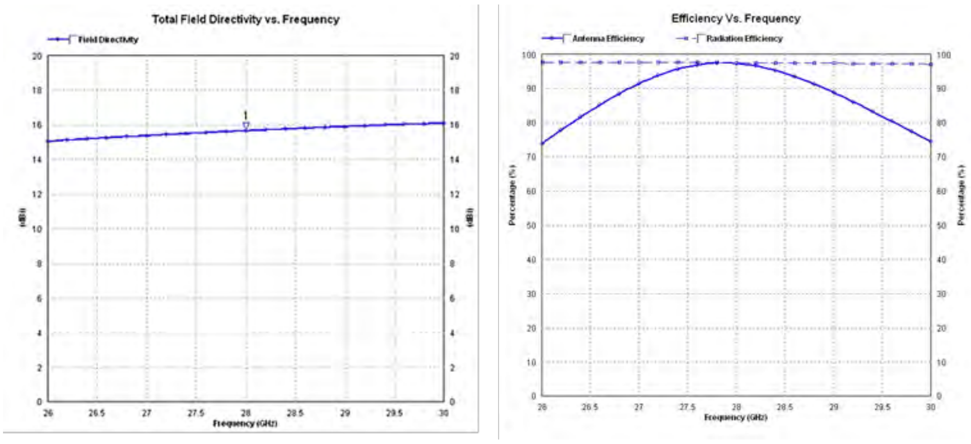

Figure 82. 8-element linear Microstrip Patch antenna array Total Field Directivity and Efficiency respectively.

Directivity is increased as well till 15.6dBi, being totally aligned with the maximum Gain presented above. Regarding the Efficiency, its Radiation Efficiency is obtained from the single element due to no mutual couplings considered on the antenna array as explained before, and its Antenna Efficiency is above 90% throughout the full -10dB bandwidth.

Maximum Scan Angle

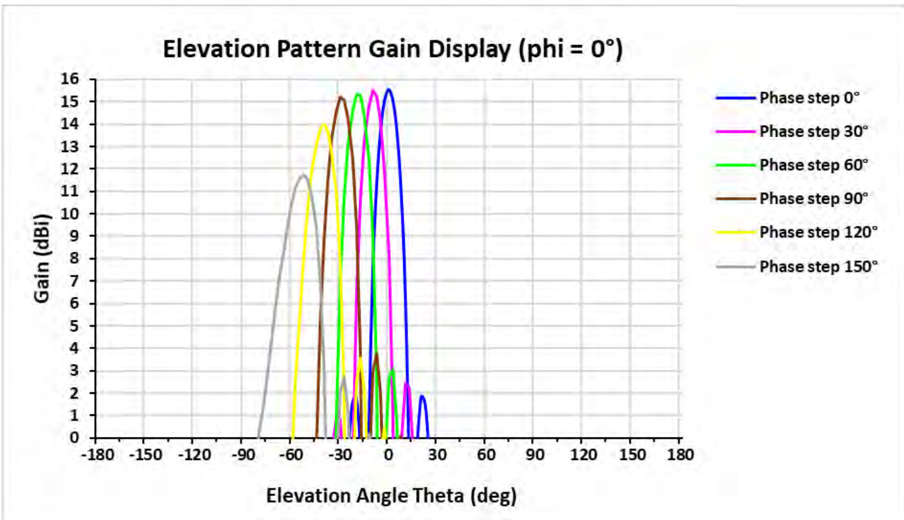

Figure 83. Maximum Scan Angle of the 8-Microstrip Patch linear antenna array solution.

Even main lobe (Phase step = 0°) maximum Gain has been increased, the -3dB point set a Maximum Scan Angle of ±45°, the same Maximum Scan Angle than the 4-element linear antenna array solution. Nevertheless, for the same angle, the Gain is greater on the 8-element solution.

It is observed so far, the same behavior for all Microstrip Patch antenna array solutions. It has to be finally confirmed with the 16-element linear case.

8-MICROSTRIP PATCH 2-D ANTENNA ARRAY

Radiation Pattern

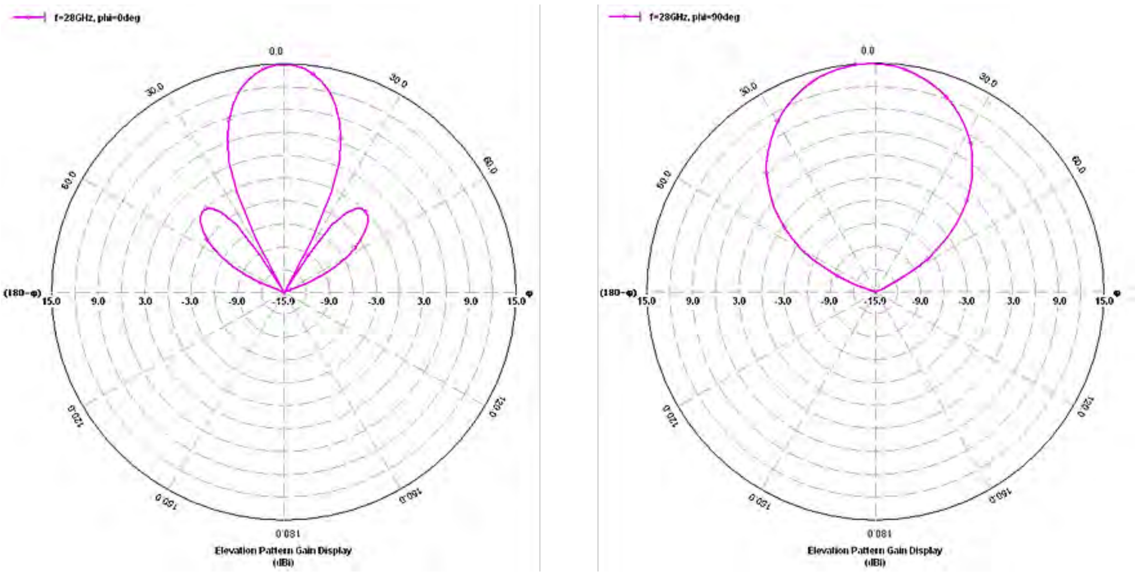

Figure 84. 8-element 2D Microstrip Patch antenna array Radiation Pattern, phi = 0° and phi = 90° respectively.

Even it is a two-dimension configuration, side lobes are present due to the difference between elements in X-direction and Y-direction, 4 and 2 respectively. Side lobes are -15dB from the main lobe maximum in phi = 0°, ensuring proper performance. From both graphs, it can be observed that maximum Gain is 14.9 dBi.

Directivity and Efficiency

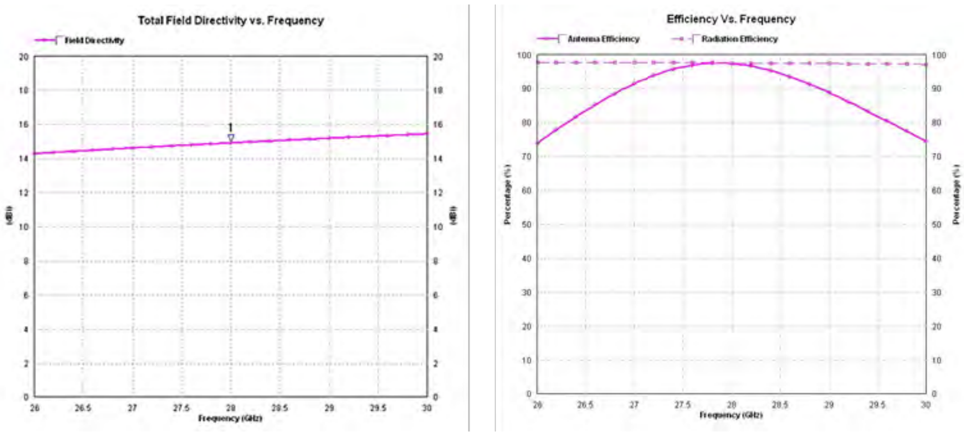

Figure 85. 8-element 2D Microstrip Patch antenna array Total Field Directivity and Efficiency respectively.

Total Field Directivity plot shows, as in previous cases, that Directivity equals the maximum Gain observed in Radiation Pattern views, which in this solution is 14.9 dBi. From the Efficiency plot, it is shown an Antenna Efficiency for the -10dB bandwidth above 90%.

Maximum Scan Angle

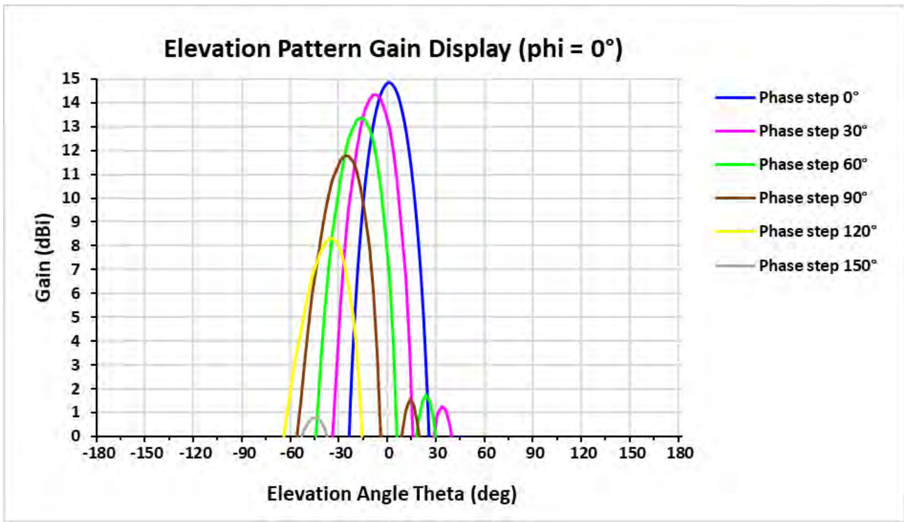

Figure 86. Maximum Scan Angle of the 8-Microstrip Patch 2D antenna array solution.

In comparison with previous solutions, it is seen that the 8-element linear antenna array achieves better performance on the Maximum Scan Angle test, which for the 8-element 2D case is ±30°.

16-MICROSTRIP PATCH LINEAR ANTENNA ARRAY

Radiation Pattern

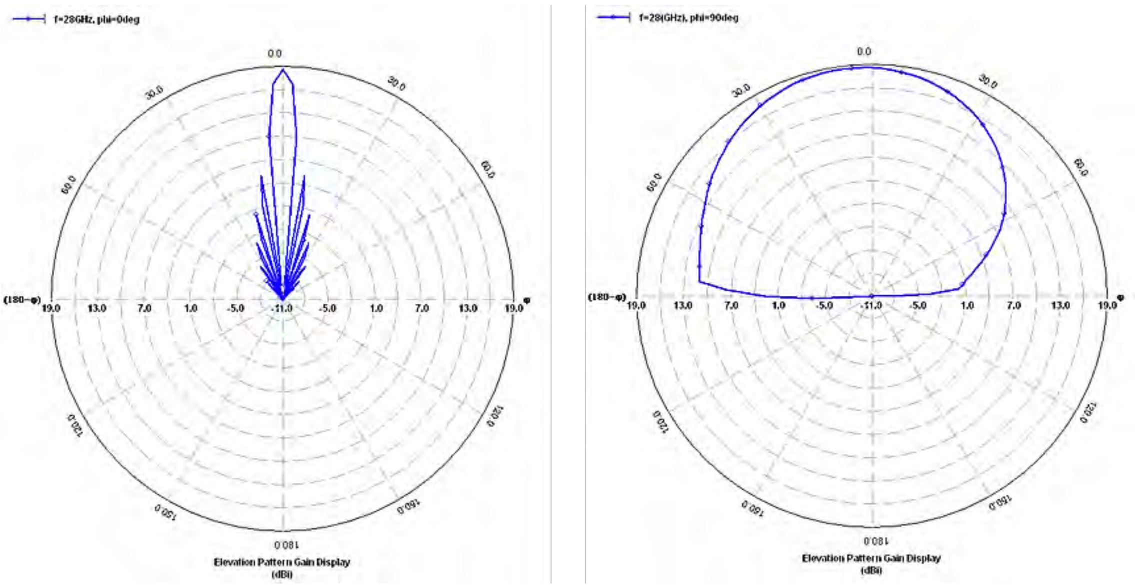

Figure 87. 16-element linear Microstrip Patch antenna array Radiation Pattern, phi = 0° and phi = 90° respectively.

As it has been observed on the 8-element linear antenna array solution, when it is increased the number of elements in one specific direction, main lobe becomes narrower and more side lobes appear. It still has side lobes -15dB from main lobe, with a maximum Gain of 18.6 dBi.

Directivity and Efficiency

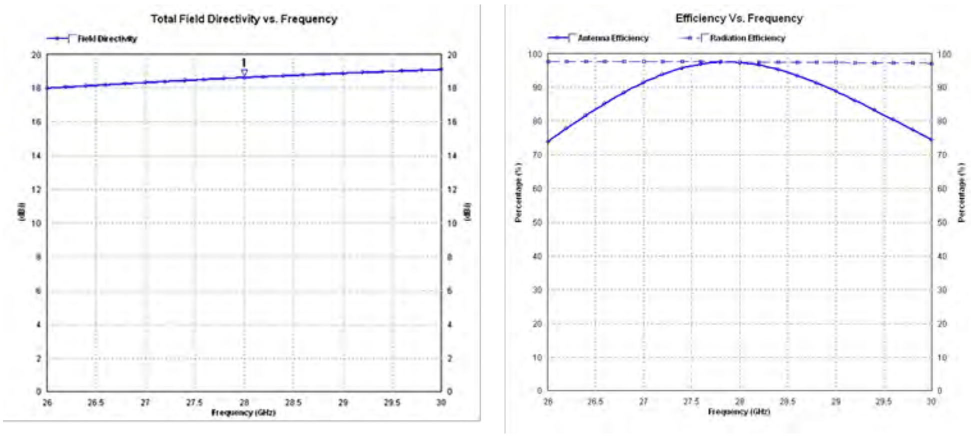

Figure 88. 16-element linear Microstrip Patch antenna array Total Field Directivity and Efficiency respectively.

Directivity is set as well to 18.6dBi, being totally aligned with the maximum Gain presented above. Regarding the Efficiency, its Radiation Efficiency is considered from the single element as it is done in all cases, and its Antenna Efficiency is above 90% throughout the full -10dB bandwidth.

Maximum Scan Angle

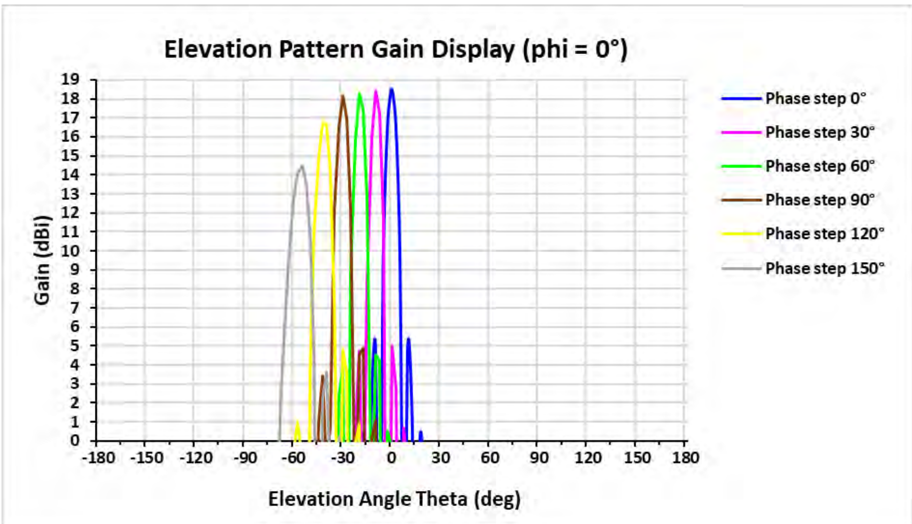

Figure 89. Maximum Scan Angle of the 16-Microstrip Patch linear antenna array solution.

From the last linear case, it can be fully confirmed that the Maximum Scan Angle performance is maintained when the Microstrip Patch antenna array is linear and reduced when it becomes two-dimensional.

As on previous linear antenna array solutions, the Maximum Scan Angle is ±45°, with a maximum gain at this point of 15.6 dBi. This is directly related to a high and stable coverage and performance of the presented Microstrip Patch antenna array solution.

16-MICROSTRIP PATCH 2-D ANTENNA ARRAY

Radiation Pattern

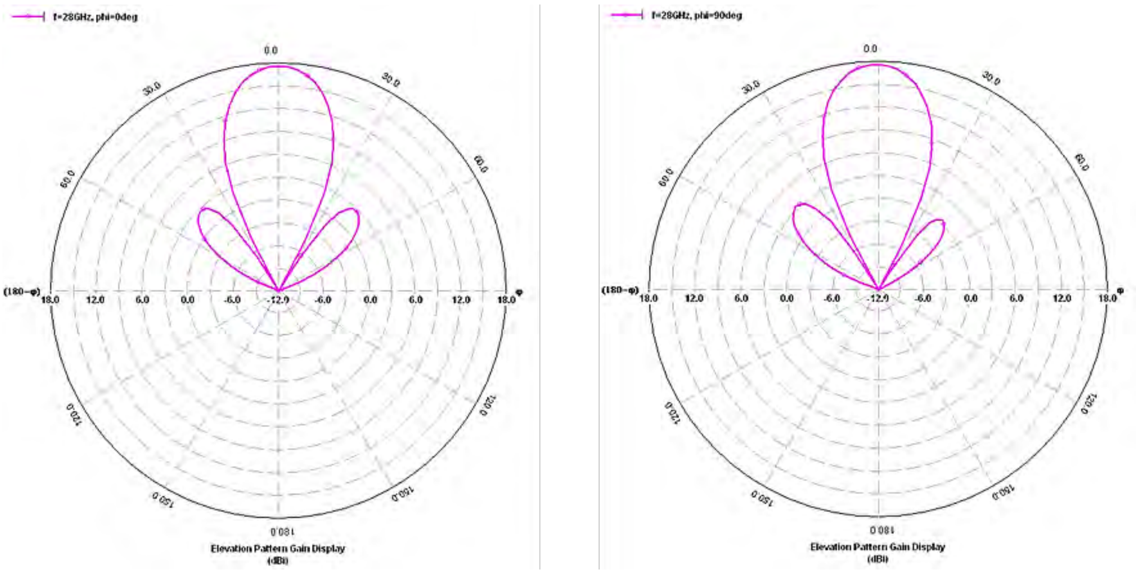

Figure 90. 16-element 2D Microstrip Patch antenna array Radiation Pattern, phi = 0° and phi = 90° respectively.

On the 4-element two-dimensional case, it has been seen that in a two-dimensional case where in both directions (X and Y) there are the same number of elements, phi = 0° and phi = 90° views have the same behavior. In the 16-element two-dimension solution, it can be observed that the maximum Gain is 17.6 dBi. Side lobes are -15dB below the main lobe maximum point, ensuring a proper radiation performance.

Directivity and Efficiency

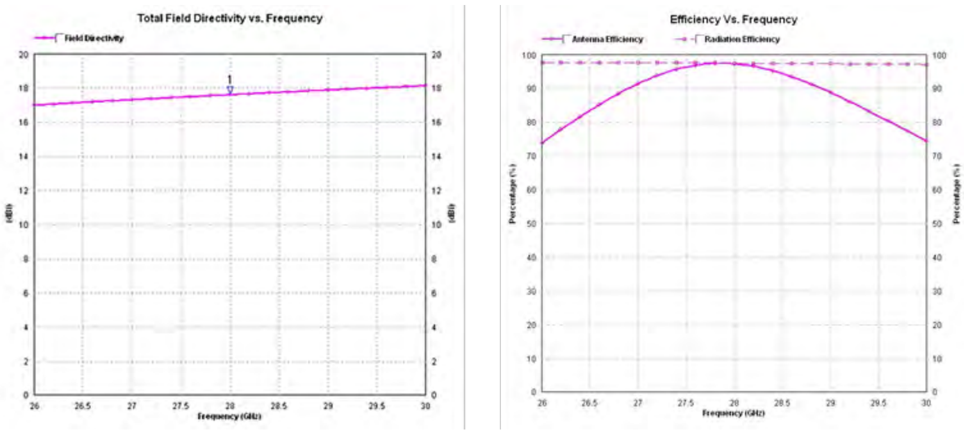

Figure 91. 16-element 2D Microstrip Patch antenna array Total Field Directivity and Efficiency respectively.

Directivity is aligned with the maximum Gain, so it is 17.6 dBi. As in all exposed cases, Antenna Efficiency is above 90% throughout the full -10dB bandwidth.

Maximum Scan Angle

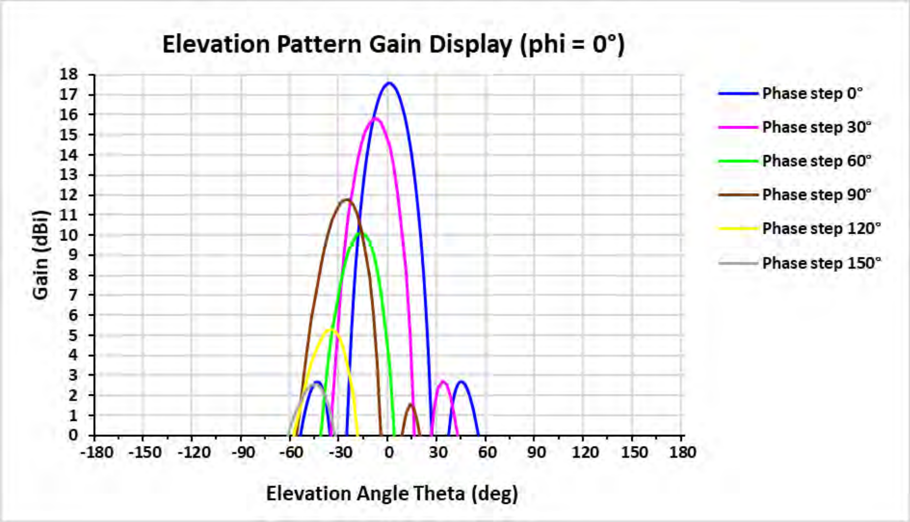

Figure 92. Maximum Scan Angle of the 16-Microstrip Patch 2D antenna array solution.

If in previous case, 16-elements linear antenna array solution, it has been confirmed that linear solutions have the same behavior and performance about the Maximum Scan Angle; moreover, from the 16-elements two-dimension antenna array it can be observed that for two-dimensional solutions the performance is decreased as soon as more elements are introduced. In this case, the Maximum Scan Angle is ±15°.

SUMMARY

Several Microstrip Patch antenna array configurations have been analyzed and presented along this section. Results show the performance variation depending on the configuration set as it can be observed in the figure below.

N-Element Antenna Type	fo	Bandwidth -10dB	Array Type	Array Total Size	Boresight Gain	Max. Scan Angle	Beam steering
4-Microstrip Patch	28GHz	2.3GHz (8.2%)	Lineal	20.1mm x 4.0mm	13.0dBi	±45°	Phase shifters
4-Microstrip Patch	28GHz	2.3GHz (8.2%)	2D	9.4mm x 9.4mm	12.1dBi	±30°	Phase shifters
8-Microstrip Patch	28GHz	2.3GHz (8.2%)	Lineal	41.5mm x 4.0mm	15.6dBi	±45°	Phase shifters
8-Microstrip Patch	28GHz	2.3GHz (8.2%)	2D	20.1mm x 9.4mm	14.9dBi	±30°	Phase shifters
16-Microstrip Patch	28GHz	2.3GHz (8.2%)	Lineal	84.3mm x 4.0mm	18.6dBi	±45°	Phase shifters
16-Microstrip Patch	28GHz	2.3GHz (8.2%)	2D	20.1mm x 20.1mm	17.6dBi	±15°	Phase shifters

Table 3. Summary of the Microstrip Patch antenna array solutions studied most important characteristics.

It has been extracted this information to properly analyze if the studied solutions would achieve the requirements set for 5G applications, as it has been presented on section 3.3. Within "Conclusions" section, it will be evaluated each solution feasibility for the upcoming 5G implementation.

4.4 Conclusions

Throughout this chapter, it has been exposed the challenges 5G demand in terms of technological requirements and specifications for its applications.

These challenges have been considered to design and analyze different solutions for 5G technology presented along this section; starting by the design of a small and high-performance single antenna element solution to thereafter integrate it in an antenna array solution.

Microstrip Patch single element has been designed considering the specifications that, in terms of performance, an antenna solution must achieve such as high gain and directivity, high efficiency, small dimensions and radiation flexibility. The results presented on section 4.2.3, validate the single element design presented as an optimal candidate to be integrated and grouped to form an antenna array solution for 5G.

Once obtained the single element which form the antenna array sought, it has been considered several Microstrip Patch antenna array configurations to achieve the specifications and characteristics set on section 3.3 and extracted from the "Review of Prior Art" analysis. These specifications have been used to properly design every antenna array solution:

- **N-elements Antenna type:** 4, 16 or greater – Microstrip Patch Antenna Array.
- **Operating frequency:** 28GHz.
- **-10dB bandwidth:** 0.5GHz to 2GHz (7.2%).
- **PCB Location:** top or bottom short edge.
- **Gain in boresight:** >12.0dBi.
- **Max scan angle:** ±60°.
- **Array type:** Linear or 2D.
- **Beam steering mechanism:** phase shifters.

The results presented within section 4.3.3, are summarized and compared with the design objectives in the table below.

	4-Microstrip Patch Lineal	4-Microstrip Patch 2D	8-Microstrip Patch Lineal	8-Microstrip Patch 2D	16-Microstrip Patch Lineal	16-Microstrip Patch 2D
N-elements	✓	✓	✓	✓	✓	✓
Op. Freq.	✓	✓	✓	✓	✓	✓
10dB BW	✓	✓	✓	✓	✓	✓
Gain	✓	✓	✓	✓	✓	✓
Max. Scan	(✓)	✗	(✓)	✗	(✓)	✗
Array Type	✓	✓	✓	✓	✓	✓
Beamsteering	✓	✓	✓	✓	✓	✓

Table 4. Microstrip Patch antenna array solutions specifications.

For instance, it has been extracted that the Maximum Scan Angle performance is better in a linear configuration than in a two-dimension configuration. In addition, it has been observed that as the number of antenna array elements increase, the maximum Gain is increased as well. Therefore, all these aspects are needed to keep in mind when designing a 5G antenna array solution.

Hence, it can be observed that all Microstrip Patch antenna array solutions designed and analyzed along this section could fit in a 5G application wireless device. They present a variety, in terms of dimensions and performance, that should be considered when selecting the required antenna array solution, analyzing the specifications desired and the device physical limitations.

5 Cover Impact on 5G Solutions

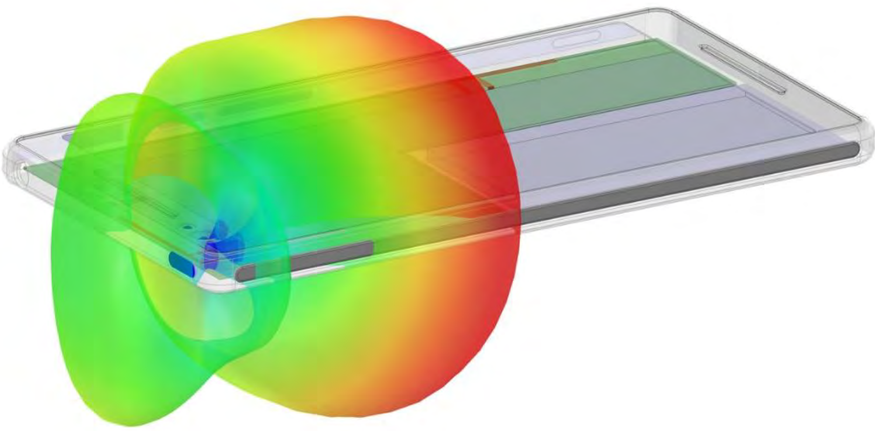

5.1 Introduction

Microstrip Patch antennas and Microstrip Patch antenna arrays are designed to be mainly implemented in a device PCB (Printed Circuit Board) due to its physical characteristics.

Therefore, and once analyzed and presented different 5G Antenna Array solutions in previous section, it is needed to characterize the behavior and the effect on the performance when the antenna solution is integrated inside a device, and hence, when a cover is placed above its radiating area.

mmW frequencies and 5G applications demand a stable and high antenna solution performance to provide the needed coverage and technical requirements. Indeed, the device cover is a critical and key point when designing the complete device, since by not choosing the correct one (type of material, thickness, etc.), the performance of the antenna solution could dramatically drop from the high performance obtained on a free-space scenario. Accordingly, product designers and RF engineers should always work together to ensure good product design but, at the same time, good radiofrequency performance.

Within this section, it is analyzed the impact of different wireless device's cover material. It is intended to characterize the 5G Antenna Array solution performance considering different covers, since when implemented in a real device, several materials can be used, so the performance must be maintained as high as possible in such different scenarios.

5.2 Cover Impact on the Array Radiation Efficiency and Radiation Pattern

At this moment in time, there are plenty of opened topics about 5G, such as new applications, impact on the daily life, frequencies bands in each region worldwide, licenses to operate, etc. which will be defined as soon as the upcoming technology starts being introduced in our life around mid-2020.

Nevertheless, in terms of performance analysis, it can be fully studied the 5G Antenna Array solution for the desired operation frequency as it has been done in previous sections and, moreover, what is presented along this section, the impact of different covers on its performance.

To characterize the impact, it has been analyzed the behavior in several scenarios, considering three material types and four different cover thicknesses.

For each case, it has been studied the Radiation Efficiency of the Microstrip Patch single element antenna and the Microstrip Patch antenna array Radiation Pattern, which are affected by the cover thickness and cover material dielectric constant, to obtain the performance of the 5G Antenna Array solution presented.

5.2.1 Design Procedure

For the purpose of correctly characterize the cover impact on the 5G Antenna Array solution designated, it is needed to clearly set a proper design procedure of the simulated set-ups to obtain the required information.

As exposed before, when placing a cover above the radiation area of an antenna, its material characteristics affect the Radiation Efficiency and the Radiation Pattern of the antenna. However, and as Antenna Theory state, it is possible to minimize the impact of the cover if its thickness is properly selected [34] . On the image below, is shown how the transmission is affected by different thicknesses in terms of wavelengths.

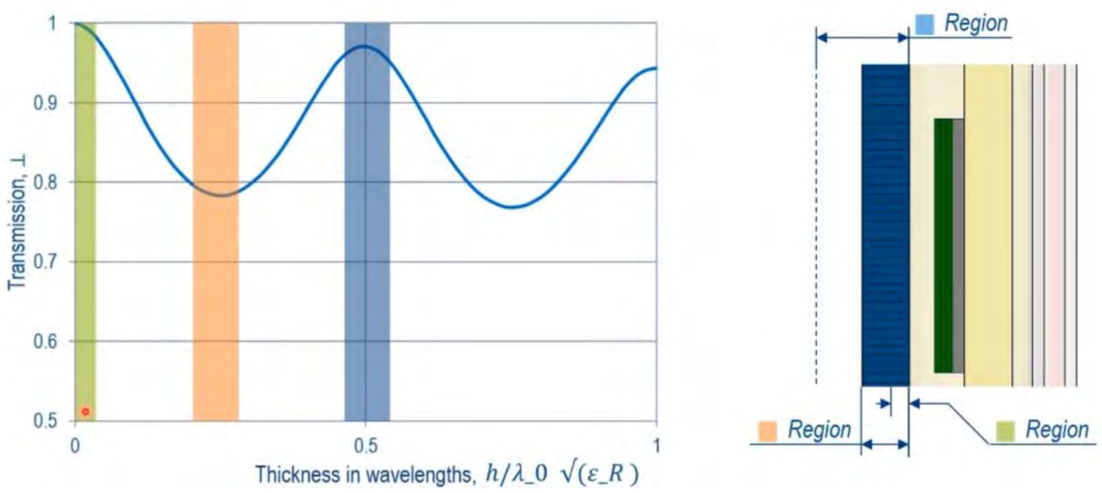

Figure 93. Transmission vs Thickness in wavelengths.

Therefore, it can be extracted than the transmission of an antenna will be maximized (i.e. cover impact minimized) every half-wavelength cycle considering the selected material dielectric constant. Hence, the cover optimal thickness to minimize its impact on the antenna performance can be defined as:

$$Optimal\ Thickness = \frac{N\lambda}{2\sqrt{\varepsilon_r}}$$

Equation 24. Optimal Thickness for a Wireless Device cover.

Along this section, three materials have been analyzed as candidates for a proper cover design to achieve maximum 5G Antenna Array performance. Their electrical characteristics are presented below [33] [34] .

- **RT/Duroid 5880:** $\varepsilon_r = 2.2$ and $tan\delta = 0.002$
- **Glass:** $\varepsilon_r = 6.84$ and $tan\delta = 0.029$
- **Aluminum Oxide:** $\varepsilon_r = 9.0$ and $tan\delta = 0.0011$

Consequently, with the electrical characteristics, it is possible to calculate the optimal thickness for each material on the first half-wavelength cycle (N = 1).

- **RT/Duroid 5880:** $Optimal\ Thickness\ RT/Duroid\ 5880 = \frac{N\lambda}{2\sqrt{\varepsilon_r}} = 3.6mm$
- **Glass:** $Optimal\ Thickness\ Glass = \frac{N\lambda}{2\sqrt{\varepsilon_r}} = 2.05mm$
- **Aluminum Oxide:** $Optimal\ Thickness\ Aluminium\ Oxide = \frac{N\lambda}{2\sqrt{\varepsilon_r}} = 1.8mm$

As it can be seen, the optimal thickness is inversely related with the dielectric constant value. On the graphic below, it is shown the trend line as the material dielectric constant increase. For instance, to achieve an optimal thickness of 1mm, the material dielectric constant would be around 29, which is high compared with the conventional wireless devices cover materials.

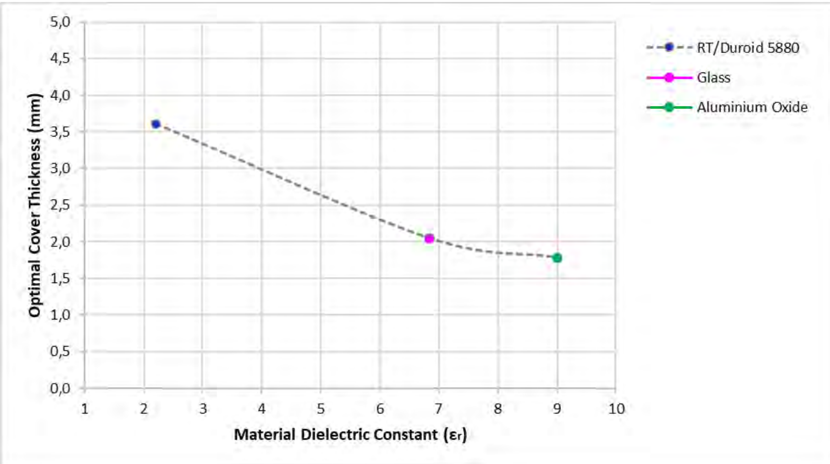

Figure 94. Optimal Thickness for the three materials considered.

Once obtained the optimal thickness for each material type, it is designed an infinite cover considering different thicknesses on top of the Microstrip Patch antenna presented on section 4.2. It has been analyzed the performance of the Optimal Thickness, 1mm, 3mm and 5mm cover thicknesses.

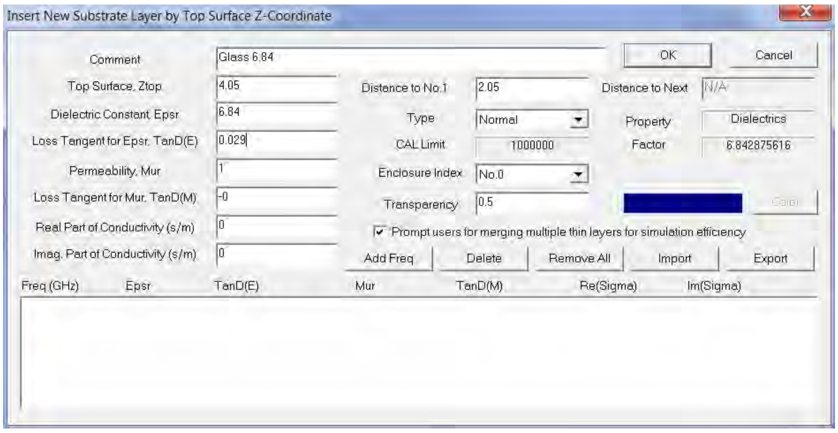

Figure 95. Example of an infinite cover layer defined on top of the Microstrip Patch single element antenna.

On IE3D MGrid tool, it has been designed all the cases of study, to properly analyze the impact on the performance. As it can be seen below, the parameters of the design have been modified to include an infinite cover at the desired height and with the desired thickness.

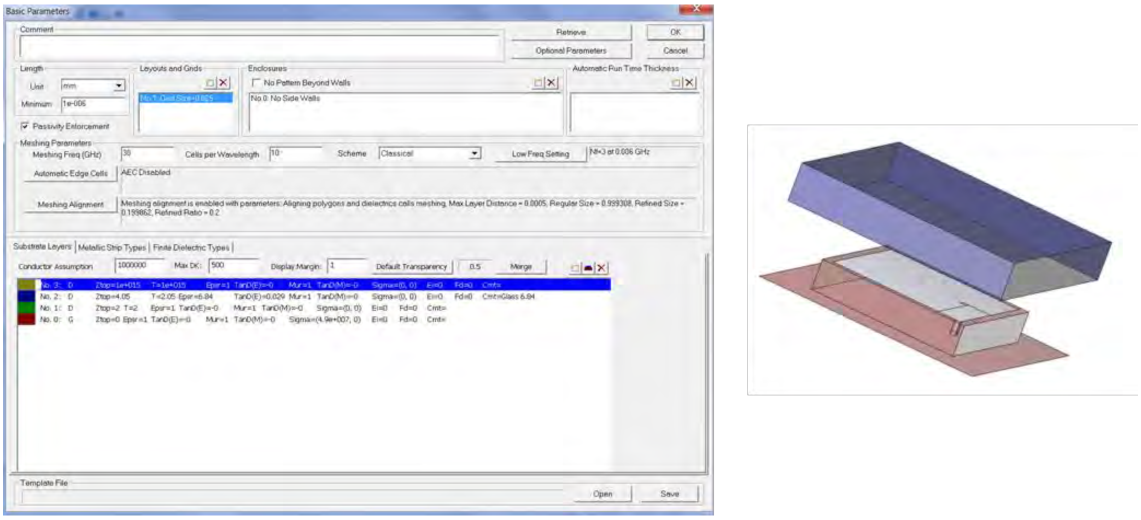

Figure 96. Example of final cover impact simulated set-up.

Microstrip Patch antenna array and its cover are defined and simulated. Thereafter, it is possible to analyze the array performance for each case of study.

The Radiation Efficiency impact is studied on the Microstrip Patch single element antenna, since, as it has been exposed on previous sections, the PatternView "Array Pattern Calculation" tool does not consider mutual couplings of the array, which make impossible to obtain an accurate Radiation Efficiency.

On the other hand, following the process exposed on section 4.3.1, it has been characterized the 8-Microstrip Patch Linear antenna array solution presented on 4.3, since its configuration and performance lead to an optimal candidate for a 5G Antenna Array solution.

Finally, 2D Radiation Pattern view is used to obtain the antenna array lobes and gain in boresight for the specific Microstrip Patch antenna array with every cover case.

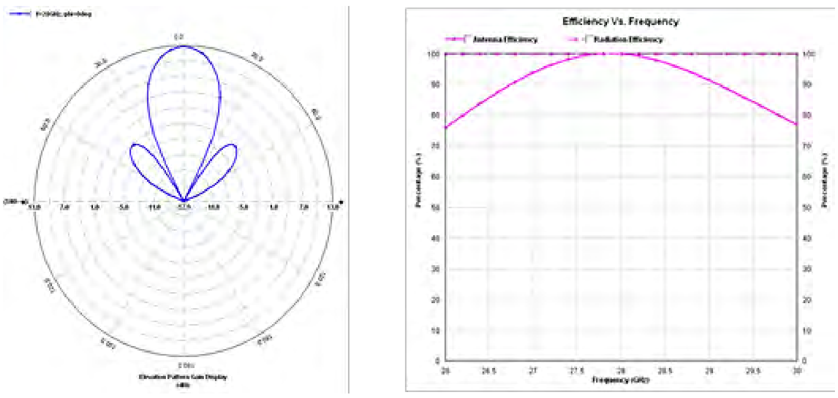

Figure 97. Example of 2D Radiation Pattern and Efficiency graphs.

5.2.2 Simulation Set-ups

Throughout the design phase, several materials with different thicknesses have been calculated to study their impact on the 8-Microstrip Patch antenna array solution designed for 5G applications.

As exposed on the "Design Procedure", in the case of study it has been selected three material types: RT/Duroid 5880, Glass and Aluminum Oxide, and with four different thicknesses: optimal for each material, 1mm, 3mm and 5mm.

To analyze the impact of the cover, it has been simulated the Microstrip Patch single element antenna used on previous section to create the antenna array solutions, including an infinite cover on top of it. Thereafter, it is characterized the antenna array for each simulated scenario.

RT/Duroid 5880

First material analyzed is the RT/Duroid 5880. This material has been also used as the substrate material for the Microstrip Patch single element antenna, since its electrical characteristics allow to ensure small dimensions on the design for 5G application.

$$\varepsilon_r = 2.2 \text{ and } tan\delta = 0.002$$

Equation 25. Dielectric Constant and Loss Tangent of RT/Duroid 5880.

Hence, four different RT/Duroid 5880 covers for each thickness have been designed:

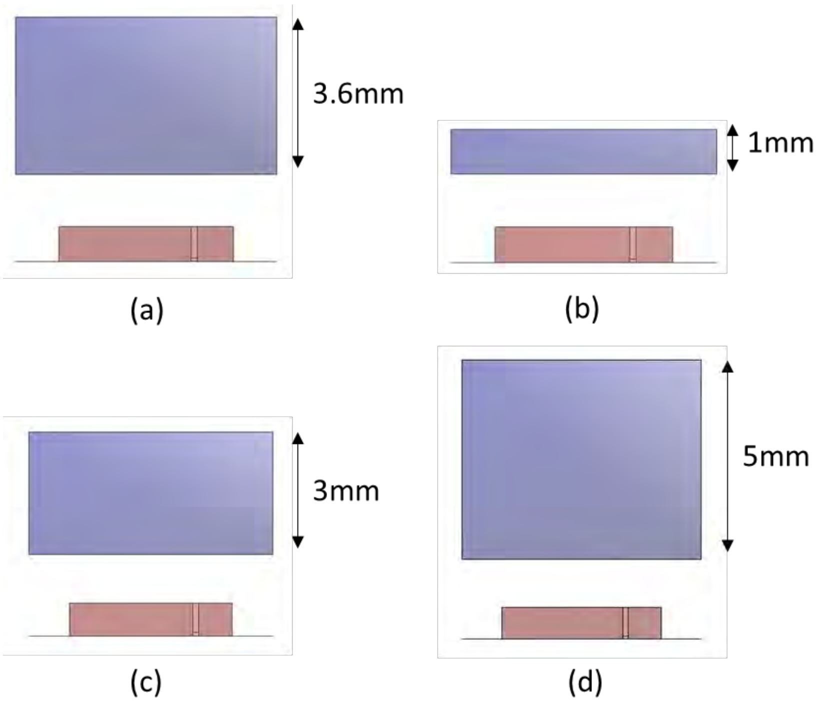

Figure 98. (a) Optimal Thickness, (b) 1mm, (c) 3mm, (d) 5mm, thicknesses simulated for RT/Duroid 5880 cover material.

Glass

As a second case, it has been selected Glass material, since it presents great electrical conditions to achieve an optimal thickness assumable for product designers.

In addition, its physical characteristics make them a great candidate to be selected. Moreover, most of the current smartphone solutions are designed with this type of material.

Glass dielectric constant and loss tangent are presented below:

$$\varepsilon_r = 6.84 \text{ and } tan\delta = 0.029$$

Equation 26. Dielectric Constant and Loss Tangent of Glass.

Its Optimal Thickness has been exposed previously in this section and it is around 2mm. In addition to the 2mm cover case, it has been also simulated the 1mm, 3mm and 5mm cases as it has been done with the RT/Duroid 5880; since by doing so, it is possible to measure the performance for each different material with same cover thickness characteristics.

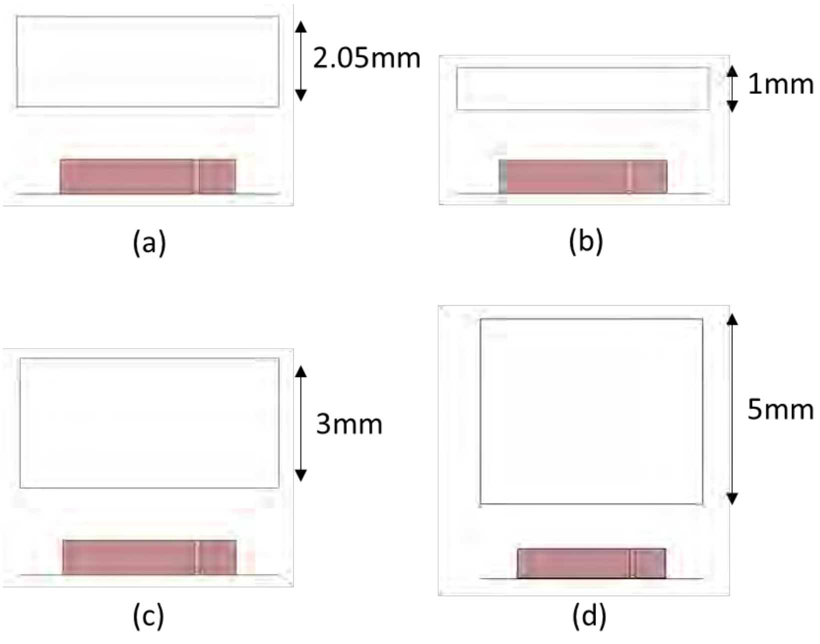

Figure 99. (a) Optimal Thickness, (b) 1mm, (c) 3mm, (d) 5mm, thicknesses simulated for Glass cover material.

In this concrete case, it has been simulated practically all thicknesses ranges feasible to be implemented on a real wireless device; since if the cover to be implemented is thicker than 5mm, the complete device would be extremely big for human being interaction.

Nevertheless, in some applications it could be needed to integrate the 8-Microstrip Patch antenna array into a device with thicker cover than 5mm; for example, for military devices, hard-condition device, etc.

Aluminum Oxide

Finally, it has been selected an extreme candidate, since it is a metallic component, with a really high dielectric constant. It is important to test such a scenario, since it enables to evaluate cases which maybe are not considered.

$$\varepsilon_r = 9.0 \text{ and } tan\delta = 0.0011$$

Equation 27. Dielectric Constant and Loss Tangent of Aluminum Oxide.

As on previous cases, the optimal thickness is evaluated together with other cover thickness cases.

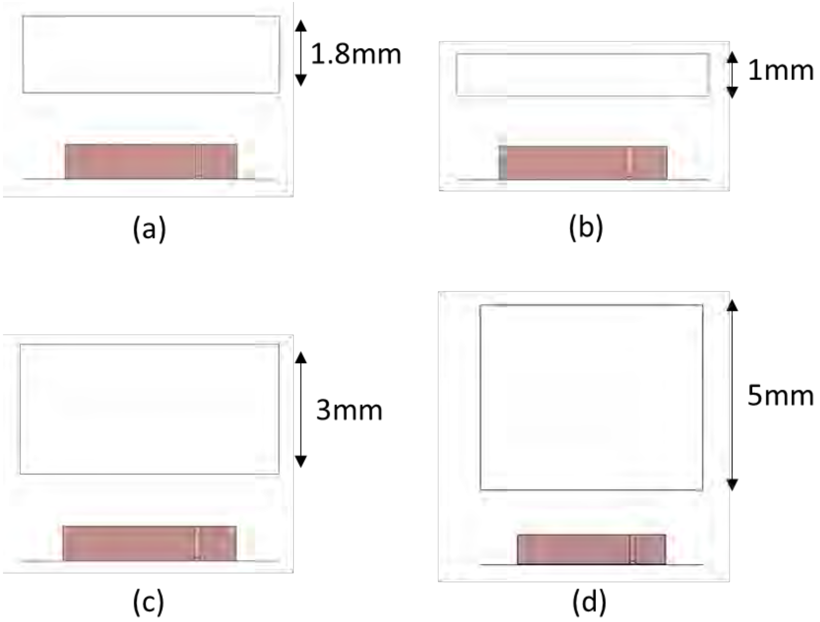

Figure 100. (a) Optimal Thickness, (b) 1mm, (c) 3mm, (d) 5mm, thicknesses simulated for Glass cover material.

8-Microstrip Patch Array characterization

To generate the 8-Microstrip Patch linear antenna array, on "Array Pattern Calculation" tool it is needed to add the array elements with the previous characteristics as it has been explained on page 54.

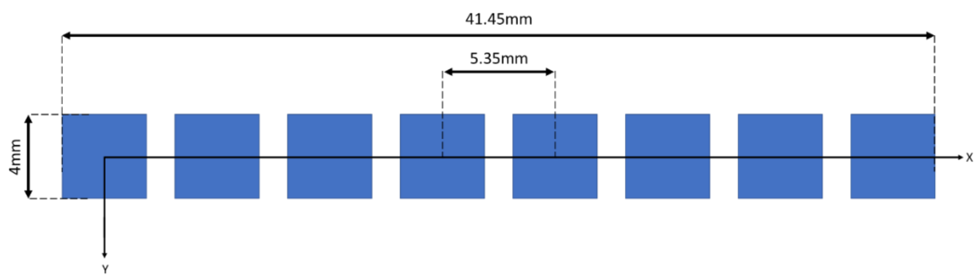

Figure 101. 8-element linear antenna array analyzed along this section.

5.2.3 Results

Within previous section, it has been exposed all the different thicknesses studied per each material. At this time, it is presented how each case affect the 8-Microstrip Patch antenna array performance.

As it has been done along this report, different figures are shown to analyze the performance and, in this case, the impact of each cover studied. For the case of study, it is presented the Efficiency and Radiation Pattern.

COVER IMPACT ON THE RADIATION EFFICIENCY

Due to a limitation with the PatternView "Array Pattern Calculation" tool, it is not possible to analyze the effect on the 8-Microstrip Patch antenna array Radiation Efficiency of the cover, since no mutual couplings are considered. Nevertheless, it is studied each cover case impact on the single element, which lead to an approach of the final array Efficiency performance.

RT/Duroid 5880

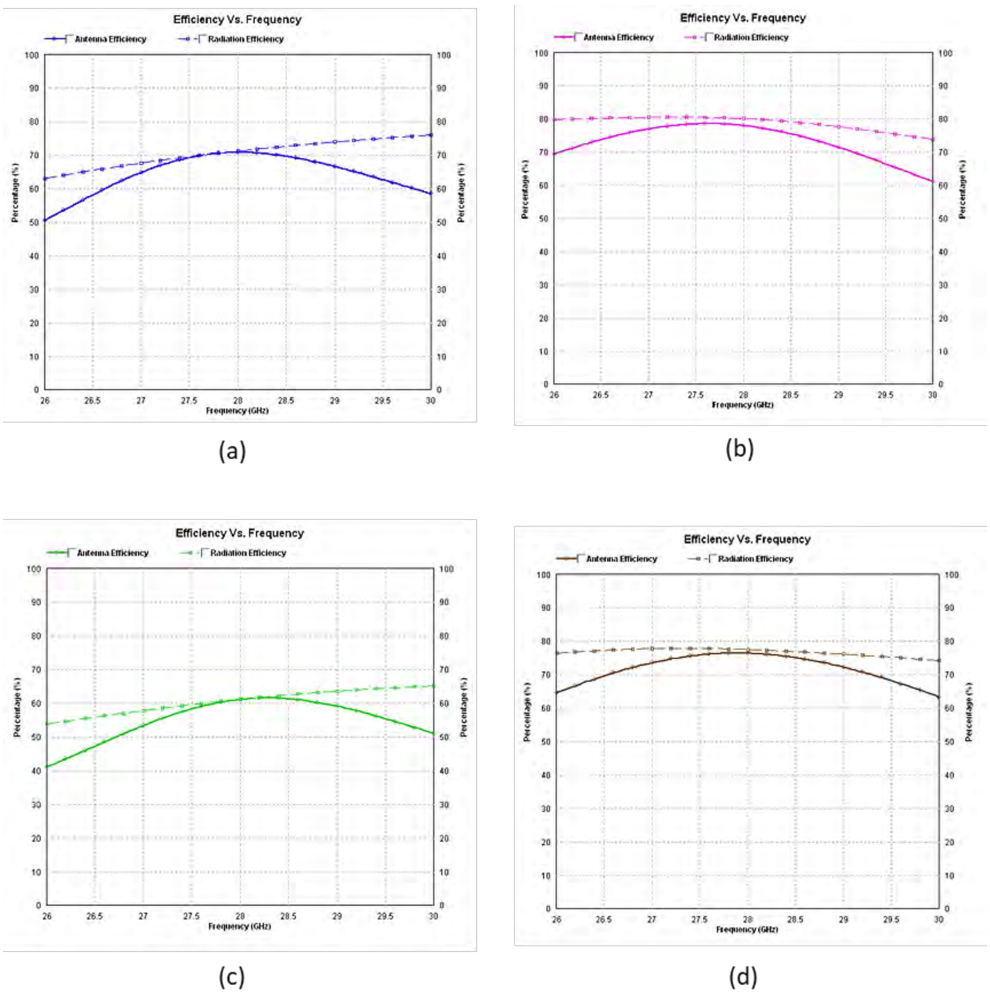

Figure 102. RT/Duroid Efficiency: (a) Optimal Thickness, (b) 1mm, (c) 3mm and (d) 5mm.

Four Efficiency vs Frequency plots are presented for each cover thickness studied. As it can be seen, the Antenna Efficiency in all cases is practically equal to the Radiation Efficiency at 28GHz, which means that the Microstrip Patch antenna is not distorted in terms of antenna impedance. Radiation Efficiency is stabilized around 60% - 80% regardless the cover thickness considered. Hence, it can be considered a candidate when a device has different casing configurations, since its performance will be maintained for different cases.

Glass

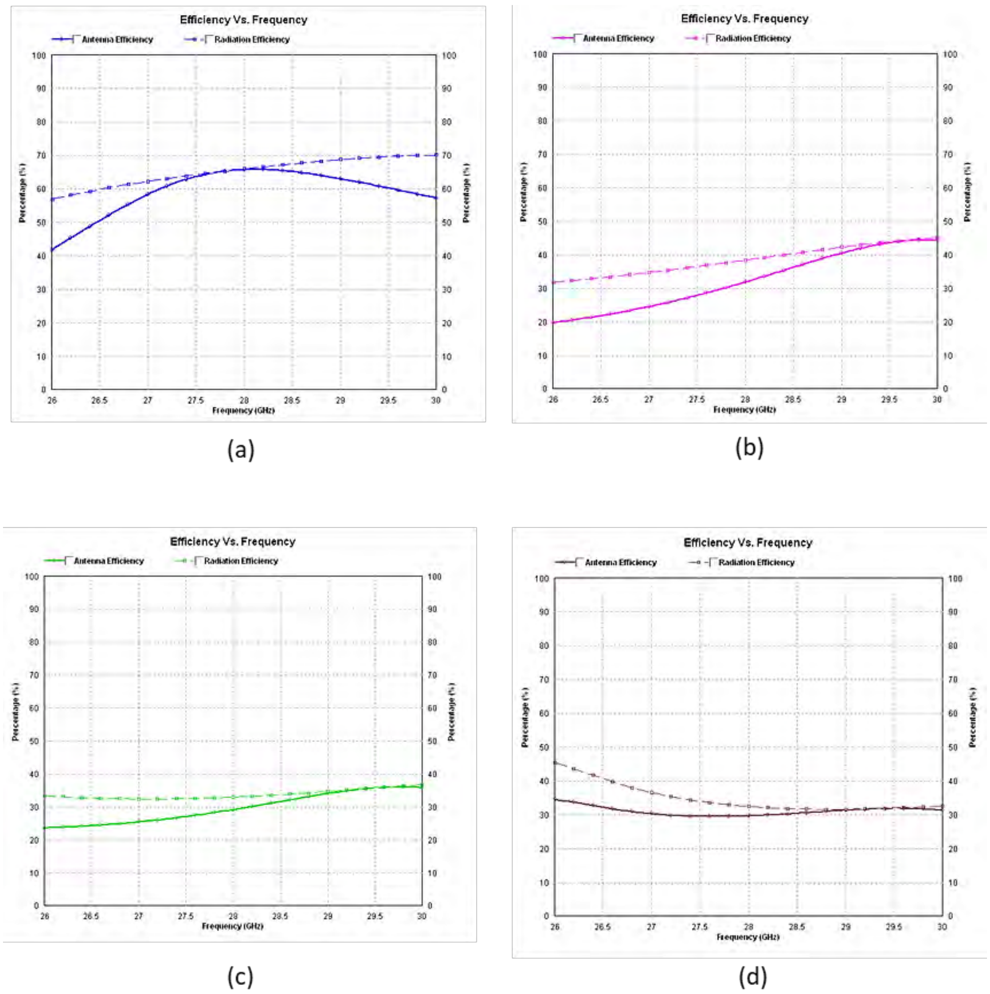

Figure 103. Glass Efficiency: (a) Optimal Thickness, (b) 1mm, (c) 3mm and (d) 5mm.

On the second case of study, it is observed a great variance on the Radiation Efficiency for each cover thickness scenario. For the Optimal Thickness, the Radiation Efficiency reaches to 66%. But, on the other thicknesses analyzed, it is faced a fall in performance since the Radiation Efficiency is below 40% in 1mm, 3mm and 5mm cases.

Therefore, on the Glass as cover material scenario, it is clearly seen the impact on the Microstrip Patch antenna Radiation Efficiency when the thickness is not considered for an optimal radiofrequency environment.

Aluminum Oxide

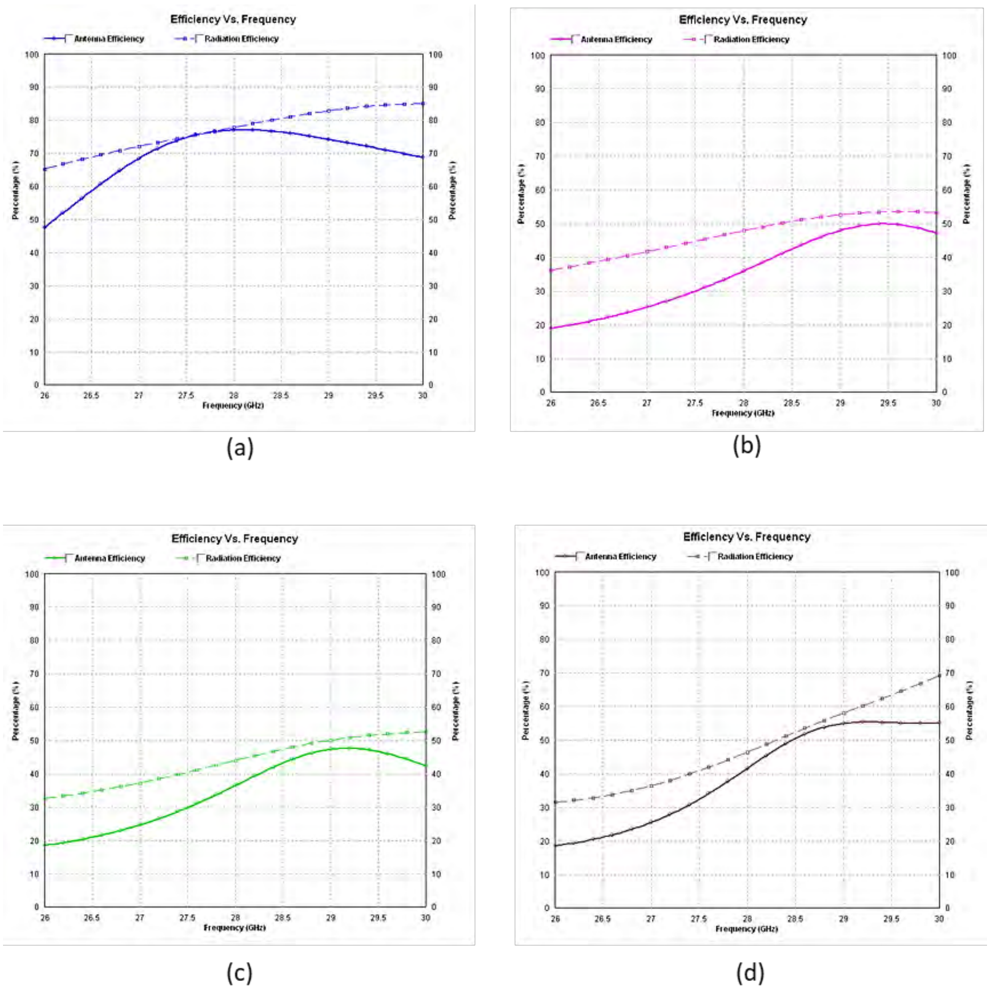

Figure 104. Aluminum Oxide Efficiency: (a) Optimal Thickness, (b) 1mm, (c) 3mm and (d) 5mm.

Finally, as a third material cover scenario, it has been analyzed the impact in the case that a metallic component, such as Aluminum Oxide, is used as a material for a wireless device cover on top of the Microstrip Patch antenna.

Surprisingly, when an Optimal Thickness is considered, Radiation Efficiency goes up to 78%, becoming the highest Radiation Efficiency value at 28GHz of the three materials and different thicknesses studied along this section, together with the 1mm RT/Duroid 5880 scenario.

On the other hand, it is significant the distortion on the Radiation Efficiency for the other use cases presented; since the its values go down until 50%. Even more, it is seen how the antenna impedance is being deformed, since the Antenna Efficiency separates from the Radiation Efficiency at 28GHz.

Hence, Aluminum Oxide could be an optimal candidate when the cover thickness is fixed and deeply analyzed the impact on the antenna performance, because otherwise, many problems could appear in terms of antenna impedance mismatch and failure on the performance.

COVER IMPACT ON THE RADIATION PATTERN

Once it has been analyzed the different covers' impact on the Microstrip Patch antenna Radiation Efficiency, it is time to present the results of the analysis regarding the covers' impact on the Radiation Pattern, i.e. the impact on the 8-Microstrip Patch linear antenna array radiation shape and maximum gain. On free-space, the 8-Microstrip Patch linear antenna array maximum Gain is 15.6dBi.

RT/Duroid 5880

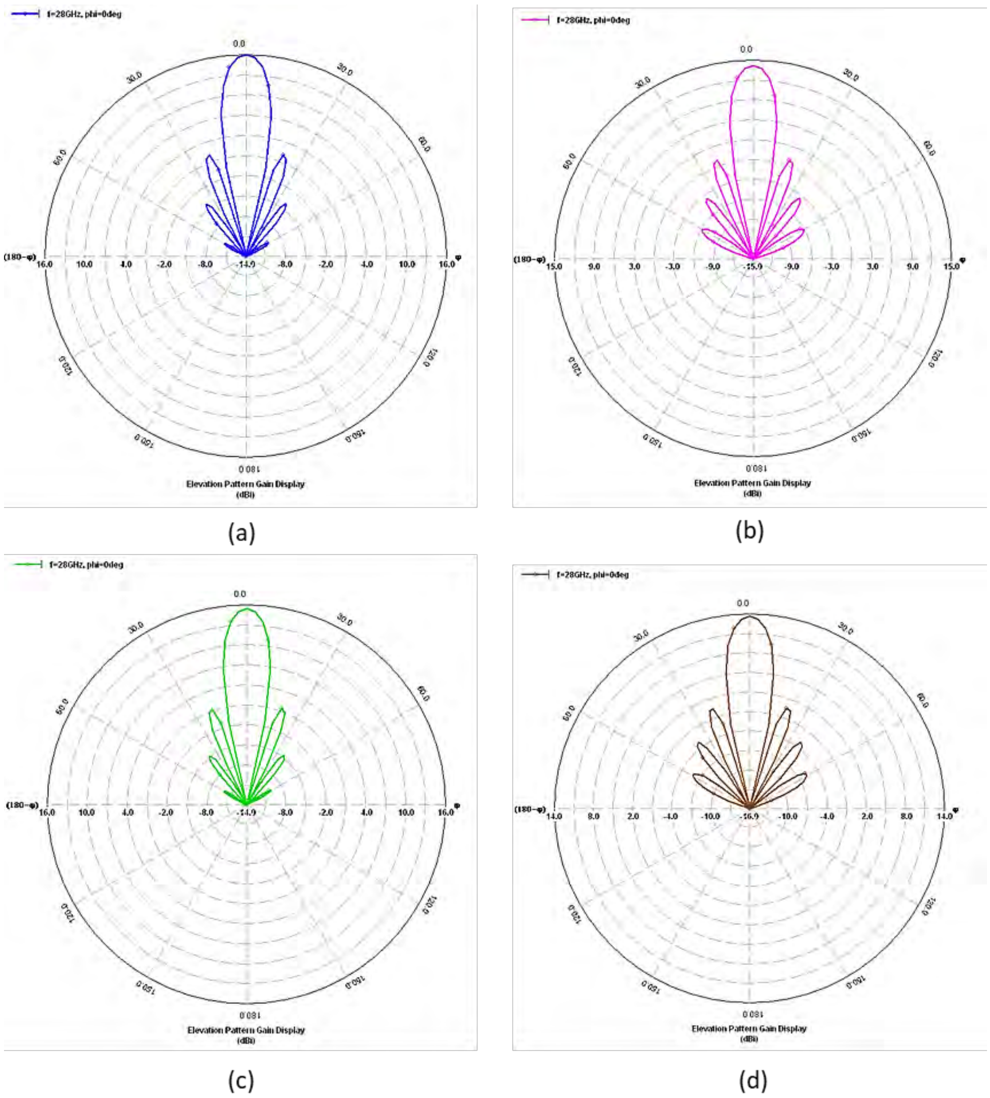

Figure 105. RT/Duroid 5880 Radiation Pattern on phi = 0°: (a) Optimal Thickness, (b) 1mm, (c) 3mm and (d) 5mm.

It can be observed that the Radiation Pattern forms on phi = 0° view are maintained from the once on free space, mainly on the Optimal Thickness and 3mm cases, since the 3mm case is close to the optimal thickness calculated for the RT/Duroid 5880. On the other hand, on cases 1mm and 5mm, side lobes become greater due to the reduction of the main lobe. This phenomenon could affect antenna array performance.

Regarding the maximum Gain for each cover thickness scenario, it can be extracted from the plots presented above that Optimal Thickness present a maximum Gain of 16.0dBi, a Gain even higher than the one obtained in free space. Otherwise, the 1mm and 5mm cases present a maximum Gain below 15.0dBi while the 3mm case gets close to the optimal thickness performance with a maximum Gain of 15.4dBi.

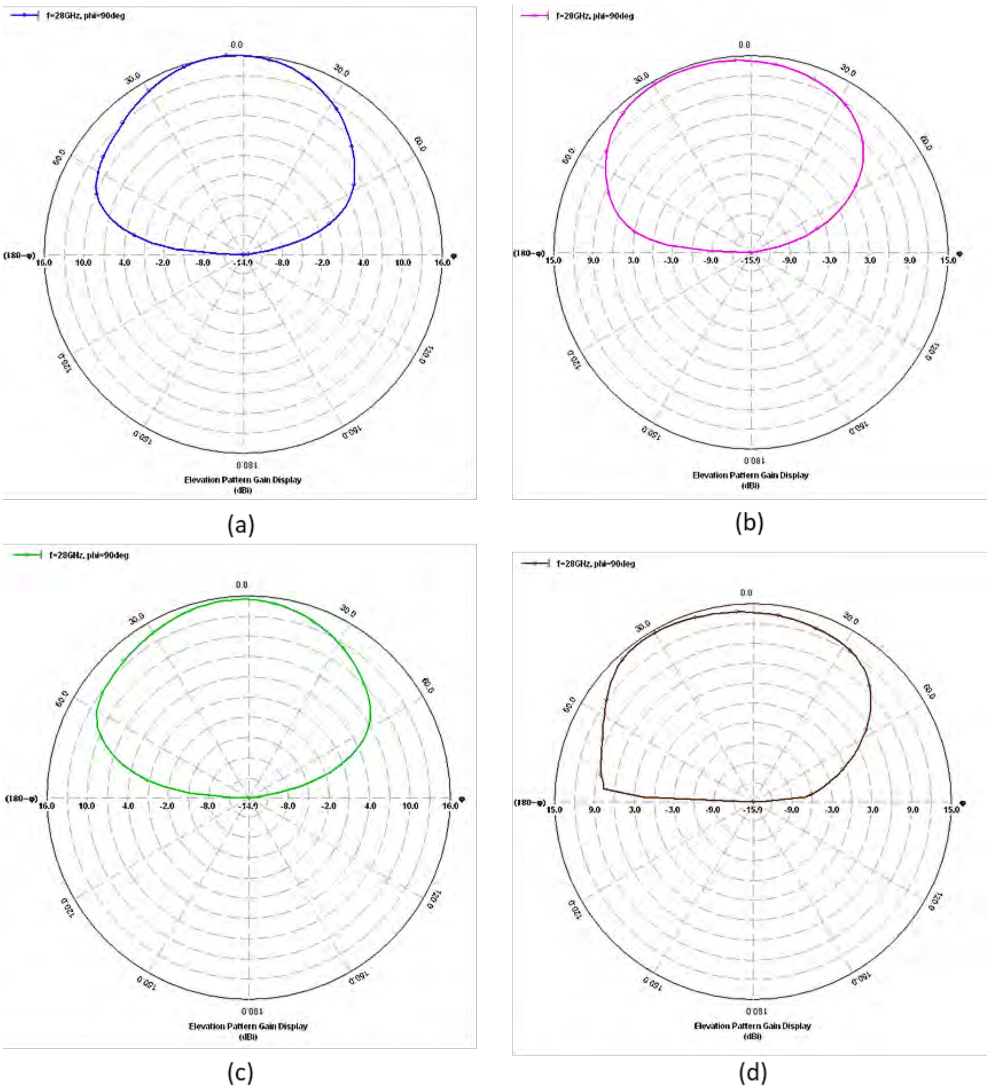

Figure 106. RT/Duroid 5880 Radiation Pattern on phi = 90°: (a) Optimal Thickness, (b) 1mm, (c) 3mm and (d) 5mm.

From the phi = 90° views, it can be observed the deviation of the Radiation Pattern for the different cover thickness analyzed. On the Optimal Thickness and 3mm case, it can be seen that the main power is being radiated on zenithal direction, while on the 1mm and 5mm case, the radiation pattern is being deviated to the left part of the pattern.

This is due to the “radiofrequency wall” that the 8-Microstrip Patch antenna array is facing, since its thickness is not optimized for the use of the RT/Duroid 5880 material.

Glass

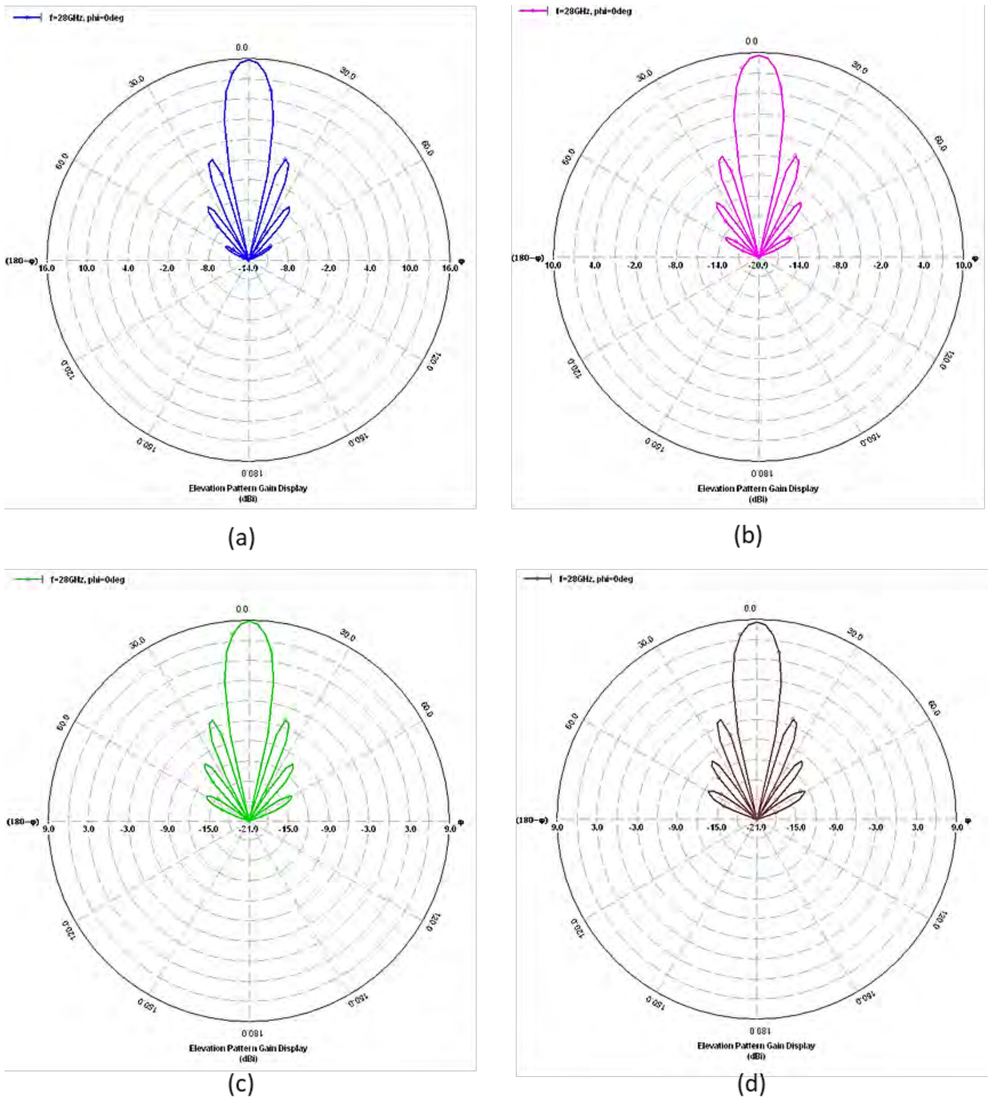

Figure 107. Glass Radiation Pattern on phi = 0°: (a) Optimal Thickness, (b) 1mm, (c) 3mm and (d) 5mm.

On the second material scenario with Glass' covers, it is observed from the phi = 0°, as it has been seen on the Radiation Efficiency impact, that the cover thickness really impacts the 8-element antenna array performance when it is not set as the calculated optimal thickness; since side lobes become greater and main lobe is reduced due to the cover.

For the Optimal Thickness it is obtained a maximum Gain of 15.9dBi, again above from the free space environment and extremely close from the RT/Duroid Optimal Thickness performance.

Regarding the 1mm, 3mm and 5mm cover thickness cases, it is observed a reduction on the maximum Gain that lead to be below 10dBi; which means that the maximum Gain is reduced by 6dBi, i.e. by a factor of 4 due to the cover presence.

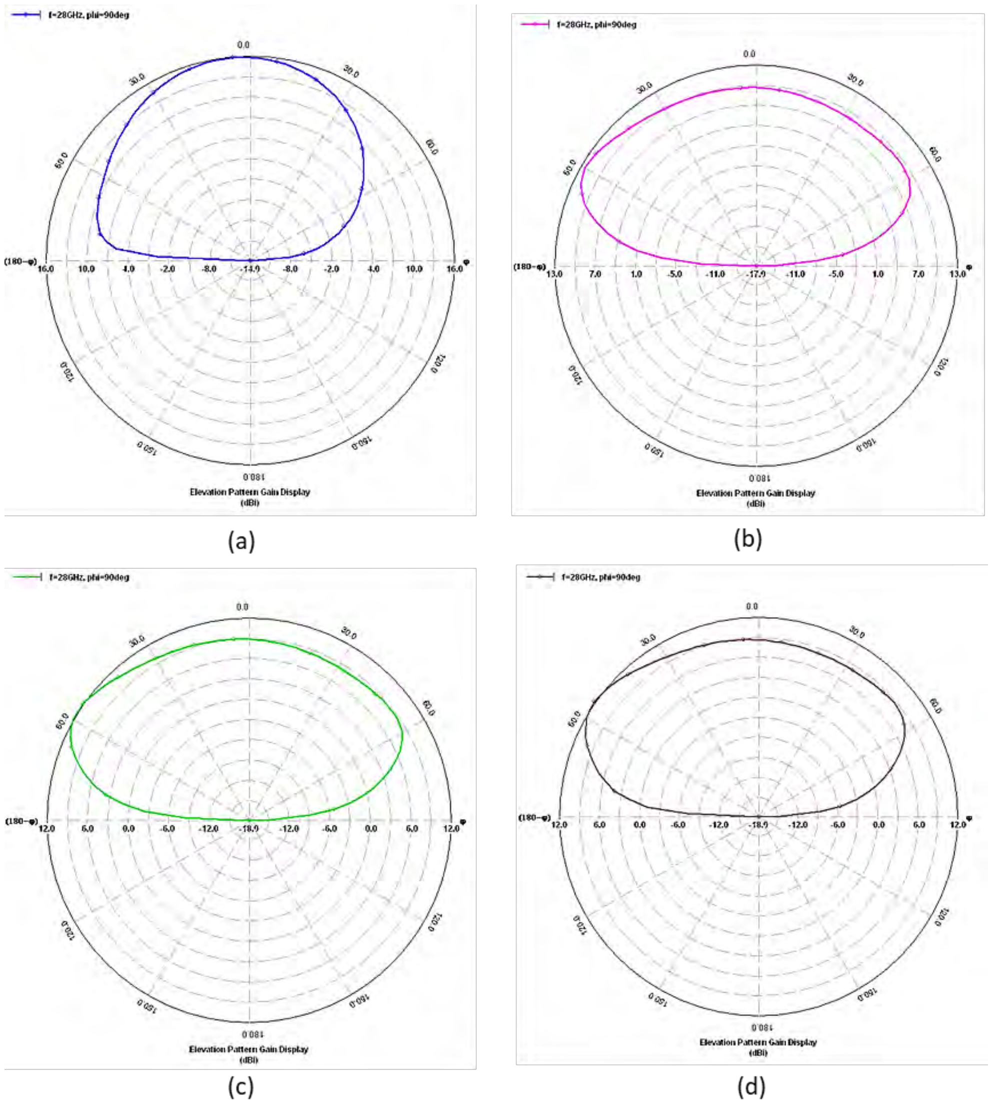

Figure 108. Glass Radiation Pattern on phi = 90°: (a) Optimal Thickness, (b) 1mm, (c) 3mm and (d) 5mm.

If it is observed the behavior on the phi = 90° views for the Glass material different cover thicknesses, it is seen that for the cases where the optimal thickness is not set, there is a deviation of the power radiated to the sides of the zenithal direction. The Radiation Pattern becomes flatter, leading to a drop of the maximum Gain on the desired direction as the 8-Microstrip Patch linear antenna array has been designed.

On the other hand, when the cover is designed to the optimal thickness calculated previously along this section, the Radiation Pattern does not face a deviation of the main lobe; since the cover becomes transparent in terms of wavelength for the 8-element antenna array transmission.

Therefore, if the Glass $\varepsilon_R = 6.84$ and $tan\delta = 0.029$ is selected as a cover material for a wireless device, it should definitely be considered the optimal thickness; since if the cover is set optimally, this material achieves a great tread off between antenna array performance and cover thickness.

Aluminum Oxide

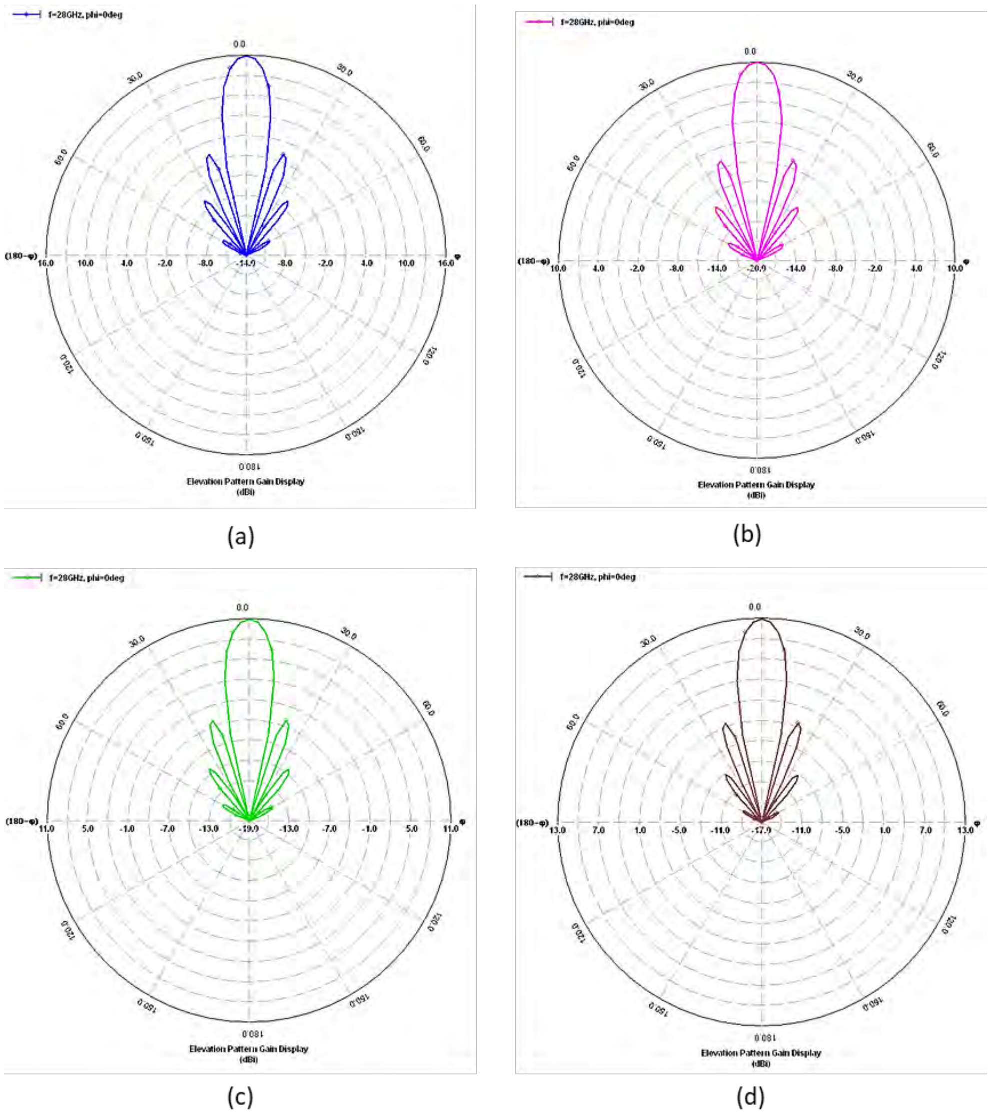

Figure 109. Aluminum Oxide Radiation Pattern on phi = 0°: (a) Optimal Thickness, (b) 1mm, (c) 3mm and (d) 5mm.

Finally, it is presented the results obtained from the Aluminum Oxide different cover thicknesses simulations and their effect on the 8-Microstrip Patch linear antenna array. This case is particularly interesting since it is a metallic component, so in principle it should extremely affect the antenna array performance.

Nevertheless, and as it is seen on the phi = 0° views, maximum Gain on the Optimal Thickness scenario is maintained up to 16.0dBi; same behavior has been observed for the other two materials studied on the optimal thickness case.

But, when the thickness is varying and is far from the optimal value, the maximum Gain is reduced below 13dBi; i.e. half of the optimal, and moreover, side lobes are reduced too. Hence, the cover is affecting the performance equally on the whole radiation pattern for the 1mm, 3mm and 5mm case.

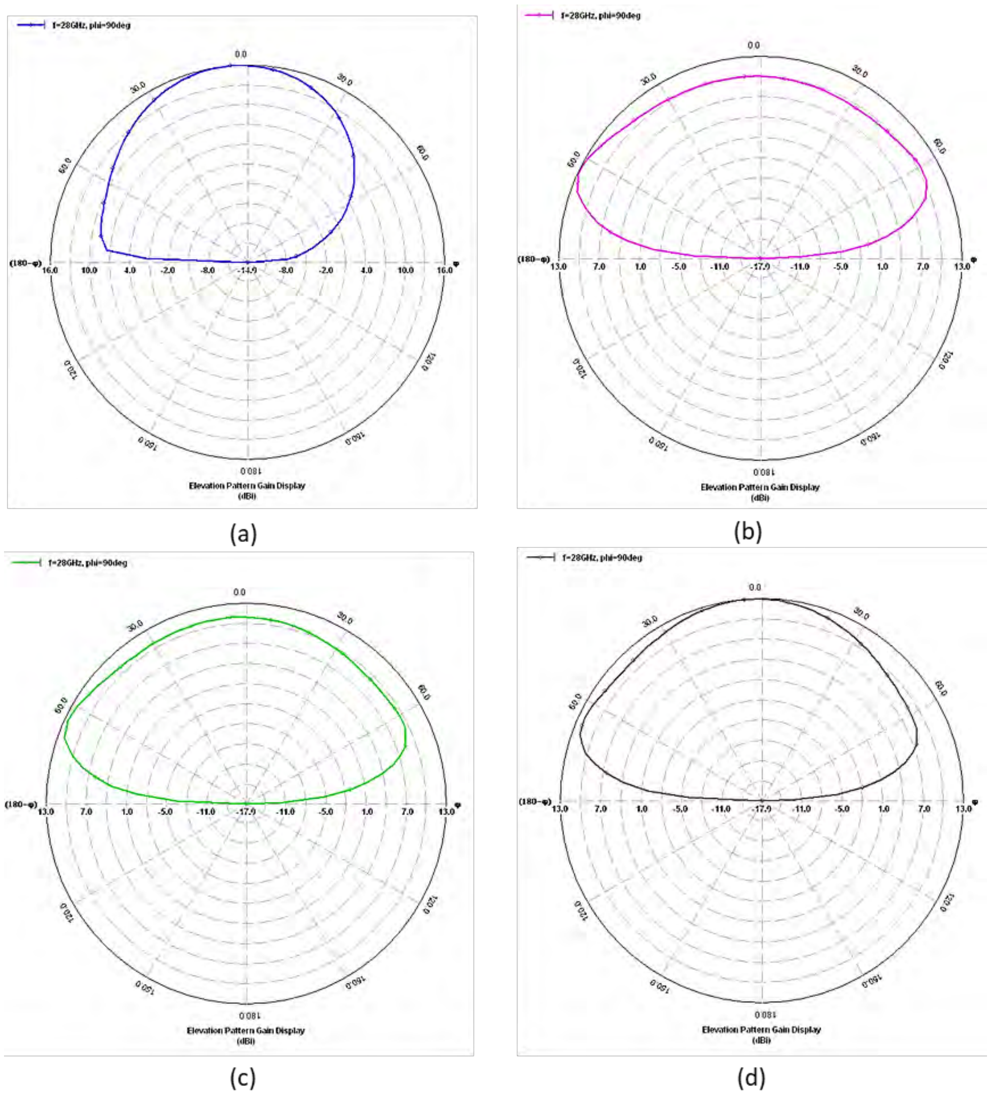

Figure 110. Aluminum Oxide Radiation Pattern on phi = 90°: (a) Optimal Thickness, (b) 1mm, (c) 3mm and (d) 5mm.

Aligned with previously shown phi = 0° views, if it is observed the 8-element linear antenna array performance on the phi = 90° views for the Aluminum Oxide cover thicknesses, it can be seen that the Optimal Thickness direction of radiation is maintained on zenithal direction as it has been observed with other materials.

However, in contrast, for cases of 1mm, 3mm and 5mm, the Radiation Pattern is deviated and becoming flatter. Hence, the performance of the antenna array is affected and reduced from the ideally designed.

Accordingly, Aluminum Oxide is a candidate to consider for product designers when modeling a new wireless device; since its performance as a cover, if the optimal thickness is selected, has been shown that can perfectly replace any other type of cover material. Even more, and due to its high dielectric constant, it allows to reduce the cover thickness to be optimal up to 2mm, dimensions that could ideally fit on a 5G wireless device design.

5.3 Conclusions

Nowadays, when a new product is being developed, there are many characteristics that should all merge to finally achieve the desired product for all parts involved in the project, such as performance, usability, design, etc. For the upcoming 5G technology, this will not change; even more, there will be more aspects to consider every time a product feasibility and design will be analyzed due to the complexity and highly demanding technical requirements (section 1.3.1).

For the case of study of this project, it has been considered the impact of the wireless device cover; since, from the antenna solution point of view, it is the most critical part which can affect the antenna performance because it sits directly on top of the antenna in most of the cases. Four cover thicknesses of three materials with different electrical characteristics have been studied to characterize the impact of a wireless device cover. For each material, it has been considered its Optimal Thickness (calculated from each material electrical characteristics), 1mm, 3mm and 5mm.

These several scenarios have been studied to analyze the cover impact on the Microstrip Patch antenna array solution Radiation Efficiency, to observe the effect on the antenna impedance; and Radiation Pattern, which is modified due to the presence of the cover.

The results presented within this section show that the Radiation Efficiency is affected in a more intense manner depending on the cover thickness simulated. As it can be seen on Figure 111 below, for both Aluminum Oxide and Glass, there is a huge difference in performance when the thickness is considered as the optimal; in fact, when an Aluminum Oxide 1.8mm cover thickness is used the Radiation Efficiency of the antenna array is close to 80%.

Otherwise, on the RT/Duroid 5880 scenario, it is observed a variation on the Radiation Efficiency which does not match with the behavior seen for the other materials, since for the optimal thickness case it is achieved a Radiation Efficiency below that the 1mm and 5mm cover thickness scenario.

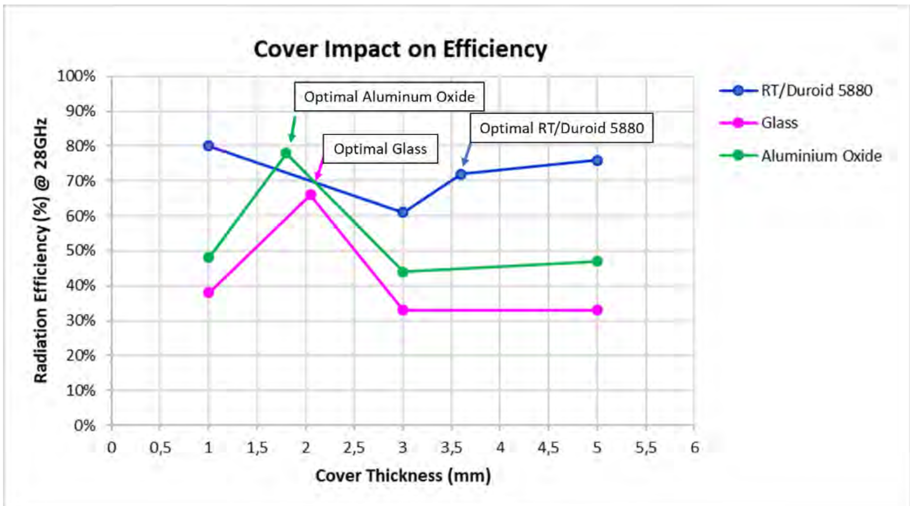

Figure 111. Materials cover thicknesses impact on the Radiation Efficiency.

In addition, it has been analyzed the cover impact on the 8-Microstrip Patch linear antenna array solution Radiation Pattern, to characterize the deviation and the effect on the main lobe and maximum Gain, since it is a key point for a successful 5G Antenna Array solution.

In this case, it has been observed the expected behavior: when the cover thickness is set to the Optimal Thickness, the impact on the 8-element antenna array is minimized; therefore, the performance of the antenna array solution is maximized, which validates what has been exposed on section 5.2.1: the transmission of an antenna is maximized every half-wavelength cycle of the cover thickness. As it is shown on the image below, for all materials studied, there is a maximum on the optimal case obtaining a maximum Gain of 16.0dBi in all cases.

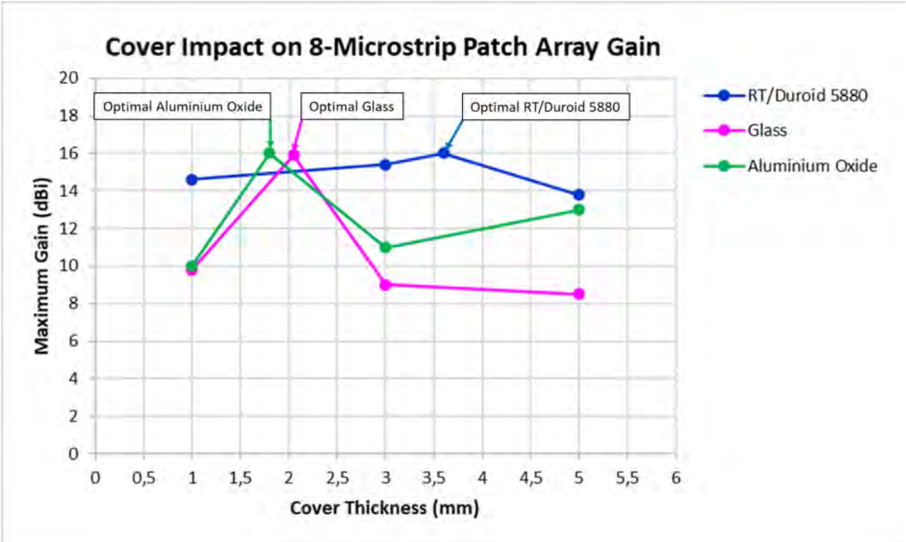

Figure 112. Materials cover thicknesses impact on the Maximum Gain.

Hence, and considering the results obtained from both the Efficiency and the Maximum Gain cover impact, it is observed that, surprisingly, the Aluminum Oxide present the best combination between minimum cover thickness and maximum antenna array performance; since when a 1.8mm cover thickness is considered its Radiation Efficiency goes up to 80% and the maximum Gain is maintained close to 16.0dBi.

Nevertheless, it should be deeply analyzed the impact of the cover material and thickness for every different antenna solution and wireless device; since every scenario could extremely change from another previously considered.

6 Conclusions

6.1 Introduction

Our world is changing day by day so fast, that new applications and technologies show up in a way that technological companies and research centers must be focused on being as updated as possible to keep track of the market demands.

The project presented has been developed within the scope of the necessity to achieve the goals and challenges that the upcoming 5G technology, which will be a reality in mid-2020, requires from an antenna solution point of view.

Consequently, it has been set a path to follow during the project and its investigation to clearly consider and establish the objectives wanted to achieve; focusing on what has been done so far, to properly design and analyze the 5G Antenna Array solution and its implementation, and exposing different solutions to cover as maximum as possible of the market demands.

Within this section, it is intended to summarize the complete investigation and the results obtained, to clearly see the objectives set and achieved along this project.

6.2 Final Conclusions

As it has been already exposed, this project aimed to investigate a feasible antenna solution for the upcoming 5G technology, focusing on the importance of the challenges that this technology demands. This project was presented as a great opportunity to "get on the wave" of 5G, conducting a research and development of a solution for plenty of new applications.

When the project topic and scope were defined, several objectives were set to satisfactorily success on the project execution. Before starting with the design of an antenna array solution, it was needed to understand what 5G is and which requirements will present from a technical point of view. Henceforth, and once set the basis of what has been studied, it has been analyzed the current antenna solutions present in the market to finally establish the technical goals for a future 5G implementation of the antenna array.

For the purpose of achieving the objectives of the project, it has been defined and scheduled the project steps which have been closely followed along the project development. Steps containing parts to be executed, meetings and deadlines have been considered. This has helped to properly structure and focus the efforts, leading to an extraordinary organization of each project phase.

One of the key parts of any investigation is to review the State of the Art of the field where the project is being conducted. From the analysis done and exposed in section 3 of this report, it has been extracted the **main characteristics a 5G antenna solution presents** on the current market, such as **huge bandwidth, high directivity/gain** and **beam steering technique**. These characteristics have been established as an objective for the 5G Antenna Array design.

Throughout the analysis and design of a 5G Antenna Array done in section 4, it has been studied the single element which has been grouped to form several antenna array solutions. The **Microstrip Patch antenna single element** has been designed to **resonate at 28GHz** with **small dimensions (4mm x 4mm)**, huge **-10dB bandwidth (2.3GHz)** and **high Efficiency** performance, being an optimal candidate for the Microstrip Patch antenna array.

Several **Microstrip Patch antenna array configurations** have been analyzed and presented, considering **4**, **8** and **16 elements** on both **linear** and **two-dimension** configurations. Obtaining high Efficiency performance, huge -10dB bandwidth and **maximum Gain from 12.1dBi to 18.6dBi**, all solutions presented could fit on a wireless device for 5G applications, considering the technical requirements demanded. However, on the beam steering performance, it has been observed that **linear configurations achieve better performance**, with a **maximum scan angle up to ±45°**.

Indeed, an 8-Microstrip Patch linear antenna array has been selected to be implemented in a real-world environment, by studying the impact of a wireless device cover on the 5G Antenna Array performance. Different materials and thicknesses have been analyzed, obtaining the impact on the Efficiency and Radiation Pattern for each case. It has been observed that considering the optimal thickness when a cover is selected, it is a key point to maximize the antenna solution performance. Surprisingly, the **Aluminum Oxide** presented the **best relation between cover thickness** and **8-element antenna array performance,** with an **Efficiency close to 80%** and a **maximum Gain of 16.0dBi** for a **1.8mm cover thickness**.

Therefore, it has been demonstrated that several antenna array configurations of the Microstrip Patch antenna developed along this project can perfectly fit as a 5G Antenna Array solution. Moreover, **it has been validated the 8-Microstrip Patch linear antenna array for a real-world wireless device for 5G applications**, such as autonomous vehicles, faster and higher quality communications with full coverage, real-time security actions, resources management and remote healthcare.

On next page, it is presented a figure summarizing the most important chapter of this project considering the objectives, results and conclusions for each of them. It helps to better understand the approach conducted and exposed along this report.

Finally, the path to follow from the investigation and development conducted along this project would be implemented by the company Fractus Antennas S.L.

	OBJECTIVE	RESULTS	CONCLUSIONS
Chapter 1.3 	Understand what 5G is, technical requirements, how will affect our life and the challenges needed to be achieved from the ICT sector.	• Up to 10Gbps data rate. • 1-millisecond latency. • 1000x bandwidth per unit area. • Up to 100x number of connected devices per unit area. • 99.999% availability. • 100% coverage. • 90% reduction in network energy usage. • Up to 10-year battery life for low power IoT devices.	Highly demanding technology in terms of antenna performance. Plenty of applications will show up, completely changing the way we live and interact with others and with things. On mid-2020 5G will be a reality on sub-6GHz frequency bands.
Chapter 2 	Present the project definition including all the steps performed during the project development. Provides an overview of the project from an organizational point of view.	Project designed to study and develop an Antenna Array solution for 5G. Main tasks list and action plan to fulfill the deadline of the project.	It is a key part of a project's success to clearly plan and schedule the project timings along its duration. A general overview of the project period is presented.
Chapter 3 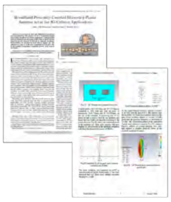	Understand how the current market products are designed and performing. Have a clear view of the timings and expects we should have from 5G technology.	• Antenna type: 4, 16 or greater – Microstrip Patch. • 28GHz frequency. • -10dB BW: 0.5GHz-2GHz. • Max Gain: >12.0dBi. • Max scan angle: ±60°. • Array type: 1D or 2D. • Beamsteering technique.	Great variety of antenna array for 5G implementation achieving high performance. Characteristics extracted to define and design the 5G Antenna Array solution of the project.
Chapter 4 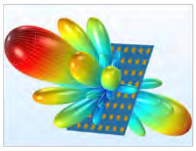	Obtain an Antenna Array solution for 5G applications achieving the performance target set on the review of Prior Art.	• Antenna type: 4, 8, 16 – Microstrip Patch. • Single element: 4mm x 4mm. • 28GHz frequency. • -10dB BW: 2.3GHz • Max Gain: 12.1dBi – 18.6dBi. • Max scan angle: ±15°-±45°. • Array type: 1D or 2D. • Beamsteering technique.	It is obtained high Efficiency performance, huge -10dB bandwidth, maximum Gain from 12.1dBi to 18.6dBi and max scan angle of ±45° at 28GHz. All solutions presented could fit on a wireless device for 5G applications.
Chapter 5 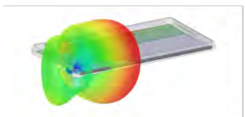	Consider one 5G Antenna Array solution on a real-world environment. Obtain the impact on the Efficiency and Radiation Pattern of a wireless device cover.	3 materials with 4 different thicknesses considered. On optimal thickness, the 5G Antenna Array performance is maximized obtaining similar performance than on free-space. Aluminum Oxide presents the best relation between cover thickness and 8-element antenna array performance, with an Efficiency close to 80% and a maximum Gain of 16.0dBi for a 1.8mm cover thickness.	It has been validated the 8-Microstrip Patch linear antenna array for a real-world wireless device for 5G applications, such as autonomous vehicles, faster and higher quality communications with full coverage, real-time security actions, resources management and remote healthcare.

7 References

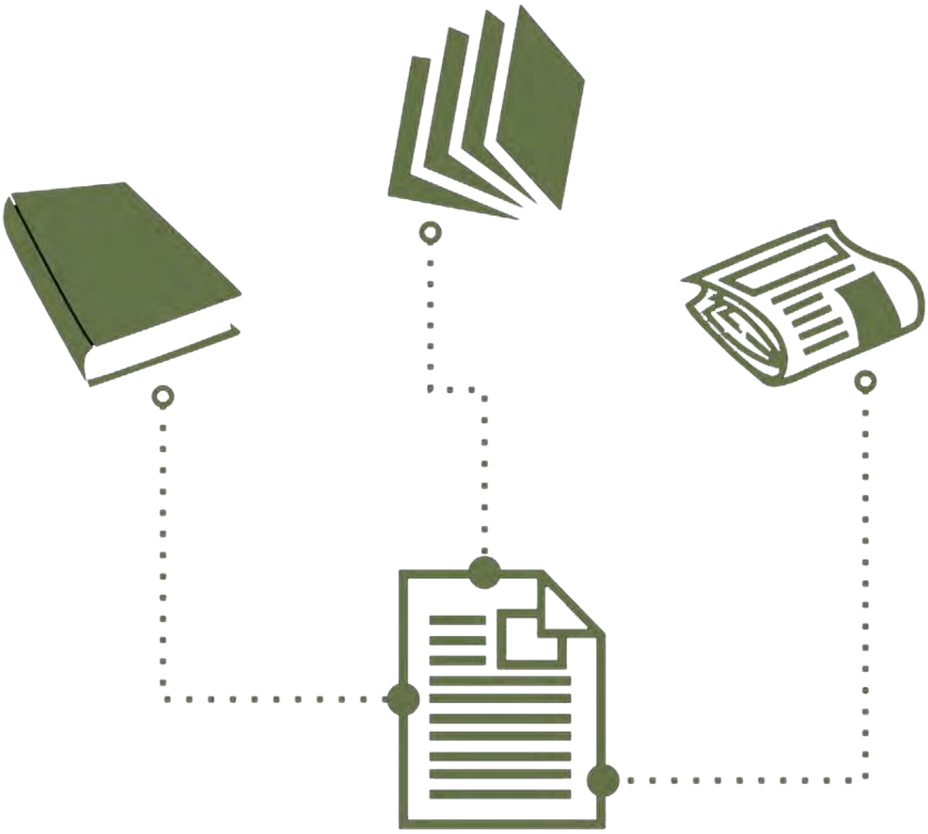

Throughout the presented report, different books, articles and papers' references have been cited to support the scientific and technological approach of this project. These references and authors are presented below in order of appearance.

[1] Internet Society. <https://www.internetsociety.org/>.

[2] IEEE Spectrum; "Everything you need to know about 5G". <https://spectrum.ieee.org/video/telecom/wireless/everything-you-need-to-know-about-5g>.

[3] 5G Infrastructure Association; "5G PAN-Europe Trials Roadmap Version 4.0".

[4] Qorvo; "Getting to 5G: Comparing 4G and 5G System Requirements" <https://www.qorvo.com/design-hub/blog/getting-to-5g-comparing-4g-and-5g-system-requirements>

[5] IEEE Future Networks; "From Standards to Service – the European Way to 5G" <https://futurenetworks.ieee.org/tech-focus/december-2017/from-standards-to-service-the-european-way>.

[6] Observatorio Empresas Vodafone; "Ocho ciudades españolas quieren actuar sobre la salud o el tráfico a través de 5G" <https://www.observatorio-empresas.vodafone.es/articulos/administraciones-publicas/smart-cities-espanolas-5g-martin-brynskov/>.

[7] BBC; "Will 5G be necessary for self-driving cars?" <https://www.bbc.com/news/business-45048264>.

[8] European Commission; "5G for Europe Action Plan" <https://ec.europa.eu/digital-single-market/en/5g-europe-action-plan>.

[9] J. Anguera and A. Pérez; "Teoría de Antenas". Universitat Ramon Llull, 2008.

[10] Constantine A. Balanis; "Antenna Theory – Analysis and Design".

[11] Jaume Anguera, Carles Puente, Carmen Borja, and Jordi Soler; "Fractal-Shaped Antennas: Review". Wiley Encyclopedia of RF and Microwave Engineering, edited by K. Chang, vol.2, pp.1620-1635, 2005.

[12] Jaume Anguera, Carles Puente, Carmen Borja, Raquel Montero, and Jordi Soler; "Small and High Directivity Bowtie Patch Antenna based on the Sierpinski Fractal". Microwave and Optical Technology Letters, vol.31, no. 3, pp.239-241, Nov 2001.

[13] Jaume Anguera, Jean-Pierre Daniel, Carmen Borja, Josep Mumbrú, Carles Puente, Tiphaine Leduc, Nancy Laeveren, and Peter Van Roy; "Metallized Foams for Fractal-Shaped Microstrip Antennas". IEEE Antennas and Propagation Magazine, vol.50, no. 6, Dec. 2008, pp.20-38.

[14] J. M. J. W. Jayasinghe, Jaume Anguera, and D.N. Uduwawala; "Genetic Algorithm Optimization of a High-Directivity Microstrip Patch Antenna Having a Rectangular Profile". Radioengineering, Vol. 22, No. 3, September 2013, pp.700-707.

[15] ElectronicsNotes; “Beamforming and Beamsteering Antennas” <https://www.electronics-notes.com/articles/antennas-propagation/smart-adaptive-antennas/beamforming-beamsteering-antenna-basics.php>.

[16] Vites; “Adaptative Beamsteering – Overview” <http://www.vites.de/index.php/en/technology>.

[17] Schaller Tech; “Tecnología Beam Steering o ¿Cómo cambiar la dirección del sonido?” < https://schallertech.com/beam-steering-o-como-cambiar-la-direccion-del-sonido/>.

[18] Muhammad Kamran Ishfaq, Tharek Abd Rahman, Yoshihide Yamada and Kunio Sakakibara; “8x8 Phased Series Fed Patch Antenna Array at 28GHz for 5G Mobile Base Station Antennas”. IEEE-APS Topical Conference on Antennas and Propagation in Wireless Communications, October 2017, pp.160-162.

[19] Ali T.Alreshaid, Oualid Hammi, Mohammad S. Sharawi and Kamal Sarabandi; “A Compact Millimeter-Wave Slot Antenna Array for 5G Standards”. IEEE 4th Asia-Pacific Conference on Antennas and Propagation (APCAP), January 2016, pp.84-85.

[20] Manoj Stanley, Yi Huang, Tian Loh, Qian Xu, Hanyang Wang and Hai Zhou; “A High Gain Steerable Millimeter-Wave Antenna Array for 5G Smartphone Applications”. 11th European Conference on Antennas and Propagation (EUCAP), May 2017, pp.1320-1323.

[21] Syeda Fizzah Jilani and Akram Alomainy; “A Multiband Millimeter-Wave 2-D Array Based on Enhanced Franklin Antenna for 5G Wireless Systems”. IEEE Antennas and Wireless Propagation Letters, Vol. 16, September 2017, pp.2983-2986.

[22] Naser Ojaroudiparchin, Ming Shen, Shuai Zhang and Gert Frølund Pedersen; “A Switchable 3-D-Coverage-Phased Array Antenna Package for 5G Mobile Terminals”. IEEE Antennas and Wireless Propagation Letters, Vol. 15, February 2016, pp.1747-1750.

[23] Henry Abu Diawuo and Young-Bae Jung; “Broadband Proximity-Coupled Microstrip Planar Antenna Array for 5G Cellular Applications”. IEEE Antennas and Wireless Propagation Letters, Vol.17, No. 7, July 2018, pp.1286-1290.

[24] Mohamed Bakry El Mashade and E.A.Hegazy; “Design and Analysis of 28GHz Rectangular Microstrip”. WSEAS Transactions on Communications, Vol. 17, March 2018, pp.1-9.

[25] Mohammed Abu Saada, Talal Skaik and Ramadan Alhalabi; “Design of Efficient Microstrip Linear Antenna Array for 5G Communications Systems”. International Conference on Promising Electronic Technologies (ICPET), November 2017.

[26] Mohsen Khalily, T.A. Rahman and M.R.Kamarudin; “Design of Phased Arrays of Series-Fed Patch Antennas With Reduced Number of Controllers for 28-GHz mm-W Applications”. IEEE Antennas and Wireless Propagation Letters, Vol. 15, February 2016, pp.1305-1308.

[27] Mohamed Mamdouh M.Ali and Abdel-Razik Sebak; “Directive Antennas for Future 5G Mobile Wireless Communications”. XXXIInd General Assembly and Scientific Symposium of the International Union of Radio Science, August 2017.

[28] Björn Thors, Davide Colombi, Zhinong Ying, Thomas Bolin and Christer Törnevik; “Exposure to RF EMF from Array Antennas in 5G Mobile”. IEEE Access, Vol. 4, August 2016, pp.7469-7478.

[29] K. Jang, M. K. Khattak, J. Jeon, H. Kim, S. Kahng, Louis J.Kim and Klaus B. Kim; “Handheld Beamforming Antennas Adoptable to 5G Wireless Connectivity”. International Workshop on Antenna Technology (iWAT), March 2015.

[30] Dennis W.Prather, Shouyuan Shi, Garrett J. Schneider, Peng Yao, Christopher Schuetz, Janusz Murakowski and Joseph C. Deroba; “Optically Upconverted, Spatially Coherent Phased-Array-Antenna Feed Networks for Beam-Space MIMO in 5G”. IEEE Transactions on Antennas and Propagation, Vol. 65, December 17, pp.6432-6443.

[31] Yue Gao, Runbo Ma, Yapeng Wang, Qianyun Zhang and Clive Parini; “Stacked Patch Antenna With Dual-Polarization and Low Mutual Coupling for Massive MIMO”. IEEE Transactions on Antennas and Propagation, Vol. 64, July 2016, pp.4544-4549.

[32] Igor Syrytsin, Shuai Zhang, Gert Frølund Pedersen and Zhinong Ying; “User Effects on the Circular Polarization of 5G Mobile Terminal Antennas”. IEEE Transactions on Antennas and Propagation, Vol. 66, June 2018, pp.4906-4911.

[33] Roger Scorp; “RT/Duroid 5880 Datasheet” <https://www.rogerscorp.com/documents/606/acs/RT-duroid-5870-5880-Data-Sheet.pdf>

[34] Marc Rütschlin; “5G Antenna Design for Mobile Phones” <https://www.cst.com/solutions/article/5g-mobile-phone-antenna-design>